**Use of Vision Sensors and Lane Maps to Aid GPS-INS Navigation**

by

John W Allen

A thesis submitted to the Graduate Faculty of
Auburn University
in partial fulfillment of the
requirements for the Degree of
Master of Science

Auburn, Alabama
May 9, 2011

Keywords: Sensor Fusion, Kalman Filter, GNSS



Approved by

David M. Bevly, Chair, Associate Professor of Mechanical Engineering
David Beale, Professor of Mechanical Engineering
Andrew J. Sinclair, Associate Professor of Aerospace Engineering

Abstract

This thesis proposes a method to increase observability of a GPS/INS system operating under limited satellite coverage. Measurements from vision sensors are used to supplement the GPS pseudorange and pseudorange-rate measurements. Both LiDAR and camera measurements are used to measure the lateral position of a vehicle in its current lane. The vision measurements provide local based positioning based off the lane. A map of the lane is used to relate the local position measurement provided by the vision systems to the global coordinate frame used by GPS and the navigation filter. Since the filter is used for ground vehicles, the height above the ground is constant. The constant height can be used to constrain position in another axis that is orthogonal to the axis in which lane position measurements are given.

In order to test the performance of the navigation filter, real data from the NCAT test track in Opelika, Alabama will be used. RTK GPS is used as a "truth" metric in order to determine filter performance. Experimental results show that using vision measurements with a precise lane map results in centimeter level global accuracy in the axis perpendicular to the road and meter level (depending on the quality of GPS measurements available) global accuracy in the axis parallel with the road. It is also shown that the navigation filter remains observable and functional if two GPS observations along with vision measurement and a lane map are available. The results also show a reduction in position drift when GPS is unavailable if vision measurements and a lane map are available.

Acknowledgments

I would like to thank god and my family without whom none of this would be possible. I would like to thank Jordan Britt and Christopher Rose for their support in this project. I would like to thank all the members of the GAVLAB for their help. I would like to thank my advisor, Dr David Bevly. I would also like the thank the Federal Highway Administration for funding this research.

Table of Contents

List of Figures

List of Tables

# Chapter 1

# Introduction

In order to reduce the number of traffic fatalities that occur due to unintentional lane departures, many vehicle manufacturers are developing lane departure warning (LDW) systems. LDW systems alert the driver before the vehicle departs the lane. Most of the LDW systems in production now are solely based off camera measurements. A LDW camera uses feature extraction to determine lateral position in the current lane. The feature used for a camera-based LDW system is the painted lane lines. A single camera can not provide three-dimensional ranging information due to the unresolved distance from the camera to the feature of interest; although the camera can provide lateral position in a lane without resolving this distance. Camera-based LDW systems are prone to failures due to road, weather, and lighting conditions. A more in-depth look at how the camera is used to determine lane position can be found in [2].

Current research is underway to provide robustness to current camera-based LDW system by adding other types of sensors. A LiDAR (Light Detection And Ranging) is an active type of vision sensor. A LiDAR works like sonar; however, instead of using sound waves, a LiDAR uses light waves to provide ranging. Unlike the camera, a LiDAR can provide three-dimensional ranging information. One drawback to the LiDAR is feature extraction can be more difficult than feature extraction using a camera. To overcome this difficulty, the LiDAR also provides reflectivity data. For the LDW case, a painted lane marker has a different reflectivity than the asphalt around it. The reflectivity data can be used to extract lane markers, and the scan angle information can be used to provide a measurement of the lateral position of the vehicle in the lane. A more in-depth look at how the LiDAR is used to determine lane position can be found in [1].

A camera and a LiDAR can both be used to estimate position in one dimension of a three-dimensional space. GPS is used to estimate position and velocity in a four-dimensional space; the fourth dimension being time. The necessity for a precise estimate of the current time is why four GPS observations are needed to maintain observability. This thesis shows how to use a way-point based map to incorporate vision measurements into a global navigation filter. The vision measurements can be used to resolve position in one axis of the local coordinate frame. Assuming a ground vehicle does not change height in the local coordinate frame, position resolution in the vertical axis can be resolved. The constant vertical height leaves the navigation filter with one unresolved axis and an unresolved clock bias; therefore the navigation filter proposed maintains sufficient observability while only using two GPS observations and vision measurements combined with a map. This could provide useful in urban navigation, or in any area where GPS observations are limited.

### 1.1 GPS Based Navigation Filter

The GPS based navigation filter is one of the most popular type of navigation filter and is well studied [4], [5]. The navigation filter works by fusing measurements from an inertial measurement unit (IMU) and GPS measurements into one solution that is updated at the rate of the IMU. The IMU measurements are integrated to estimate the filter states between GPS measurements. The GPS measurements are used to correct for the drift in states caused by integration of the error in the IMU measurements. There are many methods of combining the IMU and GPS measurements. A few examples are the extended Kalman filter, the unscented Kalman filter, and the particle filter. A discrete extended Kalman filter is used to fuse the IMU and GPS measurements for this work.

There are two methods of using GPS measurements to update the navigation filter. The first method is to use the global position and velocity computed by the GPS receiver to update the navigation filter. This method is called a loosely coupled measurement update. The loosely coupled measurement update has the advantage of being simple to implement

due to the fact that the global position and velocity are states of the filter. Therefore, the measurements represent a direct measurement of the states which results in measurement equations that are linear.

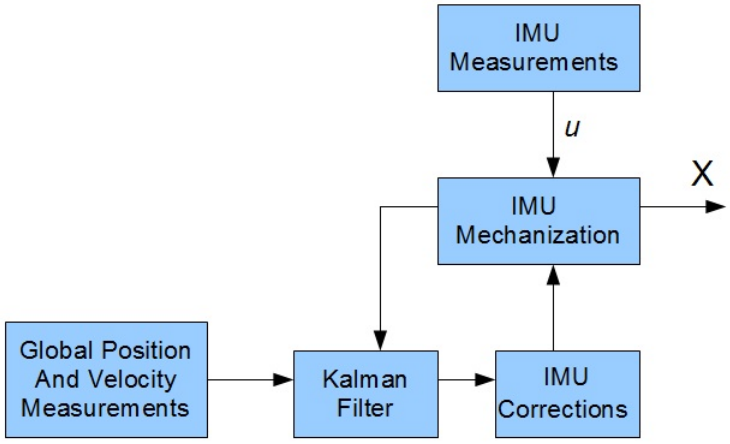


Figure 1.1: Loosely Coupled Filter Architecture

Figure 1.1 shows the block diagram for the loosely coupled filter. The IMU measurements are mechanized to determine the states of the filter (X). The mechanized IMU measurements are used to update the Kalman filter. The Kalman filter provides estimated IMU biases which are subtracted from the IMU measurements. The loosely coupled GPS measurements are used by the Kalman filter to remove accumulated error in the states of the filter.

The second method of using GPS measurements involves using the GPS range measurements. This method is a closely coupled measurement update. The range and range rate to each satellite is used for the filter measurement update. This type of measurement adds additional complexity to the navigation filter; however, it also provides a robustness benefit. When the number of GPS observations falls below four, the GPS receiver is no longer able to compute a position and velocity. Therefore, when using a loosely coupled architecture, the measurements are not available if the number of GPS observations is less than four. The

closely coupled measurement update is able to benefit from measurements when less than four GPS observations are available; however, the navigation filter is no longer observable.

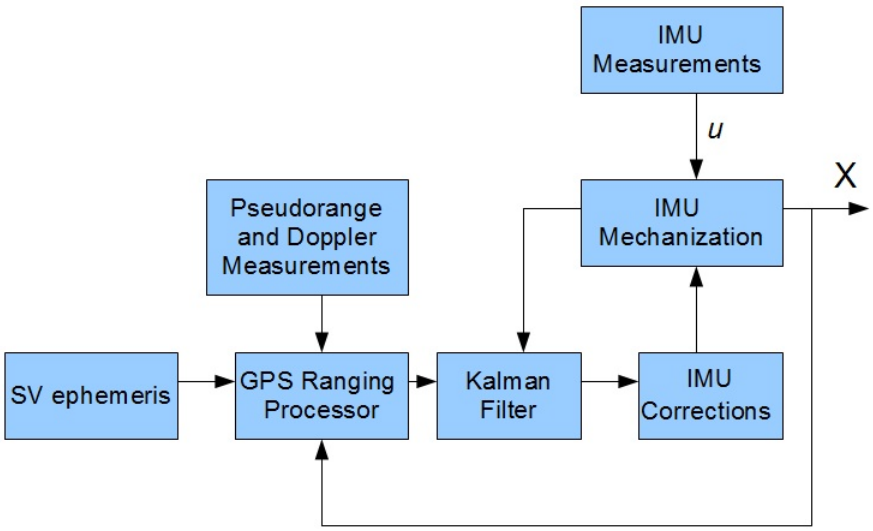


Figure 1.2: Closely Coupled Filter Architecture

Figure 1.2 shows the block diagram for the closely coupled navigation filter architecture. The only change in the system is the measurement update. The measurement update for the closely coupled system is non-linear, and requires a feedback of the states to estimate the value of the measurements. In the ranging processor, the states of the filter along with the satellite position and velocities are used to estimate the range and range rate measurements to each observable satellite. The estimated measurements are differenced from the actual measurements to determine the measurement residual. The Kalman filter uses the residual to update the states of the filter.

## 1.2 Incorporating Vision Measurments

This thesis focuses on the development of a global navigation filter that is capable of using both GPS measurements and lane position measurements from vision sensors. The vision measurements are given in a local coordinate frame (not the global coordinate frame

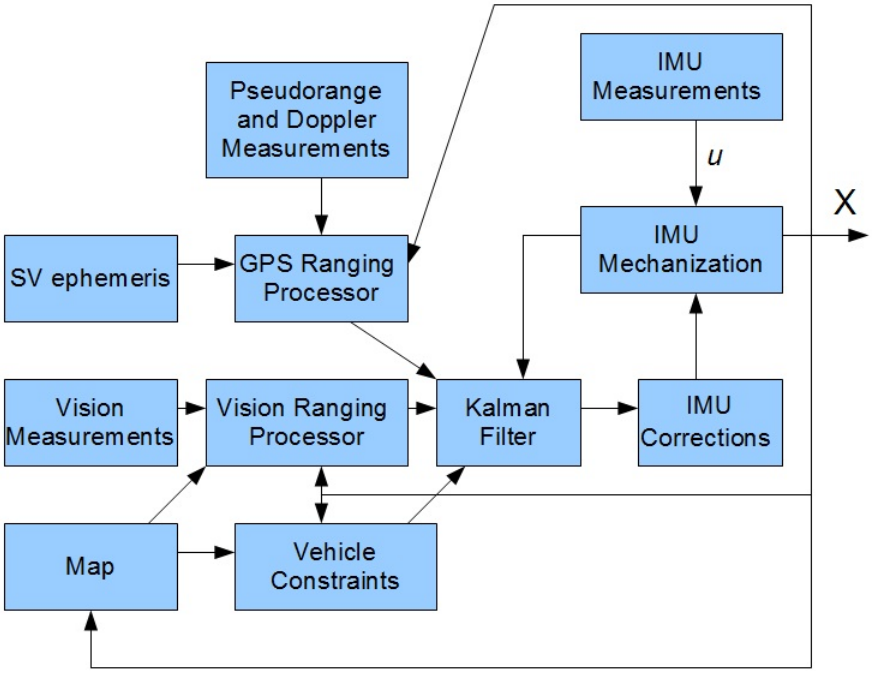


Figure 1.3: Filter Architecture

like GPS). In order to use the vision measurements to update the global filter, some information on the vision measurement coordinate frame (road based coordinate frame) is needed. This information is contained in a waypoint map of the current lane of travel.

Figure 1.3 presents the block diagram for the complete system developed and used in this thesis. This system has two measurement updates. One from the GPS receiver and the other from the vision system. Similar to the closely coupled GPS measurement, the lane position is estimated using the current states of the filter and the road map. The estimated lane position is differenced from the lane position measurement provided by the vision systems to create the measurement residual. The residual is then used to update the navigation filter. Since this work is for ground vehicles, the height above the map in the vertical direction is constant. The constant vertical height can be used to constrain the estimated position of the filter in the vertical road axis.

## 1.3 Thesis Contribution

This thesis provides a method of using measurements given in a coordinate frame that differs from the navigation coordinate frame. Lane position measurements can be used to update a global navigation filter. In order to use a measurement given in a coordinate frame the differs from the navigation coordinate frame, the location and orientation of the measurement coordinate frame must be known. The orientation and position of the lane position measurement coordinate frame is contained in a waypoint lane map. There are many benefits to adding vision based lane position measurements to a global navigation filter. These benefits include improved robustness, improved accuracy in two dimensions (vertical and lateral road axis), and the ability to navigate with only two GPS satellites. An outline of the thesis is given below.

- Backgound - Chapter 2 provides background information on navigation.
- Six Degree of Freedom Global Navigation Filter - A global navigation filter that uses inertial measurements and GPS is presented in chapter 3. The filter tracks the position, velocity, and attitude of a vehicle in a global coordinate frame.
- Method for Incorporating a Lane Map and Vision Measurements - Chapter 4 provides a method of using a lane map to update a global navigation filter with local vision measurements.
- Results - Chapter 5 provides results from the filter. Results of the navigation filter working at full capacity are provided. Also, this chapter presents results where different combinations of measurements are removed. These results shows the effects of a sensor failure or combinations of sensor failures on the navigation filter and the benefits of using vision measurements and a lane map. Results are provided to show how the filter operates when less than four GPS satellite are available.

- Coordinate Frame Rotation and Translation - Appendix A provides an explanation of coordinate frame rotation and translation as well the sequence of rotations used for this thesis

- Observability Analysis - Appendix B provides an observability analysis for the complete navigation filter with an emphasis on observability with limited GPS satellite availability.

Specific contributions are given below.

- Method for Incorporating a Lane Map and Vision Measurements - The thesis provides a method of using a lane map to update a global navigation filter with local vision measurements.

- Effects of Limited GPS Satellite Constellations - Results are provided to show how the filter operates when less than four GPS satellite are available. The results show that the navigation filter remains operational as long as two GPS satellites are available.

# Chapter 2

# Background

In the medieval ages, navigation was considered one of the seven mechanical arts. The mechanical arts were a classification of professional knowledge used before the concept of engineering. Navigation uses many principal of mathematics with an emphasis on the principles of calculus and geometry. Modern navigation also relies heavily on principles of linear algebra and estimation theory.

One basic concept of navigation is dead reckoning. Dead reckoning involves integrating a measurement of a change in a state to estimate that state. For example, the position in one axis can be estimated by integrating the velocity in that axis. Dead reckoning can also be used to predict the future position of a vehicle; however, using dead reckoning to estimate the future position of vehicle assumes velocity (and acceleration) remains constant. This method of predicting position is used by ships to estimate future position in order to avoid colliding with objects at a known location. The velocity of the ship and the course of the ship are used to estimate future two-dimensional position of the ship. Modern methods of dead reckoning involve using an inertial measurement unit (IMU) to measure acceleration and rotation along three orthogonal axes. The acceleration measurements are integrated to find velocity, which in turn are integrate to find position. The attitude can also be estimated by integrating the gyroscope measurements.

Dead reckoning involves integrating a measurement of acceleration, velocity, or rotation rate to estimate how much the derivative of the measurement has changed. For example, the derivative of velocity is position. By multiplying a measurement of velocity by some change in time ($dt$), the result will be estimated change in position over that time period. This estimated change in position can be added to the current position to get the position of the

vehicle $dt$ seconds in the future, assuming the velocity remains constant over the integration period ($dt$). After $dt$ seconds, another measurement of velocity can be used to propagate the position into the future again. Since the predicted future position is always a function of the previous position, any error in the velocity measurement will be carried over in the position. Therefore, a continual drift in error is present when using dead reckoning to navigate.

Measurements of position are used when available to correct for the accumulation of error when dead reckoning. In the past, mariners would use astronomical observations and clocks to determine position. The position is reset with the measurement, thus eliminating the drift due to dead reckoning. Dead reckoning would then continue until another measurement of position was available. Modern technique of navigation involves using IMU measurements to dead reckon, then using GPS measurements to correct for the dead reckoning drift allowing for autonomous navigation.

This chapter is used to give a brief overview on the subject of navigation and introduce the principles and sensors used in the following chapters. The first section introduces the principle of inertial navigation. The next section introduces multi-sensor fusion and the Kalman filter. The following section presents an overview of the GPS system and the ways it can be used for navigation. The last section contains a brief overview of the methods used to determine lane position with the LiDAR and camera.

## 2.1 Inertial Navigation

Inertial navigation involves using measurements from an inertial measurement unit (IMU), consisting of accelerometers and gyros, to dead reckon vehicle pose (position, velocity, and attitude). The most typical IMU configuration has three accelerometers lined up on orthogonal axes thus measuring acceleration in each axis of the three dimensional coordinate frame of the vehicle.

Accelerometers measure acceleration along a particular axis. Most accelerometers work by observing the deflection of a proof mass attached to a spring and damper. An accelerometer actually measures specific force on a known mass, then calculates acceleration. When the axis of an accelerometer is aligned vertically, the accelerometer will measure 9.81 $m/s^2$ (1g) due to gravity causing a deflection of the proof mass. Accelerometers also measure the centripetal acceleration and the Coriolis acceleration due to the rotation of the earth. Therefore, an accelerometer on earth measures the acceleration of an object along one axis plus components of the gravity vector. These components of the measurement must be removed in order to prevent a larger growth in error when dead reckoning. Accelerometer measurements also have a drifting bias that is a function of temperature and the quality of the accelerometer.

The accelerations provided by an IMU are given in the coordinate frame of the vehicle. Integrating accelerations from the IMU will not result in any significant positioning estimation. The result will be dead reckoned distance traveled laterally, longitudinally, and vertically. The positions will also be incorrect due to the fact that the body frame is a non-inertial reference frame. Therefore, the accelerometer measurements should be rotated to an inertial coordinate frame. The navigation coordinate frame, or the coordinate frame in which the position and velocity are estimated, should be inertial. Coordinate frame rotation is explained in Appendix A.

Any coordinate frame attached to the earth can be used as a inertial reference frame. Technically, a coordinate frame fixed to the earth is moving because the earth is rotating in space. The centripetal acceleration is constant for a given global position and the Coriolis acceleration is dependent on the velocity of the IMU. These values, along with the gravity vector, can be estimated in the non-inertial reference frame (navigation coordinate frame). The navigation coordinate frame used for this work is the earth centered earth fixed (ECEF) coordinate frame. The ECEF coordinate frame is fixed to the center of the earth.

In order to rotate the accelerations, the attitude of the IMU must be known. The attitude is a way of expressing the orientation of a coordinate frame with respect to another coordinate frame and is often measured using Euler angles. A more in depth explanation of Euler angles can be found in Appendix A. The most common Euler angles are roll, pitch, and yaw. These angles are used to describe the orientation of a vehicle with respect to a point on the reference ellipsoid of the earth.

Equation (2.1) shows the rotation matrix used to rotate vectors in the body coordinate frame to the ECEF coordinate frame using a particular order of rotations.

$$C_b^e = \begin{bmatrix} c_2c_3 & s_1s_2c_3 - c_1s_3 & c_1s_2c_3 + s_1s_3 \\ c_2s_3 & s_1s_2s_3 + c_1c_3 & c_1s_2s_3 - s_1c_3 \\ -s_1 & s_1c_2 & c_1c_2 \end{bmatrix} \tag{2.1}$$

The order of rotations used can be found in Appendix A. The rotation matrix is a function of the Euler angles where $s_1$ is the sine of the first angle and $c_1$ is the cosine of the first angle, $s_2$ is the sine of the second angle and $c_2$ is the cosine of the second angle, $s_3$ is the sine of the third angle and $c_3$ is the cosine of the third angle. Accelerations in the body coordinate frame can be rotated into the navigation coordinate frame using this matrix. The accelerations are then corrected for gravity and the rotation of the earth. Then they can be integrated to estimate velocity and position.

In order to rotate accelerations into the navigation coordinate frame, the attitude of the body coordinate frame (coordinate frame of the IMU) must be known. Attitude is estimated using gyroscopes. A traditional gyroscope consists of a rotating disc which has an axis rotation held in a gimbal system. The gimbaled system allows the the axis of disc rotation to rotate freely around the body of the gyroscope. The spinning disc causes the axis of rotation to maintain a constant orientation even as body of the gyroscope rotates around. The attitude of the gyroscope with respect to the spinning disc can be determined. Many IMUs report rotation around each accelerometer axis. This value can be measured from a

gyroscope, or it can be measured by observing the Coriolis acceleration on a vibrating mass spring damper system. This type of sensor is called a vibrating structure gyroscope. The IMU mechanization matrix (Equation (2.2)) is used to transform rotation rates in the body coordinate frame to rotation rates of the three Euler angles.

$$C_{MECH} = \begin{bmatrix} 1 & \frac{s_1 s_2}{c_2} & \frac{c_1 s_2}{c_2} \\ 0 & c_1 & -s_1 \\ 0 & \frac{s_1}{c_2} & \frac{c_1}{c_2} \end{bmatrix} \tag{2.2}$$

The most obvious problem with dead reckoning inertial navigation is the drift in position, velocity, and attitude estimation. The drift is caused by integration of the biases and noise present in accelerometer and gyroscope measurements. The IMU bias and noise prevents inertial only navigation for a prolonged period of time. The amount of drift over time caused by dead reckoning is based on many factors. For example, dead reckoning using acceleration to find position involves integrating twice which will cause a quicker growth of error due to the double integration. The amount of drift will also depend on the quality of the IMU. IMUs can be classified using various grades such as navigation, tactical, and automotive. The main difference between grades of IMUs is the stability of the measurement biases, which have direct effect on the rate of drift. Larger biases results in a larger growth rate of error when dead reckoning.

### 2.1.1 Crossbow IMU

The IMU used for this work is a Crossbow 440 IMU. This IMU is an automotive MEMS (Microelectromechanical systems) grade IMU. The cost of navigation and tactical grade IMUs prevent them from being used for personal vehicle navigation. The present day cost of these high grade IMUs exceeds the cost of the vehicle in most cases. The data rate of the crossbow was set to 100 $Hz$. When using the IMU to dead reckon, error in the position estimates drift quickly. Therefore, the position needs to be updated at least every few seconds

Figure 2.1: Crossbow 440 IMU

to account for the dead reckoning error growth. After only one minute of dead reckoning with this IMU, the error in estimated position is on the order of hundreds of meters. Dead reckoning attitude based off IMU rotation rates results in error on the order of a degree after one minute of dead reckoning.

## 2.2 Multi-sensor Navigation

Multi-sensor navigation is the use of multiple measurement sources to determine location. It has already been established that an IMU alone can not be used to navigate over long periods of time. There must be some other sensor that is capable of measuring location, such as GPS which can provide measurements of position and velocity. So one example of a multi-sensor navigation system consists of an IMU and a GPS receiver. The IMU is used to dead reckon position and velocity between GPS measurements. Figure 2.2 shows various methods of single axis positioning using simulated accelerometer data.

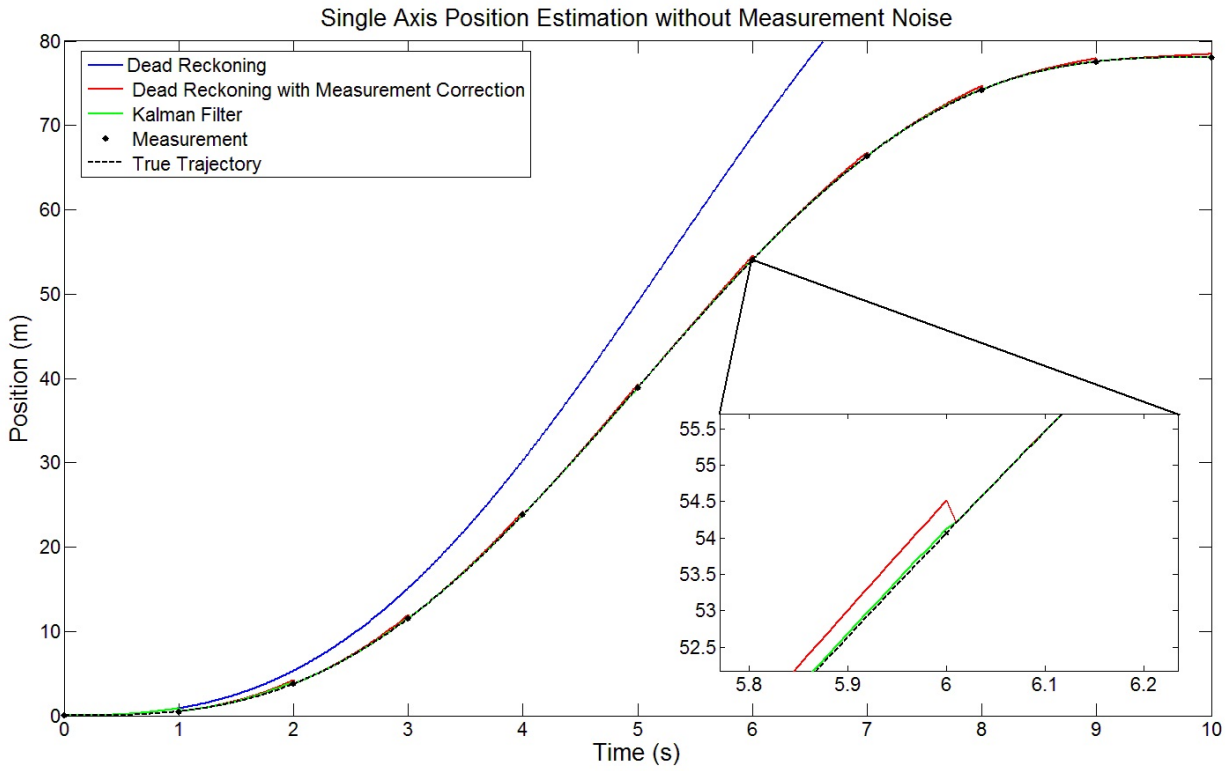


Figure 2.2: Single Axis Position Estimation without Measurement Noise

The acceleration is sinusoidal over the ten second interval. The true acceleration is corrupted with a bias and white noise. The black dashed line represents the true trajectory of the object. The blue line shows estimated position when dead reckoning over the interval. The red line is the result of dead reckoning between position measurements (black dots). The position and velocity are reset after every measurement of position. The green line represent the result using a Kalman filter to estimate the position. The Kalman filter is an optimally tuned estimator. Its optimal tuning is a result of knowledge of all the measurement and model noise statistics. The solution of the Kalman filter provides the best estimates because the estimator is able to also estimate the bias present in the accelerometer measurement. The bias can then be subtracted out, resulting in better dead reckoning performance between measurements. Figure 2.3 is the same as Figure 2.2 but with added measurement noise.

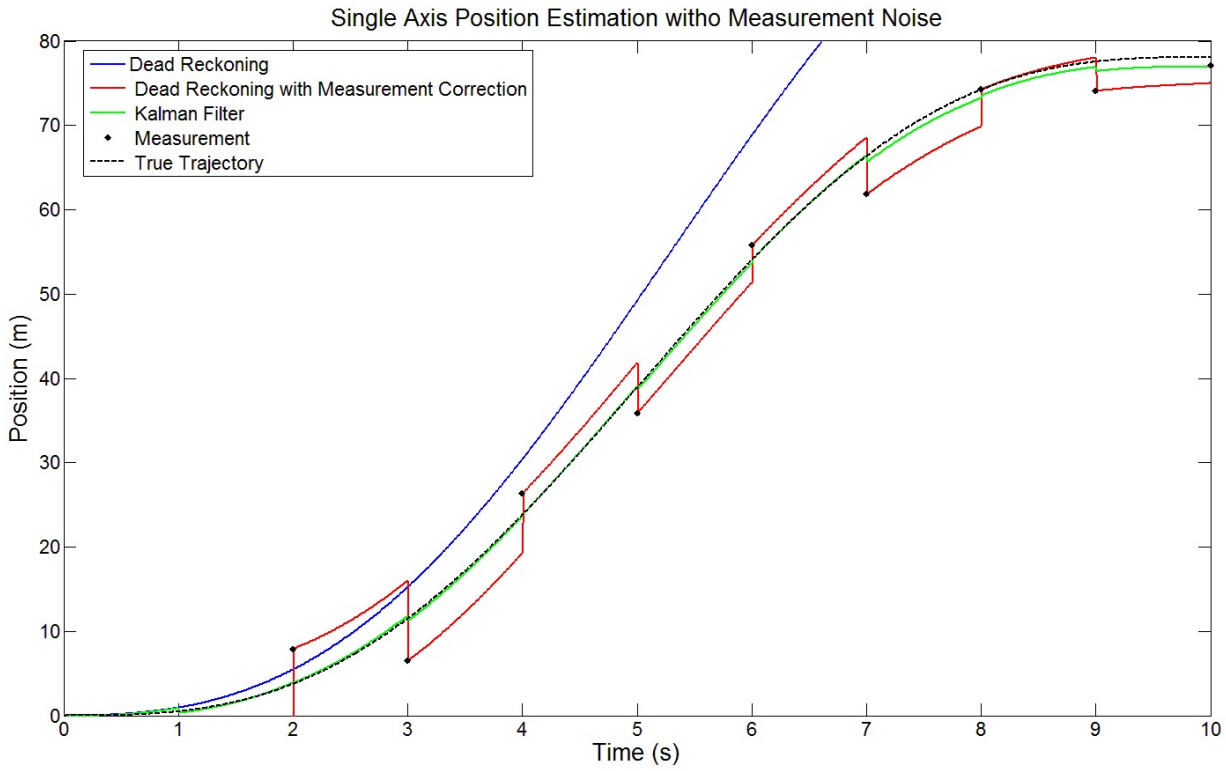


Figure 2.3: Single Axis Position Estimation with Measurement Noise

The Kalman filter is able to filter out white (unbiased) noise in the position measurements, assuming the statistics of the noise are known and the noise is white.

### 2.2.1 Discrete Extended Kalman Filter

The Kalman filter was first proposed by Rudolf Kalman in [6]. The Kalman filter is an estimator that incorporates noise statistics of the states and the measurements. The extended Kalman filter is a method of using the Kalman filter even if state and measurement equations are non-linear. The discrete filter is used because the measurements are sampled at discrete values and are not measured continuously.

The filter is split into two phases - a time update and a measurement update. The time update represents the dead reckoning section of the filter, where the states are propagated forward in time using the IMU measurements. The state noise covariance matrix is also propagated forward to reflect changes in the estimated error statistics of the states.

The measurement update is the process of measuring the states of the filter and using the measurement of the states to correct for accumulated error due to dead reckoning with IMU measurements.

## 2.3 Global Positioning System

GPS uses an antenna on earth to receive signals from GPS satellites currently orbiting the earth. The GPS signal from each satellite is a combination of the carrier wave and the course acquisition code (C/A code). The signals are used to estimate a range to each of the visible satellites. The GPS receiver is provided with one signal from the antenna which contains components of all the signals from all the GPS satellites overhead. The receiver must determine the satellites from which it is currently receiving a signal allowing the receiver to create a copy of C/A code. The copy of the code allows the GPS receiver to extract the signal of a particular satellite out of the combined signal coming from the antenna. The C/A code copy also allows the receiver to estimate how long it took the signal to travel from the satellite to the user. The travel time is multiplied by the speed of light to determine a range to the satellite. The range is called a pseudorange because it is actually a combination of the true range to the satellite plus a range bias caused by timing errors.

Figure 2.4 gives a visual representation of the GPS timing system. Each GPS satellite and the GPS receiver of the user have an on-board clock. These clocks are used to estimate GPS system time. Ideally, all the clocks will be perfectly synchronized to the GPS system time; however, perfect clock synchronization is not practical as all clocks contain errors. Since GPS depends on precise timing, any error in the satellite or receiver time will cause large position errors. For example, a one nanosecond time error (one billionth of a second) will cause a one foot error in range between satellites. Therefore, any error in the clocks must be accounted for.

There are two types of clock errors. The first type of clock error is the satellite clock error. The satellite clock error represents the difference in the estimated time of the satellite

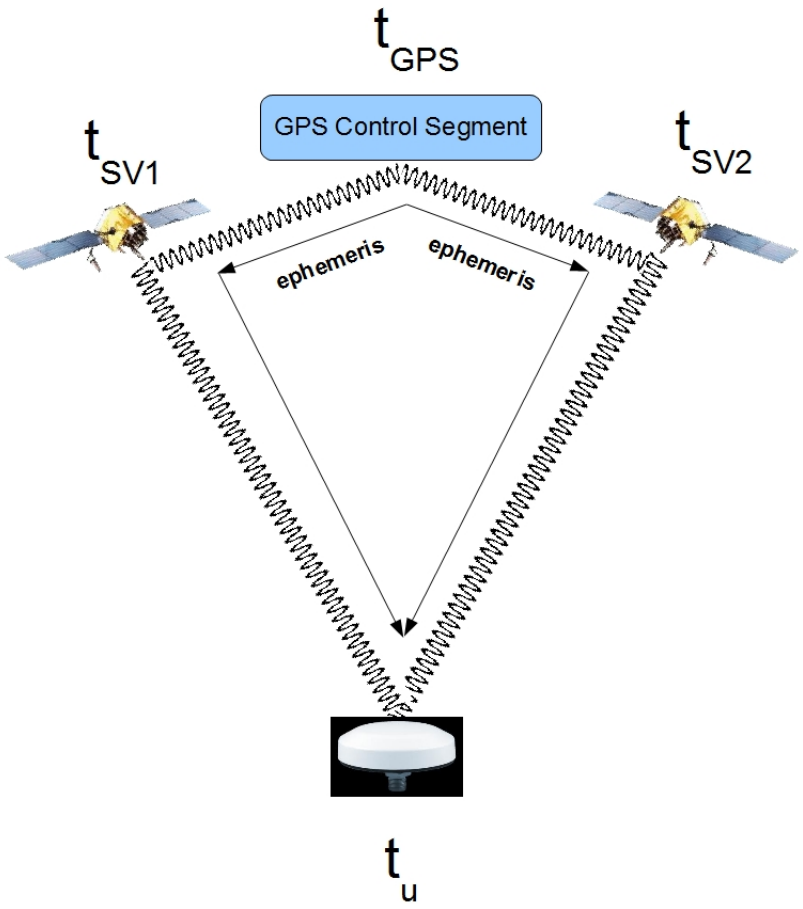


Figure 2.4: GPS Measurement Structure

and the GPS system time ($t_{GPS} - t_{SV}$). The satellite clocks are corrected periodically; however, the clock will start to drift after the correction. One source of satellite clock drift is caused by the theory of relativity. The clocks on the GPS satellites are orbiting the earth at a much faster velocity than an observer on the earth. The theory of relativity states that as the velocity of an object increases, the relative passage of time for that object decreases. Therefore, the clocks on-board GPS satellites tick at a slightly slower rate than clocks on the earth. The difference in time passage due to the velocity of the satellite is very small;

however, as stated above, even a very small error in timing can cause large errors in position estimation. The clocks on-board GPS satellites are monitored by the GPS control segment and a curve fit is created to describe how the satellite clock will drift over time. These curve fit parameters are broadcast in the ephemeris. Since the satellite clock error is a function of time and the ephemeris, a user on earth can obtain the ephemeris once and use the ephemeris to calculate a clock error of a satellite at a particular time. The clock error of the satellite allows the user to correct the estimated pseudorange for the clock errors that are present due to the satellite clock drift.

The second clock error is the error between the GPS system time and the estimated GPS system time of the receiver ($t_{GPS} - t_u$). The range bias caused by the receiver clock error can been seen on all of the pseudorange measurements. Since the bias is present and equal on all measurements, the bias can be estimated. The bias is used to correct for the clock error of the receiver. There is also a bias on the pseudorange rate measurements caused by the drift in the clock error of the receiver. The drift in receiver clock error describes the rate at which the clock error is increasing or decreasing. The receiver clock drift must also be estimated to correct pseudorange rate measurements.

There are many methods of using the pseudorange and pseudorange rates from each satellite to compute the position and velocity of the user. One method is to solve a system of equations. This method involves using four pseudorange measurements to determine four unknowns (three dimensional position and clock bias). However, in most cases, more than four pseudoranges are available. There are methods that can solve a system of overdetermined equations. One simple way is to use least squares to estimate position and velocity given the pseudorange and pseudorange rates measurements. The least squares method determines the values of the position, velocity, clock bias, and clock drift of the user that results in a minimum of the sum of the error squared. Another method is to use a Kalman filter

to estimate user position, velocity, clock bias, and clock drift given measurements of pseudorange and pseudorange rate. For any case when there is less than four GPS observations available, the system becomes under determined (or unobservable).

### 2.3.1 Measurement Structure

Equation (2.3) presents the measurement equation for one GPS observation.

$$\begin{bmatrix} \rho_m + c(dt_{sv}) \\ c\frac{f_m}{L_1} \end{bmatrix} = \begin{bmatrix} \hat{r} + dt_u \\ \hat{\dot{r}} + \dot{dt}_u \end{bmatrix} \tag{2.3}$$

The left side of the equation is the actual measurement of pseudorange and pseudorange rate. The pseudorange is calculated by taking the measured pseudorange and adding the satellite clock correction. The satellite clock correction (in meters) is calculated by multiplying the speed of light (c) by the satellite clock correction (in seconds) ($dt_{sv}$) determined by the ephemeris. The satellite clock correction will correct each pseudorange with the corresponding satellite clock error. The pseudorange-rate is calculated using received signal frequency ($f_m$). The Doppler shift can be determined by comparing the received signal frequency to the actual frequency of the signal ($L_1$). The Doppler shift is multiplied by the signal velocity (speed of light) to determine pseudorange rate.

The right side of Equation (2.3) represents the estimated pseudorange and pseudorange rate. The pseudorange and pseudorange rate is estimated using the states of the filter. The range ($\hat{r}$) and range rate ($\hat{\dot{r}}$) can be estimated using the estimated position and velocity of the filter along with the satellite position and velocity. The filter must also estimate the receiver clock bias ($dt_u$) and drift ($\dot{dt}_u$). The clock bias and drift are estimated in units of meters and meters per second. These values are added to the estimated range and range rate to estimate pseudorange and pseudorange rate.

### GPS Ephemeris

The GPS ephemeris is a set of variables that describes the orbit of a particular GPS satellite. These constant variables can be used to determine the satellite position and velocity at a particular time. The satellite positions and velocities are needed in order to compute the position of the user. The GPS ephemeris also contains clock correction values. These values are used to determine the satellite clock error at a particular time. The GPS interface control document (IDC) gives the format of the ephemeris. The IDC also provides the calculations necessary to use the ephemeris to calculate satellite position, velocity, and clock error at a certain time [7].

### 2.3.2 Septentrio GPS Receiver


Figure 2.5: Septentrio GPS Receiver

The GPS receiver used in the results of this thesis was a Septentrio PolaRx2eH triple antenna GPS receiver. This GPS receiver uses three antennae which makes it capable of measuring the attitude of the three antennae. The principles of RTK differential GPS is used to determine the precise baselines between the antennae. This information is then used to solve for the attitude of the vehicle. The attitude computed by the receiver was not used as a measurement for the filter, since the navigation filter developed in this thesis is designed to work with a single antenna GPS receiver. However, the attitude feature of the receiver did provide a method to verify the estimating attitude of the navigation filter.

The Septentrio GPS receiver is also capable of using RTK differential GPS corrections broadcast by a base station to determine a very accurate global position. RTK GPS is able to provide global position with centimeter level accuracy [8]. The NCAT test track has an on-site base station. The base station uses another Septentrio GPS receiver to obtain, format, and broadcast the GPS observables. The RTK position and velocity were used as a truth measurement. The truth measurement is used to determine the error in the estimated

position and velocity. The RTK position and velocity are not error free; however, they represent the best available method of determining position and velocity. The RTK position and velocity were also used as a measurement update to show how the filter performs in a situation where RTK corrections and good satellite geometry are available.

The Septentrio GPS receiver provides access to the raw GPS measurements (pseudo-range, carrier phase, received signal frequency, and carrier-to-noise ratio) for each GPS satellite from which a signal was received. These measurements were logged along with the RTK position, velocity and attitude providing various methods of updating the navigation filter. The RTK position and velocity can be used as a measurement update. The RTK position and velocity reflects the highest quality GPS measurements available. This filter is also capable of using the raw GPS measurements for a measurement update to the filter. Performance of positioning using the raw GPS measurements is similar to stand-alone GPS when using the full GPS satellite constellation. The main advantage of using the raw GPS measurements is the ability to continue measurement updates when the number of GPS satellite observations fall below four. The raw measurements are used to study the affects on the navigation filter when using less than four GPS observations. The Septentrio GPS receiver was set up to measure position, velocity, and attitude at 10 Hz, and the raw measurement were provided at 2 Hz.

The Septentrio GPS receiver is considered a high grade GPS receiver. The Septentrio and similar grade receivers are very expensive. The navigation filter presented is capable of working with any GPS receiver that provides access to the raw measurements; however, many receivers do not provide access to these measurements. The receivers that do provide the raw measurements are usually of a very high grade and very expensive. This price gap is starting to decrease as manufactures that mass produce GPS receivers realize the benefits of using the raw measurements to update the navigation filter.

## 2.4 Lane Positioning Methods

Two methods of lane positioning are presented in this section. The first is using a LiDAR scanner for lane positioning. Currently, LiDAR scanners are very expensive. The cost of LiDAR scanners has prevented implementation of LiDAR-based LDW systems on civilian vehicles; however, the cost of LiDAR scanners is expected to decrease as demand for these devices increases. The second method of lane positioning involves using a camera. Ideally, both cameras and LiDAR scanners will be used in future LDW systems. Each device has different strengths and weaknesses. Using both devices will improve the robustness of both the LDW system and navigation system aiding. Both of these sensors provides a measurement of the lateral position in the lane.

### 2.4.1 LiDAR

Light Detection and Ranging (LiDAR) measures the range to an object by pulsing a light wave at the object. The light wave for LiDAR applications is a laser. LiDAR is very similar to sonar, but instead of using a sound wave, LiDAR uses a light wave. LiDAR scanners combine the laser with a moving mirror that rotates the laser beam (Figure 2.6). The rotation of the beam provides ranging information in multiple directions, both vertically and horizontally. LiDAR also provides reflectivity measurements, a measurement known as echo width. Reflectivity data can be used to classify objects that the LiDAR encounters.

#### LiDAR Based Lane Positioning

A LiDAR scanner with reflectivity measurements can be used to search for lane markings. Painted lane markings are more reflective than the asphalt that surrounds the lane marking. Therefore, the echo width data from a LiDAR scanner can be used to find lane markings, and then the scan angle information from the LiDAR can be used to determine the vehicles lateral distance from the lane marking. Figure 2.7 shows sample reflectivity data

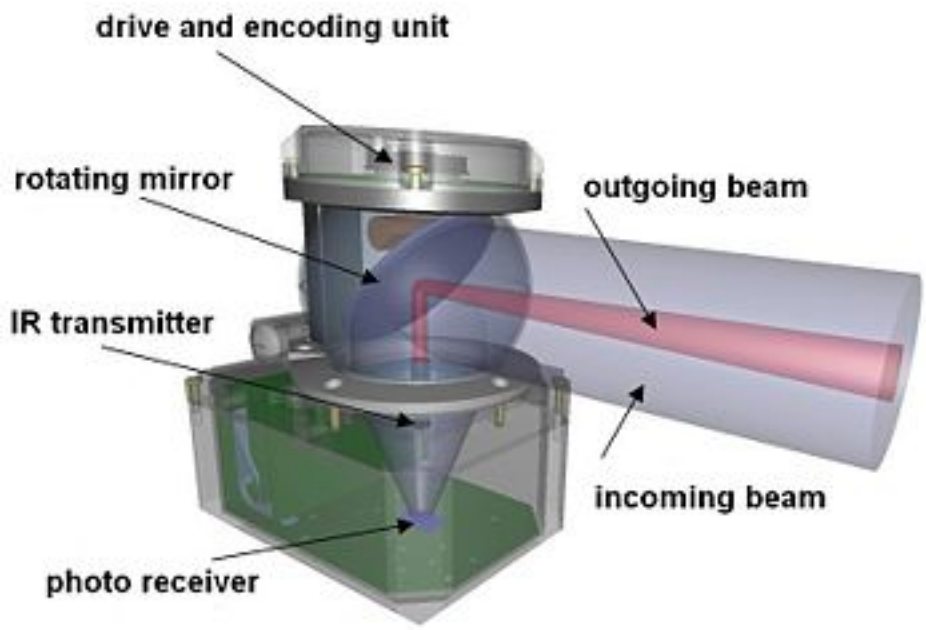


Figure 2.6: Laser Scanner

from a LiDAR scanner, and Figure 2.8 shows a picture taken from a camera aligned with the LiDAR scanner.

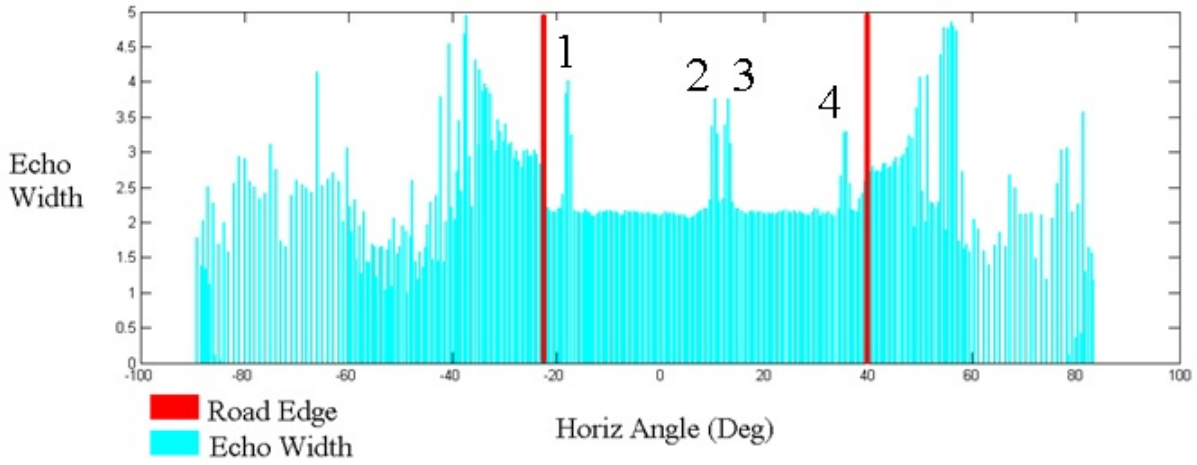


Figure 2.7: Average echo width for 100 scans [1]

The distinct spikes in the echo width are a result of the laser hitting a lane marking. At the start and end of the laser scan when the laser is not contacting the road, the echo width measurements become noisy resulting in spikes in the echo width that do not correspond

to a lane marking. Therefore, it is necessary to use search bounds on the echo width measurements. Testing has shown that the standard deviation of a LiDAR based lane position measurement under ideal circumstances is around .044 meters [1].


Figure 2.8: Corresponding echo width to lane markings [1]

One advantage of using a LiDAR scanner based LDW system is the robustness of LiDAR scanners to varying lighting and weather conditions. Currently, the largest disadvantage of LiDAR based LDW systems is the cost of the hardware. LiDAR is a relatively new technology, and there are a limited number of manufactures. Also, using LiDAR scanners to detect lane markings is a relatively new concept and not as well tested as camera based lane positioning.

**T**

he LiDAR scanner used for this research is an IBEO ALASCA XT. This LiDAR is a multi-scan automotive grade LiDAR with a ten hertz update rate.

### 2.4.2 Camera

#### Camera Based Positioning

Cameras are the most popular type of hardware used to determine lane position for LDW systems. Camera based LDW systems are available as an option on some production vehicles.

The first step of camera based lane positioning is lane line extraction. Line extraction involves searching the image for a lane marking. Thresholding is the process of filtering out unwanted features in the image. Thresholding extracts areas of the image that are white to yellow in color. Then, edge detection and the Hough transform are used to extract lines or edges in the image, as in Figure 2.9. Other camera-based lane detection systems employ optical flow, neural networks, and alternatives to the Hough transform such as peak and edge finding. The vehicles position in the lane can be estimated after the image is searched for lane markings. One simple method of estimating lateral lane position is counting the number of pixels from the center of the image to the lane marking. The number of pixels is multiplied by a scale factor to determine the distance from the center of the vehicle to the lane line. Testing has shown that standard deviation of a camera based lane position measurement under ideal circumstances is around 0.059 meters [2].

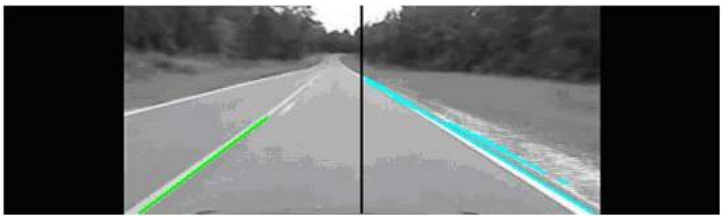

Figure 2.9: Lane lines extracted from the Hough transform [2]

One advantage of using a camera based LDW system is the cost of the hardware involved. Digital cameras have been in production for decades, and the cost of these devices is relatively cheap. Also, methods of lane positioning using a camera were pioneered in the 90s; therefore, the algorithms used for lane positioning using a camera are well established. Some disadvantages to camera based LDW systems include vulnerability to lighting and weather conditions. At dawn and dusk, when the sun is low in the sky, a camera may be saturated by the sun. Also, camera based lane detection can be difficult in rural environments where lane markings are in poor condition or urban environments where visibility of lane markings are blocked by surrounding traffic [2].

### Camera Hardware

The camera used for this work is a Logitech Quickcam Pro 9000. This camera is a standard low resolution web camera with a ten hertz update rate.

# Chapter 3

## Six Degree of Freedom Navigation Filter

This chapter describes the navigation filter used in this thesis. The chapter only covers the time update and the GPS measurement update. The inclusion of the lane map and vision measurements are presented in Chapter 4. There are two methods of using GPS measurements to update the filter. The first method is the loosely coupled measurement update. This method uses positions and velocities calculated by the GPS receiver to update the filter. The second method is the closely coupled measurement update. This method uses the GPS ranges and received signal frequency to each GPS satellite in order to update the navigation filter. Both type of measurement updates are covered in this chapter. The filter is set up to use loosely or closely coupled GPS measurement updates allowing the filter to use a loosely coupled measurement update as long as the receiver provides a solution. If the receiver is not able to provide a solution due to insignificant GPS satellite visibility, the navigation filter can switch over to the closely coupled GPS measurement update allowing the filter to be updated with the GPS observations available.

The navigation coordinate frame used is the earth centered earth fixed (ECEF) coordinate frame. The filter tracks the three-dimensional position and velocity of a vehicle in the ECEF coordinate frame. Measurements from an inertial measurement unit (IMU) are integrated to determine vehicle position and velocity states. Any error in the IMU measurements causes an increasing error in position and velocity estimates due to the integration. In order to eliminate this drift, measurement updates are used to update the states. The measurement updates correct the error in the position and velocity states due to integration of IMU errors. IMU measurements are also biased. Integrating biased IMU measurements

will result large error growth in estimated position and velocity. The filter estimates the biases in the IMU measurements to compensate for this effect.

In order to rotate the IMU measurements (given in the body coordinate frame) to the coordinate frame of the navigation filter (ECEF coordinate frame) the filter must estimate the attitude of the IMU with respect to the ECEF coordinate frame. The attitude is represented by the three Euler angles necessary to rotate between the vehicle body coordinate frame and the ECEF coordinate frame. The conventional roll, pitch, and yaw angles can be calculated using the Euler angles when the location of the vehicle is also known. More on coordinate frame rotations can be found in Appendix A. The ECEF coordinate frame is fixed to the center of the earth and rotates with the earth (denoted by sub/superscript e).

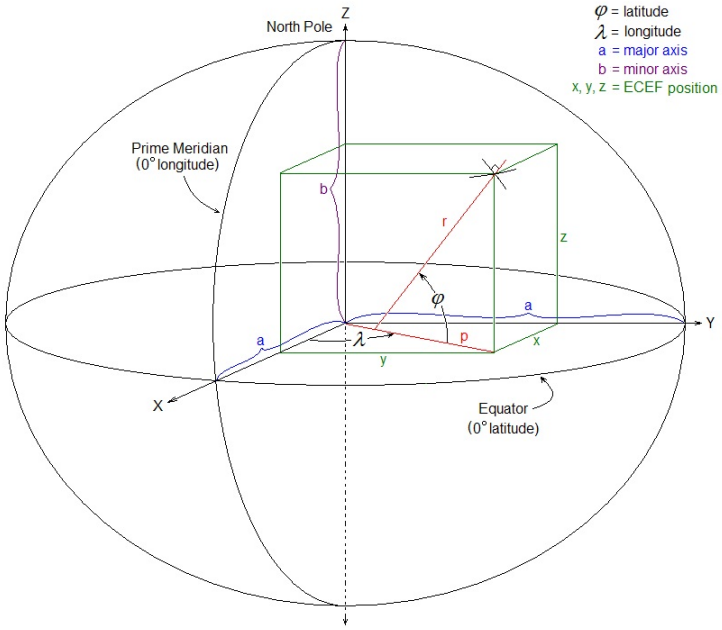


Figure 3.1: Earth Centered Earth Fixed Coordinate Frame

The vehicle body frame (denoted by sub/superscript b) used is the standard vehicle body coordinate frame in which the x axis points in the direction of travel, the y axis points out the passenger side and the z axis points down.

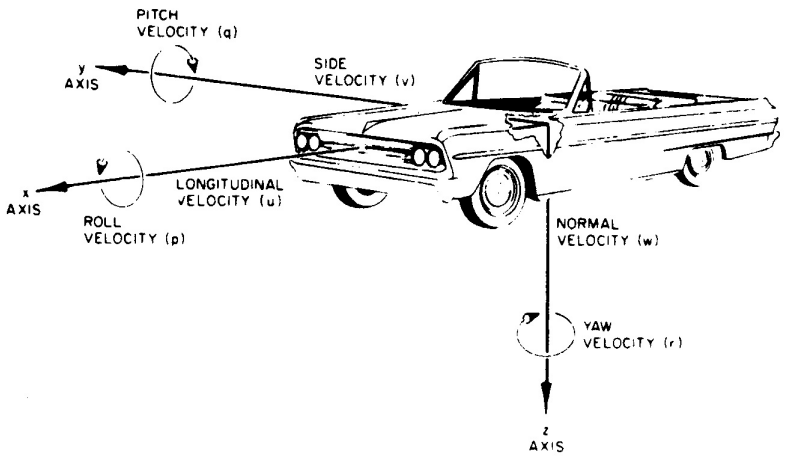


Figure 3.2: Vehicle Body Coordinate Frame [3]

### 3.1 States and State Equations

The following equation shows the state vector.

$$\vec{x} = \begin{bmatrix} \vec{r}_{eb}^{\,e} & \vec{v}^{\,e} & \vec{\psi}^{\,e} & \vec{b}_a^{\,b} & \vec{b}_g^{\,b} & \vec{dt}_{gps} \end{bmatrix}^T \tag{3.1}$$

The state vector contains estimates of the position, velocity, and attitude of the vehicle. The state vector also contains IMU bias and GPS receiver clock bias/drift. $\vec{r}_{eb}^{\,e}$ is a three state vector containing the estimated three-dimensional position of the vehicle in the ECEF coordinate frame (in meters). $\vec{v}^{\,e}$ is a three state vector containing the estimated three-dimensional velocity of the vehicle with respect to the ECEF coordinate frame (in meters per second). $\vec{\psi}^{\,e}$ is a three state vector containing the estimates for the three Euler angles (in radians) that describe the attitude of the vehicle. The attitude is expressed in terms of the three necessary rotations to rotate the ECEF coordinate frame to align with the body coordinate frame. $\vec{b}_a^{\,b}$ is a three state vector containing the estimated IMU accelerometer biases given in the IMU or body coordinate frame. $\vec{b}_g^{\,b}$ is a three state vector containing the estimated IMU gyro biases also given in the body coordinate frame. $\vec{dt}_{gps}$ is a two state vector containing clock bias and drift terms necessary to use GPS pseudorange and pseudorange rate measurements. The $\vec{dt}_{gps}$ is only necessary if these measurements are used; therefore,

the state vector can consist of 15-17 states depending on the type of GPS measurements currently being used.

Equations for the change in each state are necessary to perform the time update and propagate the states forward in time. These equations are given in Equation (3.2).

$$\dot{\vec{x}} = \begin{bmatrix} f_1(\vec{x},\vec{u},\vec{v}) \\ \vdots \\ f_n(\vec{x},\vec{u},\vec{v}) \end{bmatrix} = \begin{bmatrix} \vec{x}_{4:6} \\ C_b^e(\vec{u}_{1:3} - \vec{x}_{10:12} - \vec{v}_{1:3}) + \omega_e \begin{bmatrix} \omega_e\vec{x}_1 + 2\vec{x}_5 \\ \omega_e\vec{x}_2 - 2\vec{x}_4 \\ 0 \end{bmatrix} - GM(\vec{x}_1^2 + \vec{x}_2^2 + \vec{x}_3^2)^{-1.5}\vec{x}_{1:3} \\ C_{MECH}(\vec{u}_{4:6} - \vec{x}_{13:15} - \vec{v}_{4:6}) - \begin{bmatrix} 0 \\ 0 \\ \omega_e \end{bmatrix} \\ -\vec{v}_{7:12} \\ \vec{x}_{17} - \vec{v}_{13} \\ -\vec{v}_{14} \end{bmatrix} \tag{3.2}$$

The equations for the change in each state is a function of all the states ($\vec{x}$) and inputs ($\vec{u}$). The equations are determined by creating a kinematic model. The kinematic model describes the change in position, velocity, and attitude based off measurements of acceleration and rotation rates. IMU accelerations minus their biases are rotated into the ECEF coordinate frame using the rotation matrix $C_b^e$. The rotated unbiased accelerations are corrected and integrated to determine position and velocity. Change in attitude is determined by multiplying the gyro inputs by the IMU mechanization matrix ($C_{MECH}$).

The first three states are the position states. The change in the position states is equal to the velocity states ($\vec{x}_{4:6}$). The next three states are the velocity states. The change in velocity is equal to the acceleration. The acceleration is an input from the IMU; however, the accelerometers provide accelerations in the body coordinate frame. The acceleration

measurements are also biased. The accelerometer bias estimates ($\vec{x}_{10:12}$) are subtracted from the IMU measurements. The result is then rotated into the ECEF coordinate frame using the rotation matrix given in Equation (3.3).

$$C_b^{\ e} = \begin{bmatrix} c_8c_9 & s_7s_8c_9 - c_7s_9 & c_7s_8c_9 + s_7s_9 \\ c_8s_9 & s_7s_8s_9 + c_7c_9 & c_7s_8s_9 - s_7c_9 \\ -s_8 & s_7c_8 & c_7c_8 \end{bmatrix} \tag{3.3}$$

The rotation matrix is constructed using the attitude estimates ($\vec{x}_{7:9}$). $c_i$ is the cosine of the $i^{th}$ state and $s_i$ is the sine of the $i^{th}$ state. More on coordinate frame rotation and translation can be found in Appendix A.

Accelerometers also measure the specific force due to gravity along with centripetal acceleration and the Coriolis acceleration due to the rotation of the earth. The estimated values of the forces must be subtracted from the rotated unbiased accelerations. Equation (3.4) is used to estimate the specific force caused by gravity.

$$g = GM(\vec{x}_1^2 + \vec{x}_2^2 + \vec{x}_3^2)^{-1.5}\vec{x}_{1:3} \tag{3.4}$$

The equation splits the specific force into its vector components in the ECEF coordinate frame. The norm of this vector is equal to approximately 9.81 $m/s^2$. The vector is subtracted from the rotated unbiased IMU accelerations. GM is the standard gravitational parameter. The standard gravitational parameter for earth is $3.896004418 \times 10^{14}\ m^3/s^2$. Equation (3.5) shows the estimated specific force vector cause by centripetal acceleration and the Coriolis acceleration (in the ECEF coordinate frame) due to the rotation of the earth.

$$\begin{bmatrix} -\omega_e^2\vec{x}_1 - 2\omega_e\vec{x}_5 \\ -\omega_e^2\vec{x}_2 + 2\omega_e\vec{x}_4 \\ 0 \end{bmatrix} \tag{3.5}$$

The IMU will also measure centripetal acceleration and the Coriolis acceleration due to the rotation of the earth. Since the ECEF axis is attached to the earth, the axis is spinning at a rate of one revolution per day. $\omega_e$ is the rotation rate of the earth around the z axis of the ECEF coordinate frame. The value used for this work is $7.2921159 \times 10^{-5}$ rad/s. The rotation rate of the earth along with the current vehicle position and velocity are used to determine the centripetal and Coriolis accelerations due to the earth's rotation. These values are subtracted from the rotated unbiased IMU accelerations to correct for the fact that the ECEF coordinate frame is non inertial reference frame.

The change in attitude states is equal to the product of the IMU mechanization matrix (Equation (3.6)) and the unbiased gyro measurement vector.

$$C_{MECH} = \begin{bmatrix} 1 & \frac{s_7 s_8}{c_8} & \frac{c_7 s_8}{c_8} \\ 0 & c_7 & -s_7 \\ 0 & \frac{s_7}{c_8} & \frac{c_7}{c_8} \end{bmatrix} \tag{3.6}$$

The rotation rate of the earth ($\omega_e$) is present in the gyro measurements. The rotation rate of the earth can be subtracted out after the IMU mechanization matrix is multiplied by unbiased rotation rates. The change in the bias states is set to zero. The change in GPS receiver clock bias is equal to the receiver clock drift ($\vec{x}_{17}$). The change in the GPS receiver clock drift is set to zero.

Inputs to the system ($\vec{u}$) are measurements from an IMU. The first three inputs in the input vector ($\vec{u}_{1:3}$) are the accelerometers' measurements of acceleration ($m/s^2$) in the x, y, z (in that order) axis of the vehicle body coordinate frame. The fourth through sixth elements of the input vector ($\vec{u}_{4:6}$) are the gyro measurements of rotation rate (rad/s) around the x y z (in that order) axis of the vehicle body coordinate frame.

The process noise sources ($\vec{v}$) are included in Equation (3.2). These variables are present in the equations to show the noise sources in the system. They are not actually used when updating the states. The process noise sources are only used to determine the noise input

matrix ($B$) (Equation (3.10)). The first three noise sources ($\vec{v}_{1:3}$) are from the IMU accelerometers. The fourth through sixth elements of the noise source vector ($\vec{v}_{4:6}$) are from the gyro measurements. The seventh through twelfth elements of the noise source vector ($\vec{v}_{7:12}$) are artificial noise sources that are added in to allow for IMU bias estimation. These noise sources prevent the IMU bias estimation from falling asleep by ensuring a non-zero steady state gain in the Kalman filter gain matrix. Without the added noise sources, the estimated variance of the biases (contained in the state covariance matrix $P$) would not increase during time updates and cause the estimated variance to reach some steady state value after so many measurement updates. Once the estimated variance reaches a steady state value, the filter will not update the bias estimates. Since the biases in a IMU are know to drift over time, ideally, the estimated bias should be capable of changing over time to track the change in IMU bias. Adding artificial noise to the estimated biases will ensure that the estimated variance of the bias will also increase over time and allow the biases to change after measurement updates. The last two elements of the noise source vector ($\vec{v}_{13:14}$) are for the GPS receiver clock bias and drift. These values are only used when using GPS pseudorange and pseudorange rate measurements (closely coupled measurement structure).

## 3.2 Time Update

The measurements from the IMU can be used to propagate the states between GPS, camera, and LiDAR measurements. Equation (3.2) shows the state equations used to propagate the states. The IMU inputs ($\vec{u}$), current estimates, and state equations are used in conjunction with $4^{th}$ order Runge-Kutta integration to predict the value of the estimates at the next IMU input. The $\vec{v}$ is the noise source vector and is ignored when integrating the states. Once the states are propagated forward in time, the state covariance matrix must be updated to reflect the new variances/covariance of the state estimates.

Equation (3.7) is used to update the state covariance matrix at each time update.

$$P = A_D P A_D^T + (BQB^T)dt \tag{3.7}$$

The IMU measurements are received at a discrete time. Equation (3.7) represents a discrete update of the state covariance matrix. The state matrix ($A$) must be discretized in order to use this equation. The discretization period ($dt$) represents the change in time between the time updates. A time update is conducted at every IMU measurement; therefore $dt = 1/f_{IMU}$ where $f_{IMU}$ is the frequency of the IMU. The IMU used for this work had a 100Hz update rate so $dt = .01$. The noise input section of the equation ($BQB^T$) can be roughly discretized by multiplying each element of the product of $BQB^T$ by $dt$.

The state matrix ($A$) is a Jacobian matrix. The state matrix is obtained by taking the partial derivative of each change in state equation (Equation (3.2)) with respect to each state (Equation (3.1)) evaluated at the current estimate.

$$a_{i,j} = \frac{\delta f_i(\vec{x}, \vec{u}, \vec{v})}{\delta \vec{x}_j} \tag{3.8}$$

The discrete version of the $A$ matrix can be obtained using Equation (3.9).

$$A_D = e^{(A)dt} \tag{3.9}$$

Using Equation (3.9) requires solving a matrix exponential at every time update. Another method of determining $A_d$ is to discretize all of the state equations in Equation (3.2) and repeat Equation (3.8) using the discretized equations. This method would prevent the filter from solving a matrix exponential at every time update which greatly reduces the processing requirements.

The process noise input matrix is also a Jacobian matrix. Each element of the processes noise input matrix is obtained by taking the partial derivative of each change in state equations (Equation (3.2)) with respect to each noise source ($\vec{v}$) evaluated at the current estimate.

$$b_{i,j} = \frac{\delta f_i(\vec{x}, \vec{u}, \vec{v})}{\delta \vec{v}_j} \tag{3.10}$$

$Q$ is the process noise covariance matrix. The process noise covariance matrix is a diagonal matrix since the noise sources are assumed to be uncorrelated. The size of the process noise covariance is defined by the number of noise sources (12-14 depending on GPS measurement type). The diagonal elements of the process noise covariance matrix correspond to the variances of each process noise source. In order to be optimally tuned, the value of the $i^{th}$ diagonal element of the process noise covariance should be set equal to the true variance of the $i^{th}$ noise source in the process noise source vector ($\vec{v}$). The values for the variances of the accelerometer and gyro noise sources were estimated using static IMU data. The seventh through twelfth noise sources were added to allow for bias estimation. The values for the variance of these noise sources is used to tune the dynamics of the bias estimation. The last two noise sources are only present when GPS pseudorange and pseudorange rate measurements are being used. The values of the process noise covariance that correspond to these noise sources are used to tune the dynamics of the GPS clock errors estimates. Table 3.1 gives the values used for the diagonal elements of the process noise covariance matrix.

Table 3.1: Diagonal Elements of the Process Noise Covariance Matrix

| i | Noise Source | $Q_{i,i}$ | Units |
|---|---|---|---|
| 1 | X Accelerometer | .00049765 | $m^2$ |
| 2 | Y Accelerometer | .00049765 | $m^2$ |
| 3 | Z Accelerometer | .00049765 | $m^2$ |
| 4 | X Gyro | .0000054925 | $(m/s)^2$ |
| 5 | Y Gyro | .0000054925 | $(m/s)^2$ |
| 6 | Z Gyro | .0000054925 | $(m/s)^2$ |
| 7 | X Accelerometer Bias | .0001 | $(m/s^2)^2$ |
| 8 | Y Accelerometer Bias | .0001 | $(m/s^2)^2$ |
| 9 | Z Accelerometer Bias | .0001 | $(m/s^2)^2$ |
| 10 | X Gyro Bias | .0000001 | $(rad/s)^2$ |
| 11 | Y Gyro Bias | .0000001 | $(rad/s)^2$ |
| 12 | Z Gyro Bias | .0000001 | $(rad/s)^2$ |
| 13 | Clock Bias | .001 | $m^2$ |
| 14 | Clock Drift | .01 | $(m/s)^2$ |

## 3.3 Measurement Update

A measurement update is conducted whenever a measurement of the states becomes available. With no measurement updates, the states would have constantly increasing error due to integration of the IMU error and biases. The measurement update uses measurements of the states to determine how the state estimates and state covariance matrix should be changed to account for the new measurement.

The extended Kalman filter measurement update is capable of using measurements that are non-linear with respect to states of the filter. In the extended Kalman filter, the Kalman gain is multiplied by the residual vector to determine the correction to the state estimates. The residual vector (Equation (3.11)) is a vector that represents the difference between the measurements vector ($\vec{y}$) and the estimated values of the measurement vector using the current states ($\hat{\vec{y}}$).

$$\vec{z} = \vec{y} - \hat{\vec{y}} \tag{3.11}$$

$\vec{y}$ is the measurement vector. The measurement vector is $m \times 1$ vector of measurements where $m$ is the number of measurements. $\hat{\vec{y}}$ is the estimated measurement vector. the measurement vector is a $m \times 1$ vector of estimated values of the measurements using the current states. Subtracting the estimated measurement vector from the measurement vector results in the residual vector ($\vec{z}$).

The estimated measurement vector is created by substituting the states into the measurement equations ($f_i(\vec{x})$).

$$\hat{\vec{y}} = \begin{bmatrix} f_1(\vec{x}) \\ \vdots \\ f_m(\vec{x}) \end{bmatrix} \tag{3.12}$$

The measurement equations are equations that are a function of the states and represents a mathematical description of the measurement. The measurement equations are used to predict the value measurement using the states of the filter. The equations are also used to construct the observation matrix ($H$).

$K$ is the Kalman gain matrix. Equation (3.13) is used to compute the Kalman gain.

$$K = PH^T(HPH^T + R)^{-1} \tag{3.13}$$

The Kalman gain equation is a function of the current state noise covariance matrix ($P$), the observation matrix ($H$), and the measurement noise covariance matrix ($R$). $H$ is the measurement model. It is a $m \times n$ Jacobian matrix where $m$ is the number of measurements and $n$ is the number of states. Equation (3.14) is used to calculate each element of the observation matrix.

$$h_{i,j} = \frac{\delta f_i(\vec{x})}{\delta \vec{x}_j} \tag{3.14}$$

$R$ is the measurement noise covariance matrix. $R$ is a diagonal matrix (assuming no cross correlation) that is $m \times m$ where $m$ is the number of measurements. The diagonal element $r_{i,i}$ is set to the variance of the $i^{th}$ measurement in the measurement matrix.

$$r_{i,i} = \sigma^2_{\vec{y}_i}; \tag{3.15}$$

The the Kalman gain matrix determines how much to change the states based on the variance ($R$) of the current measurements and the current state noise covariance matrix ($P$). Therefore, $R$ acts as a weighting matrix that governs how much the states should be changed by the current set of measurements. Setting the diagonal values of the measurement noise covariance matrix to true variances of the current measurements will result in optimal performance of the extended Kalman filter.

The Kalman gain along with the observation model ($H$) and measurement residual vector ($\vec{z}$) are used to update the states and state noise covariance matrix. Equation (3.16) is used to update the state vector.

$$\vec{x} = \vec{x} + K\vec{z} \tag{3.16}$$

Equation (3.17) is used to update the state noise covariance matrix.

$$P = (I_{nxn} - KH)P \tag{3.17}$$

### 3.3.1 Loosely Coupled GPS Measurement Update

The loosely coupled GPS measurement update uses position and velocity values provided by the GPS receiver to update the navigation filter. The GPS receiver used provides estimated position and velocity in the ECEF coordinate frame. The measurement provided is a direct measurement of the first six states since the first six states of the filter are position and velocity in the ECEF coordinate frame. The receiver also provides estimated variance and covariance of both the position and velocity measurements.

Equation (3.18) shows the measurement vector for the loosely coupled GPS measurement update. The GPS position and velocity measurements are placed in this vector

$$\vec{y} = \begin{bmatrix} \vec{r}^{\,e}_{eb} \\ \vec{v}^{\,e} \end{bmatrix} \tag{3.18}$$

Equation (3.19) shows the measurement equations for the loosely coupled GPS measurement. The loosely coupled GPS measurement provides a direct measurement of the first six states of the filter.

$$\hat{\vec{y}} = \vec{x}_{1:6} \tag{3.19}$$

Equation (3.20) shows the $H$ matrix for the loosely coupled GPS measurement. Since the measurements are direct measurements of the first six states, the $H$ matrix is constructed with an $6 \times 6$ identity matrix and a $6 \times 9$ matrix of zeros.

$$H = \begin{bmatrix} I_{6\times6} & 0_{6\times9} \end{bmatrix} \tag{3.20}$$

The diagonal values of the measurement noise covariance matrix ($R$) are set using the measurement variances provided by the GPS receiver.

$$R = \begin{bmatrix} \sigma_x^2 & 0 & 0 & 0 & 0 & 0 \\ 0 & \sigma_y^2 & 0 & 0 & 0 & 0 \\ 0 & 0 & \sigma_z^2 & 0 & 0 & 0 \\ 0 & 0 & 0 & \sigma_{vx}^2 & 0 & 0 \\ 0 & 0 & 0 & 0 & \sigma_{vy}^2 & 0 \\ 0 & 0 & 0 & 0 & 0 & \sigma_{vz}^2 \end{bmatrix} \tag{3.21}$$

If the GPS receiver gives the full position and velocity covariance matrices, then they can be added into the measurement noise covariance matrix,

$$R = \begin{bmatrix} R_{position} & 0_{3x3} \\ 0_{3x3} & R_{velocity} \end{bmatrix} \tag{3.22}$$

where $R_{position}$ is the position measurement covariance matrix and $R_{velocity}$ is the velocity measurement covariance matrix.

### 3.3.2 Closely Coupled GPS Measurement Update

The closely couple GPS measurement update is a measurement update using the pseudorange and received signal frequency to all satellites in view of the receiver. The pseudorange is an estimated range to a GPS satellite. It is called a pseudorange (not a range) because the measured range to a satellite contains a bias due to the clock error of the receiver. The

clock error is the difference in time between the receiver clock estimated time and the GPS system time. This bias is constant on all ranges; therefore, it can be estimated given enough pseudorange measurements. The estimated range rate using the received signal frequency also contains an error due to receiver clock drift, thus the estimated range rate is called pseudorange rate.

When using closely coupled GPS measurements, two extra states must be added to the state vector. The extra states are the clock bias and clock drift. The clock bias is the range bias (in meters) caused by the difference in the receiver clock and the GPS system clock. The clock drift is the range rate bias (in meters per second) caused by the change in receiver clock and the GPS system clock. Since these two biases are observed on all the observations, they can be estimated. However, since these values must be estimated, it takes four GPS satellites instead of just three to calculate three-dimensional position and velocity.

In order to use pseudorange and pseudorange rate measurements, the position and velocity the satellites from which observations where made must be known. The satellite position and velocity can be computed using the ephemeris data provided by the satellites. The ephemeris parameters are constant for a several hours after first being broadcast. Therefore, the ephemeris only needs to be obtained on startup and when a new ephemeris has been issued. The satellite position and velocity for a particular observation are solved using the GPS time of the observation and ephemeris values. The ephemeris also contains a satellite clock correction term that must be multiplied by the speed of light and added to the measured pseudorange to account for errors in that particular satellite clock. More on how the GPS ephemeris is obtained and how these values can be used to calculate satellite position, velocity, and clock correction can be found in [7].

Equation (3.23) shows the measurement vector for a measurement from one GPS satellite.

$$\vec{y} = \begin{bmatrix} \rho_m + c(dt_{sv}) \\ c\frac{f_m}{L_1} \end{bmatrix} \tag{3.23}$$

The values in the measurement matrix are pseudorange and pseudorange rate. The GPS receiver provides an estimated pseudorange (with a satellite clock error) and received signal frequency to all the satellite signals received by the GPS receiver. The pseudorange must be corrected for the satellite clock error. The pseudorange rate can be calculated using the received signal frequency measurement.

The pseudorange must be corrected for the satellite clock errors. The satellite clock error should not be confused with the receiver clock error. The satellite clock error is the error between the satellite clock and GPS system time. Like the satellite position and velocity, the satellite clock correction can be calculated as a function of time using the ephemeris values. The satellite clock correction is multiplied by the speed of light (meters/second) to determine the range correction (meter).

A range rate or closure speed can be calculated using the received signal frequency ($f_m$). The Doppler effect states that dividing the received signal frequency by the frequency of the signal at transmission ($L_1$) and then multiplying by the speed at which the signal travels (speed of light) results in an estimated range rate. The frequency of the $L_1$ GPS signal is 1.57542 GHz. Only GPS measurements from the $L_1$ signal were used for this work; however, if using measurements from the $L_2$ signal, the received signal frequency must be divided by the $L_2$ signal frequency (1.2276 GHz).

Equation (3.24) shows the measurement equations used to obtain the measurement prediction ($\hat{\vec{y}}$).

$$\hat{\vec{y}} = \begin{bmatrix} \hat{r} + \vec{x}_{16} \\ \hat{\dot{r}} + \vec{x}_{17} \end{bmatrix} \tag{3.24}$$

The pseudorange measurement is equal to the estimated range ($\hat{r}$) plus the receiver clock bias ($\vec{x}_{16}$). The receiver clock bias is the sixteenth state when using GPS pseudorange and pseudorange rate measurements. The clock bias is estimated in meters and represents the error (in meters) caused by the difference in the vehicle GPS receiver clock and the GPS system time. The clock bias state can be divided by the speed of light to determine the actual clock difference in seconds. The estimated pseudorange rate measurement is equal to the estimated range rate ($\hat{\dot{r}}$) plus the receiver clock drift ($\vec{x}_{17}$). The receiver clock drift is the seventeenth state of the filter when using GPS pseudorange and pseudorange rate measurements. The clock drift estimate is estimated in meters per second and represents the rate of change of the receiver clock bias.

Equation (3.25) shows how to estimate the range to a satellite.

$$\hat{r} = \sqrt{(x_{sv} - \vec{x}_1)^2 + (y_{sv} - \vec{x}_2)^2 + (z_{sv} - \vec{x}_3)^2} \tag{3.25}$$

The equation is simply the distance formula and is a function of the position states ($\vec{x}_{1:3}$) and the position of the satellite ($[x_{sv}\ y_{sv}\ z_{sv}]$). The position of the satellite is calculated using the GPS time of the measurement and the ephemeris data for the satellite.

Equation (3.26) shows how to estimate the range rate to a satellite.

$$\hat{\dot{r}} = \vec{e} \begin{bmatrix} (\dot{x}_{sv} - \vec{x}_4) \\ (\dot{y}_{sv} - \vec{x}_5) \\ (\dot{z}_{sv} - \vec{x}_6) \end{bmatrix} \tag{3.26}$$

The equation is a function of the velocity states ($\vec{x}_{4:6}$) and the velocity of the satellite($[\dot{x}_{sv}\ \dot{y}_{sv}\ \dot{z}_{sv}]$). The velocity of the satellite relative to the earth is calculated using the GPS time of the measurement and the ephemeris data for the satellite. The range rate equation is also a function of the unit vector that points from the satellite to the GPS antenna ($\vec{e}$). The difference in the three dimensional vehicle velocity and satellite velocity is rotated into the one dimensional axis that points from the satellite to the GPS antenna.

The unit vector that points from the satellite to the vehicle ($\vec{e}$) can be calculated using the state position estimates ($\vec{x}_{1:3}$) and the satellites position ($[x_{sv}\ y_{sv}\ z_{sv}]$). Equation (3.27) shows how to calculate the unit vector that points from the satellite to the vehicle.

$$\vec{e} = \begin{bmatrix} (\vec{x}_1 - x_{sv})/\hat{r} & (\vec{x}_2 - y_{sv})/\hat{r} & (\vec{x}_3 - z_{sv})/\hat{r} \end{bmatrix} \tag{3.27}$$

Taking the partial derivative of the pseudorange measurement equation with respect to each position states results in a unit vector that points from the satellite to the vehicle. Similarly taking the partial derivative of the pseudorange rate measurement equation with respect to the velocity states results in a unit vector that points from the satellite to the vehicle. Thus, the unit vector is placed in the observation matrix ($H$) as shown in Equation (3.28). The size of the observation matrix for each GPS observation is $2 \times 17$. All the pseudorange and pseudorange rate measurements can be processed at the same time by stacking the $H$ matrix show below.

$$H = \begin{bmatrix} \vec{e} & 0_{1x3} & 0_{2x9} & I_{2x2} \\ 0_{1x3} & \vec{e} & & \end{bmatrix} \tag{3.28}$$

Equation (3.29) shows the observation matrix for a closely coupled GPS measurement update with four satellite observations.

$$H = \left[\begin{array}{cccc} \vec{e_1} & 0_{1x3} & 0_{2x9} & I_{2x2} \\ 0_{1x3} & \vec{e_1} & & \\ \hline \vec{e_2} & 0_{1x3} & 0_{2x9} & I_{2x2} \\ 0_{1x3} & \vec{e_2} & & \\ \hline \vec{e_3} & 0_{1x3} & 0_{2x9} & I_{2x2} \\ 0_{1x3} & \vec{e_3} & & \\ \hline \vec{e_4} & 0_{1x3} & 0_{2x9} & I_{2x2} \\ 0_{1x3} & \vec{e_4} & & \end{array}\right] \tag{3.29}$$

$\vec{e_i}$ is the unit vector that points from the $i^{th}$ satellite to the vehicle. Each observation is represented by two rows in the H matrix. The first row represents a pseudorange measurement, and the second row represents a pseudorange rate measurement. Four independent satellite observations are needed for the navigation filter to be fully observable. If more than four observations are available, the $H$ matrix can be modified by adding two rows for each additional observation. If less than four observations are available, then the navigation filter will not be fully observable; however, a measurement update can take place using the available observations. The size of $H$ will be $2m \times n$ where $m$ is the number of satellites observed and $n$ is the number of states.

Equation (3.30) is used to estimate the standard deviation of a GPS pseudorange measurement based off the carrier to noise ratio ($C/N_0$) of the received GPS signal [9].

$$\sigma_\rho = K_\rho + \lambda_c \sqrt{\frac{4d^2 B_n}{C/N_0}\left(2(1-d) + \frac{4d}{T_s C/N_0}\right)} \tag{3.30}$$

The estimated standard deviation of the pseudorange is squared and placed into the diagonal element of the measurement noise covariance that corresponds to the pseudorange measurement. The $K_\rho$ term is the unmodeled error term and represents all nonreceiver based error such as multipath and atmospheric delays. The remaining terms in Equation (3.30) represents the estimated error in the delay lock loop used to track the satellite.

Equation (3.31) is used to estimate the standard deviation of a GPS pseudorange rate measurement based on the carrier to noise ratio ($C/N_0$) of the received GPS signal [9].

$$\sigma_{\dot{\rho}} = \frac{f_e}{3} + \frac{\lambda}{2\pi T_s}\sqrt{\frac{4B_n}{C/N_0}\left(1 + \frac{1}{T_s C/N_0}\right)} \tag{3.31}$$

The estimated standard deviation of the pseudorange rate is squared and placed into the diagonal element of the measurement noise covariance that corresponds to the pseudorange rate measurement. The $f_e$ term is the dynamic stress factor. The dynamic stress factor is dependent on the tracking loop bandwidth and order. The remaining terms Equation (3.30)

represents the estimated error in the frequency lock loop. Table 3.2 shows the values used for Equations (3.30) and (3.31).

Table 3.2: Tracking Loop Parameters

| Parameter | Value | Units |
|---|---|---|
| $B_n$, code loop noise bandwidth | 2 | Hz |
| $d$, correlator spacing | 0.5 | Chips |
| $f_e$, dynamic stress error | 3 | m/s |
| $K_\rho$, unmodeled range error | 5 | m |
| $\lambda$, carrier wavelength | 0.1902 | m |
| $\lambda_c$, code chip width | 293.5 | m |
| $T_s$, predetection integration time | 0.005 | s |

The estimated pseudorange and pseudorange rate standard deviations are squared and placed into measurement covariance matrix $R$ as shown below.

$$R = \begin{bmatrix} \sigma^2_{\rho,1} & 0 & 0 & 0 & 0 \\ 0 & \sigma^2_{\dot{\rho},1} & 0 & 0 & 0 \\ \vdots & \vdots & \ddots & \vdots & \vdots \\ 0 & 0 & 0 & \sigma^2_{\rho,m} & 0 \\ 0 & 0 & 0 & 0 & \sigma^2_{\dot{\rho},m} \end{bmatrix} \tag{3.32}$$

The measurement covariance matrix is a $2m \times 2m$ diagonal matrix where $m$ is the number of satellite observations. $R$ is a diagonal matrix because the noise sources are assumed to be non-correlated. This assumption is valid because the measurements are originating from different satellites; therefore, the error in one pseudorange/pseudorange rate measurement has no correlation with the error in other observations.

## 3.4 Conclusions

This chapter has presented the structure of the navigation filter used for this thesis. The navigation filter tracks the pose (position, velocity, and attitude) of the vehicle along with the three IMU accelerometer biases and the three IMU gyro biases. The filter also

estimates the receiver clock bias and drift if necessary. The navigation filter is split into time updates and measurement updates. Time updates are conducted at every IMU measurement. The IMU measurements are used to propagate the states (along with the state covariance matrix) forward in time. The measurement update is conducted whenever a measurement of the states is available. GPS measurements are used to update the states (and state covariance matrix). The GPS measurements can either be loosely or closely coupled. The loosely coupled measurement is a measurement of position and velocity provided by the GPS receiver. The closely coupled measurement is a measurement pseudorange and received signal frequency from each visible GPS satellite. The filter is constructed to work with either measurement type. The filter can use loosely coupled GPS measurement until the number of visible satellite falls below four. When the number of GPS observation falls below four, the GPS receiver can no longer compute a position or velocity; however, the navigation filter can then switch over to closely coupled GPS measurements. The closely coupled measurement allows from some additional measurements when the GPS receiver can not compute a solution. The closely coupled measurement structure is also advantages because the noise sources with the pseudorange and received signal frequency measurements are uncorrelated between GPS observations. The assumption that the measurement noise covariance matrix $R$ is diagonal is more correct for the closely coupled measurement update. Equation (3.22) provides a method of constructing the $R$ matrix for the loosely coupled measurement update that reflects the cross covariances between the position and velocity measurements (provided the receiver provides the cross covariance terms of the estimated position and velocity).

# Chapter 4

## Vision Measurement and Vehicle Constraint Updates Using a Map

The vision measurements, either from the LiDAR[1] or camera[2], give an estimated lateral position in the current lane. The road coordinate frame is the coordinate frame in which the vision measurements are given. The road coordinate frame can be approximated using a waypoint map. For this work, each lane is assumed to have its own associated lane map. The waypoints lie in the center of the mapped lane, where the distance between waypoints is defined by the road geometry. Complex road geometry will require waypoints to be close together. For example, in a turn, the waypoints will need to be close enough to capture the geometry of the road. On a straightaway, the waypoints can be very spread out due to the lack of change in road geometry.

The road coordinate frame is a three dimension coordinate frame and is denoted by the sub/superscript $r$. The x-axis of the road coordinate frame points from the last waypoint passed to the next waypoint. The y-axis of the road coordinate frame is perpendicular to the x-axis. If facing the direction of travel, the y-axis points to the right. The road coordinate frame is assumed to have no bank; therefore, the y-axis is always parallel with the plane tangent to reference ellipsoid. The z-axis is perpendicular to the x-y plane and points down. This type of coordinate frame was chosen because the vision measurements give a direct measurement of the y-axis position. Also, since this work is for ground vehicles, the position in the z-axis of the road coordinate frame is fixed, can be measured once, and added in as a measurement update. The change in vertical height on any point on the vehicle is a function of the roll angle of the vehicle and the height of the point above the roll axis; however, this angle and height above the roll axis is small for normal operating conditions. Figure 4.1 shows a visual representation of the road coordinate frame.

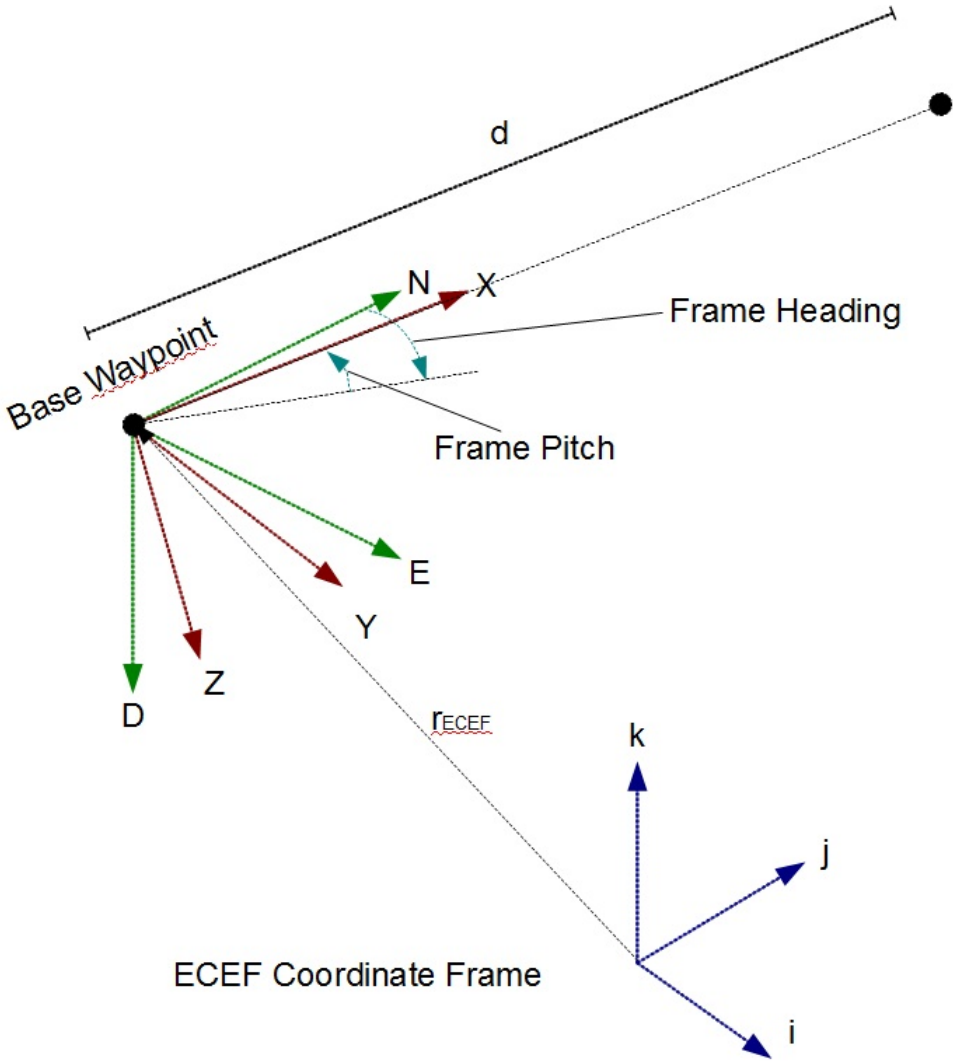


Figure 4.1: Road Coordinate Frame

In order to use measurements given in the road coordinate frame, the estimated position in the navigation (ECEF) coordinate frame must be mapped into the road coordinate frame. Equation (4.1) is used to map position from the navigation coordinate frame to the road coordinate frame.

$$\vec{r}^{\,r}_{rb} = C_e^{\,r}\,[\vec{r}^{\,e}_{eb} - \vec{r}^{\,e}_{er}] \tag{4.1}$$

$\vec{r}^{\,e}_{eb}$ is the estimated position vector in the navigation coordinate frame and $\vec{r}^{\,r}_{rb}$ is the estimated position vector in the road coordinate frame. In order to use this equation, the position of the origin of the road coordinate frame must be known ($\vec{r}^{\,e}_{er}$). The position of the origin of the road coordinate frame is the last waypoint the vehicle passed in the waypoint map. The rotation matrix from the navigation coordinate frame to the road coordinate frame ($C_e^{\,r}$) must also be known. In order to construct this rotation matrix, the attitude of the road coordinate frame with respect to the navigation coordinate frame must be known and is represented by three Euler angles. More information of how rotation matrix and set up and used can be found in Appendix A.

## 4.1 Waypoint Based Lane Map

The information needed to use the lane map is the position of each waypoint in the ECEF coordinate frame, the three Euler angles necessary to rotate the ECEF coordinate frame to the road coordinate frame for each waypoint, and the distance to the next waypoint for each waypoint. Therefore, the map database takes the form:

$$Map\ Database = \begin{bmatrix} \vec{r}^{\,e}_{er,1} & \vec{\gamma}_1 & d_{r,1} \\ \vdots & \vdots & \vdots \\ \vec{r}^{\,e}_{er,m} & \vec{\gamma}_m & d_{r,m} \end{bmatrix} \tag{4.2}$$

where $\vec{r}^{\,e}_{er,i}$ is the position vector of waypoint $i$ in the ECEF coordinate frame, and $\vec{\gamma}_i$ is the attitude vector of the road coordinate frame. Like the attitude states of the vehicle, the attitude of the road coordinate frame is represented with three Euler angles. $d_{r,i}$ is the distance from waypoint $i$ to waypoint $i+1$. This value is used to check if the vehicle has passed the next waypoint in order to keep up with the vehicles location along the map.

The form of the rotation matrix from the ECEF coordinate frame to the road coordinate frame is given in Equation (4.3).

$$C_e^{\,r} = \begin{bmatrix} c_2c_3 & c_2s_3 & -s_2 \\ s_1s_2c_3 - c_1s_3 & s_1s_2s_3 + c_1c_3 & s_1c_2 \\ c_1s_2c_3 + s_1s_3 & c_1s_2s_3 - s_1c_3 & c_1c_2 \end{bmatrix} \tag{4.3}$$

The elements from the road coordinate frame attitude ($\vec{\gamma}_i$) are used to construct the rotation matrix. The rotation matrix from ECEF to the road coordinate frame and the position of the road coordinate frame (position of the last waypoint passed) can be substituted into Equation (4.1) to solve for estimated position in the road coordinate frame, where $c_1$ is the cosine of the first attitude angle in the attitude vector and $s_1$ is the sine of the first attitude angel in the attitude vector. Similarly, $c_2$ and $s_2$ are the trigonometric functions of the second angle, and $c_3$ and $s_3$ are the trigonometric functions of the third angle.

The next three sections discuss how to obtain the information needed for the waypoint map. Section 4.1.1 shows how to obtain the waypoint positions ($\vec{r}^{\,e}_{er,i}$). Section 4.1.2 covers how to obtain the three Euler angles need to describe the attitude of the road coordinate frame ($\vec{\gamma}_i$). Section 4.1.3 shows how to obtain the distance between waypoints ($d_{r,i}$).

### 4.1.1 Determining Waypoint Position

#### Saving a Road Survey

Differential GPS provides a very accurate baseline between the base station antenna and the receiver antenna; however, global position and the accuracy of the global position are based off the base station antenna position and the accuracy to which the base station antenna is known. For example, if the track is surveyed with differentially corrected GPS with corrections provided by a different base station than the one that will be used by GPS used to determine lane position, then a bias will be present in the lane position estimate. This bias will be a function of the errors in the base station global position. Therefore, if both base stations are perfectly know, this bias will not be present; however, any error in either of the base stations position will result in a bias lane estimation. Surveying a specific

location that can be found and surveyed at a later date will ensure that any global error in the survey base station is eliminated. Surveying this location also provides a method of using the lane survey in conjunction with a base station that is not precisely known in order to determine lane position. This map-marker can be used to determine the amount the map must be shifted to work with the different base station. The map-marker should be in a location with a good visibility of the sky, and it should be marked with something that can be easily found at a later date. The map-marker ensure that the map can be used with any base station instead of just the base station used for the survey.


Figure 4.2: Waypoint Baselines

Surveying the road with differential GPS will ensure the waypoints of the lane map are very accurate with respect to the map-marker location. An accurate position vector between waypoints and the marker location can be solved by subtracting the global position of the marker location from the global positions of each lane map waypoint (represented by the

red lines in Figure 4.2). These vectors can be saved as the actual map survey. Saving the base-line vectors eliminates any global component to the survey.

#### Setting Up a GPS Base Station

When a base station is set up to broadcast corrections used to determine lane position, the position vectors in the map survey can be added to the global solution computed at the map-marker using corrections from the new base station (represented by the blue line in Figure 4.2). The NCAT test track was surveyed using a survey GPS system providing accuracy on the centimeter level. The test track also has a GPS base station that provides RTK (Real Time Kinematic) corrections. The survey of the track was conducted using GPS corrections provided by a different base station than the corrections used by the onboard/rover GPS receiver. For this reason, the map had to be aligned to the different base stations. The shift in the map (global position of map) can determined by surveying the map marker position using the same corrections used by the rover GPS receiver.

#### Effects of Map Accuracy

In order to ensure that RTK differential GPS alone can provide lane level position, the lane map must be very accurate. Any inaccuracies in the lane map will result in a bias lane position. If vision measurements are available, the filter will still produce a non biased lane position; however, if vision measurements become unavailable, the navigation filter will report a biased lane position. If the lane map is not accurate to the centimeter level, then any benefit from using RTK differential GPS is lost. An inaccurate lane map will cause differential GPS measurements to resemble standalone GPS measurements when compared to the lane map.

### 4.1.2 Determining Euler Angles Between Global Axis and Road

The rotation matrix from the ECEF coordinate frame to the road coordinate frame:

$$C_e^{\ r} = \begin{bmatrix} c_2c_3 & c_2s_3 & -s_2 \\ s_1s_2c_3 - c_1s_3 & s_1s_2s_3 + c_1c_3 & s_1c_2 \\ c_1s_2c_3 + s_1s_3 & c_1s_2s_3 - s_1c_3 & c_1c_2 \end{bmatrix} \tag{4.4}$$

can be thought of as a sequence of two rotations (Equation (4.5)).

$$C_e^{\ r} = C_n^{\ r} C_e^{\ n} \tag{4.5}$$

The first rotation is from the ECEF coordinate frame to the North, East, Down (NED) coordinate frame ($C_e^{\ n}$). This rotation matrix is based off two angles. $\phi_i$ is the latitude of the $i^{th}$ coordinate frame, and $\lambda_i$ is the longitude of the $i^{th}$ coordinate frame. The origin of the NED coordinate frame is at the $i^{th}$ waypoint ($\vec{r}^{\ e}_{er,i}$). The second rotation is from the NED coordinate frame to the road coordinate frame ($C_n^{\ r}$). This rotation matrix is also based off two angles; $\psi_i$ is the heading of the $i^{th}$ coordinate frame, and $\theta_i$ is the pitch of the $i^{th}$ coordinate frame.

$C_e^{\ n}$ maps coordinates in the ECEF coordinate frame to the NED coordinate frame. The longitude and latitude of the $i^{th}$ road coordinate frame correspond to the global position of the $i^{th}$ waypoint. The latitude and longitude can either be surveyed, or solved for using the position of the $i^{th}$ waypoint. Equation (4.6) show the rotation matrix from ECEF coordinate frame to the NED coordinate frame.

$$C_e^{\ n} = \begin{bmatrix} -\sin(\phi_i)\cos(\lambda_i) & -\sin(\phi_i)\sin(\lambda_i) & \cos(\phi_i) \\ -\sin(\lambda_i) & \cos(\lambda_i) & 0 \\ -\cos(\phi_i)\cos(\lambda_i) & -\cos(\phi_i)\sin(\lambda_i) & -\sin(\phi_i) \end{bmatrix} \tag{4.6}$$

$C_n^{\ r}$ maps coordinates in the NED coordinate frame to the road coordinate frame. The pitch and heading angles can be solved by looking at the change in position between waypoint $i$ and waypoint $i+1$. Equation (4.6) shows the rotation matrix from ECEF coordinate frame to the NED coordinate frame.

$$C_n^{\ r} = \begin{bmatrix} \cos(\theta_i)\cos(\psi_i) & \cos(\theta_i)\sin(\psi_i) & -\sin(\theta_i) \\ -\sin(\psi_i) & \cos(\psi_i) & 0 \\ \sin(\theta_i)\cos(\psi_i) & \sin(\theta_i)\sin(\psi_i) & \cos(\theta_i) \end{bmatrix} \tag{4.7}$$

The first step in solving for the road heading and pitch angles is to express the position of the $i+1$ waypoint in the NED coordinate frame based at the $i^{th}$ waypoint using Equation (4.8).

$$\begin{bmatrix} n_{r,i} \\ e_{r,i} \\ d_{r,i} \end{bmatrix} = C_e^{\ n} \left[ \vec{r}^{\,e}_{er,i+1} - \vec{r}^{\,e}_{er,i} \right] \tag{4.8}$$

Once the position of waypoint $i+1$ is expressed in the NED coordinate frame with the origin located at waypoint $i$, then the road coordinate frame heading and pitch can be calculated as fallows.

$$\psi_i = atan2(e_{r,i}, n_{r,i}) \tag{4.9}$$

$$\theta_i = atan\left( \frac{-d_{r,i}}{\sqrt{n_{r,i}^2 + e_{r,i}^2}} \right) \tag{4.10}$$

The roll of the road coordinate frame is assumed to be zero; however, knowledge of this roll angle could be incorporated to more accurately model the road coordinate frame in areas where the road is banked.

The longitude ($\lambda_i$), latitude ($\phi_i$), pitch ($\theta_i$), and heading ($\psi_i$) are all substituted into their corresponding rotation matrices resulting in a rotation matrix that maps coordinates in the ECEF coordinate frame to the road coordinate frame. The three attitude angles in the map database ($\vec{\gamma}_i$) can be extracted from this rotation matrix. The following set of equations

show how to solve for the road coordinate frame attitude using the longitude, latitude, pitch, and heading angles.

$$\vec{\gamma}_{i,1} = atan2(-\cos(\phi_i)\sin(\psi_i), \cos(\phi_i)\sin(\theta_i)\cos(\psi_i) - \sin(\phi_i)\cos(\theta_i)) \tag{4.11}$$

$$\vec{\gamma}_{i,2} = asin(\cos(\phi_i)\cos(\theta_i)\cos(\psi_i) + \sin(\phi_i)\sin(\theta_i)) \tag{4.12}$$

$$\vec{\gamma}_{i,3} = atan2 \begin{pmatrix} -\sin(\phi_i)\sin(\lambda_i)\cos(\theta_i)\cos(\psi_i) + \cos(\lambda_i)\cos(\theta_i)\sin(\psi_i) + \cos(\phi_i)\sin(\lambda_i)\sin(\theta_i) \\ , -\sin(\phi_i)\cos(\lambda_i)\cos(\theta_i)\cos(\psi_i) - \sin(\lambda_i)\cos(\theta_i)\sin(\psi_i) + \cos(\phi_i)\cos(\lambda_i)\sin(\theta_i) \end{pmatrix} \tag{4.13}$$

### 4.1.3 Determining Distance Between Waypoints

The distance between the waypoints can be determined using the distance equation. This value is included in the lane map database for use by the algorithm that keeps track of the vehicles location within the lane map.

$$d_{r,i} = \sqrt{(\vec{r}^{\,e}_{er,i+1} - \vec{r}^{\,e}_{er,i})^T(\vec{r}^{\,e}_{er,i+1} - \vec{r}^{\,e}_{er,i})} \tag{4.14}$$

## 4.2 Vision Measurement Update

### 4.2.1 Vision Measurement Model

In order to use lateral lane position measurements, the lateral lane position with respect to the lane map must be estimated using the current states of the navigation filter. Equation (4.15) is used to find the position estimates in the road coordinate frame.

$$\begin{bmatrix} \widehat{x} \\ \widehat{y} \\ \widehat{z} \end{bmatrix} = C_e^{\ r} \left[ \vec{r}_{eb}^{\,e} - \vec{r}_{er,i}^{\,e} \right] \tag{4.15}$$

$\vec{r}_{eb}^{\,e}$ denotes the current position estimate in the ECEF coordinate frame. $\vec{r}_{er,i}^{\,e}$ denotes the position of the last waypoint passed in the ECEF coordinate frame. $\widehat{y}$ is the lateral lane position estimate, $\widehat{x}$ is the distance into the current road coordinate frame, and $\widehat{z}$ is the vertical position in the current road coordinate frame. The z-axis of the road coordinate frame points down. $C_e^{\ r}$ is the rotation matrix from the ECEF coordinate frame to the road coordinate frame and has the form:

$$C_e^{\ r} = \begin{bmatrix} c_2c_3 & c_2s_3 & -s_2 \\ s_1s_2c_3 - c_1s_3 & s_1s_2s_3 + c_1c_3 & s_1c_2 \\ c_1s_2c_3 + s_1s_3 & c_1s_2s_3 - s_1c_3 & c_1c_2 \end{bmatrix} \tag{4.16}$$

The three Euler angles that are substituted into Equation (4.16) come from the map database ($\vec{\gamma}_i$) along with the position of the last waypoint passed ($\vec{r}_{er,i}^{\,e}$). The first three states of the filter ($\vec{x}_{1:3}$) is the position vector of the vehicle in the ECEF coordinate frame ($\vec{r}_{eb}^{\,e}$).

In order to perform a measurement update, three things must be known. The first is the measurement vector ($\vec{y}$). Equation (4.17) shows the measurement vector.

$$\vec{y} = \begin{bmatrix} y_{vision} \\ y_{height} \end{bmatrix} \tag{4.17}$$

The first measurement is lane position measured by the LiDAR or camera. The second measurement is the height above the lane determine by the vehicle constant. Since this work deals with ground vehicles, the height above the road (ground) can be measured once and assumed to be constant. This constant height is measured and included as a measurement.

The second requirement needed to perform a measurement update is the measurement equations. Equation (4.18) shows the measurement equations for the $y$ and $z$ axis of the road coordinate frame.

$$\vec{\hat{y}}(\vec{x}, \vec{r}^{\,e}_{er,i}, \vec{\gamma}_i) = \begin{bmatrix} \hat{y} \\ \hat{h} \end{bmatrix} = \begin{bmatrix} C^{\,r}_{e(2,1)} \left(\vec{x}_1 - \vec{r}^{\,e}_{er(i,1)}\right) + C^{\,r}_{e(2,2)} \left(\vec{x}_2 - \vec{r}^{\,e}_{er(i,2)}\right) + C^{\,r}_{e(2,3)} \left(\vec{x}_3 - \vec{r}^{\,e}_{er(i,3)}\right) \\ -C^{\,r}_{e(3,1)} \left(\vec{x}_1 - \vec{r}^{\,e}_{er(i,1)}\right) - C^{\,r}_{e(3,2)} \left(\vec{x}_2 - \vec{r}^{\,e}_{er(i,2)}\right) - C^{\,r}_{e(3,3)} \left(\vec{x}_3 - \vec{r}^{\,e}_{er(i,3)}\right) \end{bmatrix} \tag{4.18}$$

The measurement equations are a function of the states of the filter and the map parameters. The states and map parameters are substituted into these equations to estimate the measurement based off the current states. These equations are also used to determine the measurement model matrix ($H$). The first measurement equation is for the lateral lane position. This measurement is provided by a camera or LiDAR. The second measurement equation is the height above the road coordinate frame.

The last thing needed to perform a measurement update is the measurement model matrix ($H$). The measurement model is created by taking the partial derivative of the measurement equations with respect to each state. Equation (4.19) shows the measurement model matrix,

$$H = \begin{bmatrix} e_1 & 0_{1x3} & 0_{1x3} & 0_{1x3} & 0_{1x3} & 0_{1x2} \\ e_2 & 0_{1x3} & 0_{1x3} & 0_{1x3} & 0_{1x3} & 0_{1x2} \end{bmatrix} \tag{4.19}$$

where Equation (4.20) is the unit vector in the navigation coordinate frame that points in the direction of the y axis of the road coordinate frame

$$e_1 = \left[C^{\,r}_{e(2,1)}, C^{\,r}_{e(2,2)}, C^{\,r}_{e(2,3)}\right] \tag{4.20}$$

and Equation 4.21 is the unit vector in the navigation coordinate frame that points in the direction of the negative z axis of the road coordinate frame

$$e_2 = \left[-C^{\,r}_{e(3,1)}, -C^{\,r}_{e(3,2)}, -C^{\,r}_{e(3,3)}\right] \tag{4.21}$$

Both of these unit vectors are taken directly from rows of the rotation matrix from the navigation coordinate frame to the road coordinate frame.

The height and lane position measurements provide measurements in two of the three position axis. The system is almost fully observable just using these measurements. The only missing piece of information is position in the x axis of the road coordinate frame. If this value is measured (using something other than GPS), then the navigation filter will remain fully observable even without GPS measurements. The results also show that when using vision measurement updates, the navigation filter remains observable even if only two GPS ranges are available (instead of the typical four needed to maintain observability).

### 4.2.2 Map Keeping

In order to use vision updates, the navigation filter must know what map to use and where along this map the vehicle is located. Determining the vehicle location within a certain map is done by searching through the map to find the closest waypoints. Determining which map a vehicle currently resides is a much more difficult problem. For example, when initializing map location on road with multiple lanes of travel in each direction, the global position used to search the maps has to be level accurate as to not cause any ambiguity as to what lane the vehicle currently resides. Stand alone GPS has meter level biases; therefore, there would be no way to determine the vehicle current lane on a multi lane road. Map intersections could also cause ambiguity as to which map the vehicle is current traveling in. Also, once the lane of the vehicle is determined, the navigation filter will have to successfully track all lane changes in order to maintain use of the correct lane map. RTK differential GPS is considered to be accurate on the centimeter level. Therefore, if available, RTK differential GPS position can be used to initialize location on a multi-lane road with a correct guess at what lane map to use.

### Initializing Map Location

Determining which map the vehicle is currently residing poses an interesting problem. One method of initializing the map is to do a distance calculation from the estimated GPS position to all nearby waypoints from all nearby maps. The waypoint that is closest to the vehicle is assumed to be the last waypoint the vehicle passed, thus, the current map is set to the map containing the closest waypoint and map index is set to the index corresponding to the closest waypoint to the vehicle. This method searching every waypoint in every lane map would not be the most efficient method of finding the closest waypoint. Furthermore, there would also be an issue with how the search algorithm would continuously search for when the vehicle entered map coverage. Once entering a mapped area, accuracy of current global position becomes important in properly estimating which the lane vehicle entered at the start of a multi-lane map.

After the map and map index is selected, the distance into the current road coordinate frame is calculated using Equation (4.22) to determine if the closest waypoint is in front or behind the vehicle.

$$\widehat{x} = C^{\,r}_{e(1,1)} \left( \vec{r}^{\,e}_{eb,1} - \vec{r}^{\,e}_{er(i,1)} \right) + C^{\,r}_{e(1,2)} \left( \vec{r}^{\,e}_{eb,2} - \vec{r}^{\,e}_{er(i,2)} \right) + C^{\,r}_{e(1,3)} \left( \vec{r}^{\,e}_{eb,3} - \vec{r}^{\,e}_{er(i,3)} \right) \tag{4.22}$$

If the closest waypoint is in front of the vehicle (the result of Equation (4.22) is negative), the map index should be shifted down until the result of Equation (4.22) is positive.

### Maintaining Map Location

After every measurement update and time update, the states of the navigation filter will change. Every time the states of the filter are updated, the distance into the current road frame must be checked to ensure that the vehicle has not passed into the next road coordinate frame. Substituting the position states into Equation (4.22) will result in the

current longitudinal distance into the road coordinate frame. If this value is larger than $d_{r,i}$ (from map database), then the vehicle has passed into the next coordinate frame. The map index $i$ should then be incremented by one. It may be necessary to increment the map index by more than one if the vehicle passes through a section of the map with no update. This problem becomes more likely if the waypoints are very close together and can be overcome by using a continuous check that will increment the map index until the distance estimated by Equation (4.22) is less than $d_{r,i}$. In order to improve the robustness of the filter, the map checking system is also set up to decrease the map index if the result of Equation (4.22) is less than zero.

**End of Map**

Once the vehicle passes the last waypoint in a map, then the vehicle is assumed to have left the area covered by the current map. Once the vehicle leaves the map, it can no longer use lane position measurements to update the filter. Without the map, there is no way to incorporate lane position measurements into the global navigation filter. The vision measurements can continue to operate and estimate lane position; however, this information can not be used to update the global position used by the navigation filter. As long as GPS remains available, the navigation filter will continue to operate even with no map. The position estimated by the filter can be used to determine when the vehicle has entered an area that has map coverage and reinitialize the map.

Information on what to do once the vehicle leaves the map can be saved in the map database. For example, each waypoint could also have an associated lane map for right and left lane departures. This association would allow the filter to know if there was a lane to the right or left and what lane map to hand off to if the vehicle changes lanes. The map used for this work was circular. Therefore, the map tells the filter to simply go back to the start of the map once it reaches the end. For non-circular paths, the current map can contain information on what map should be used next after leaving the current map.

## 4.3 Conclusions

This chapter presents a method of using lane position measurements to update a global navigation filter using a waypoint based map. The map database is not considered to have any standard form. The database must contain the position of the waypoints in the coordinate frame of the navigation filter. The waypoint positions is the only necessary information; however the rotation between the ECEF coordinate frame and the road coordinate frame must also be know in order to use the vision measurements. The waypoints can be used in conjunction with Equations (4.6-4.10) to determine the rotation between the ECEF and the road coordinate frame; however, this requires quite a bit of computational overhead which can be reduced by either saving the three Euler angles (Equations (4.11-4.13)) or every element of the rotation matrix ($C_e^r$) itself in the map database.

The method of using measurements given in a coordinate frame of than the navigation coordinate frame assumes the position of the measurement coordinate frame contains no error. The filter assumes the lane map is perfectly accurate. If the map is not perfectly accurate, the filter will continue operate. However, lane position accuracy will be maintained and the global position estimates will be biased. This error works similarly with any error in RTK GPS base station antenna global position. Any error in the global position of the base station GPS antenna will cause a bias in RTK GPS measurements with respect to the lane map. This chapter presents a method of overcoming both of these biases given a survey marker location (assuming all waypoints and the survey marker location are centimeter accurate in relation to each other).

This chapter also presents a primitive method of map tracking. Using the map and vision measurements hinges on knowing the current lane the vehicle resides (or which lane map to use) and the vehicles current location within the lane map (determining the proper map index to use). The area of lane tracking shows the strongest potential in system improvement.

# Chapter 5

## Results

This chapter presents results from the navigation filter and an evaluation of the performance of the filter. Along with showing the filter working at full capacity, various sensor outages are simulated to show how the loss of a particular sensor affects the estimates of the navigation filter. The results also show how the filter reacts when no lane map is available. Finlay, the results will show how the filter performs when less than four GPS satellites are available, and the result of losing vision measurements or the lane map under a limited satellite constellation.

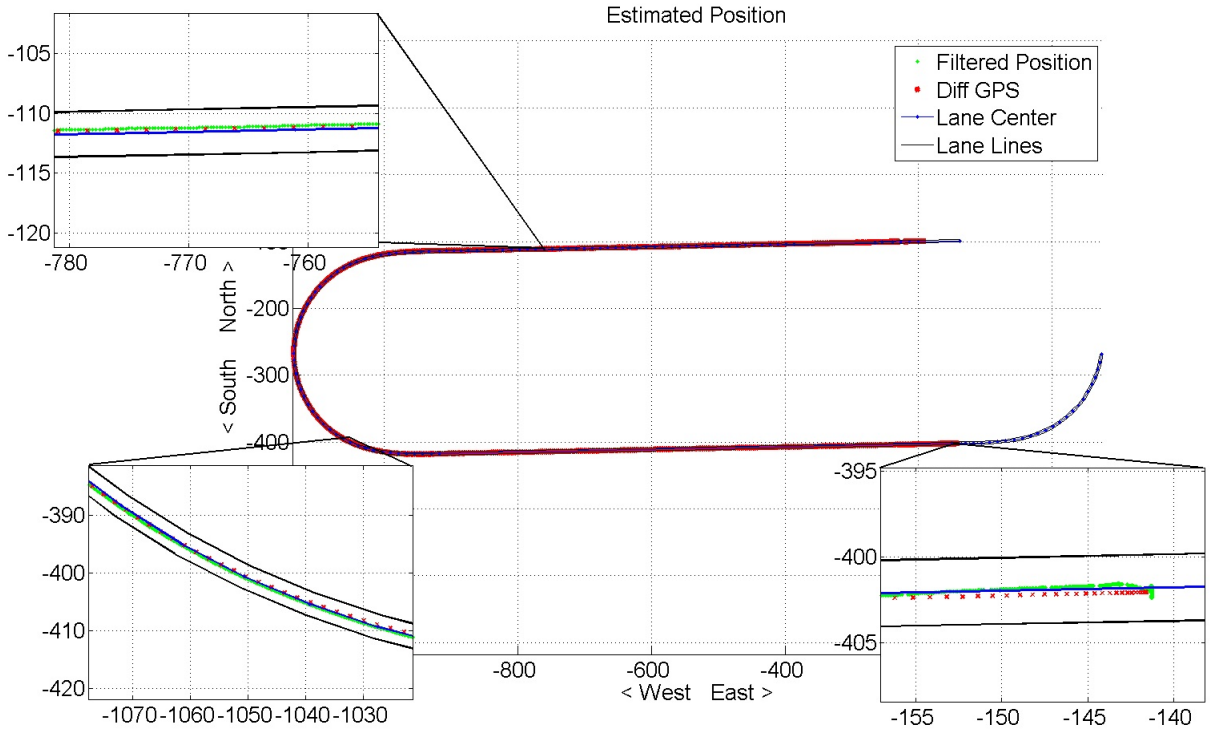


Figure 5.1: Estimated Vehicle Position Using Loosely Coupled RTK GPS Updates

All the error plots where created using the unfiltered RTK GPS position and velocities from the Septentrio GPS receiver. The RTK corrections were provided by an on site base

station. The close proximity to the base station ensures that RTK GPS position is accurate on a centimeter level. These RTK positions and velocities (taken at $10Hz$) were used in conjunction with the IMU measurements to determine a ”’true”’ trajectory. The truth trajectory represents the best available metric of the actual states of the navigation filter. The error was estimated by differencing the ”’true”’ trajectory and the estimates of the navigation filter.

The data for the following results was collected at the NCAT test track is Opelika Alabama. For this data set, the vehicle starts in the outside lane at the end of the front (north) straight. The test vehicle drives down the front straight at 55 mph, through a 180 degree turn, then down the back straight at 70 mph. The vehicle comes to a complete stop at the end of the back straight.

Figure 5.1 shows the estimated position when using differential GPS measurements. The red dots represent the GPS measurements (at 10 Hz). As can be seen, the GPS measurements reside close to the center of the lane. The green dots represent the filtered solution (at 100 Hz) with differential GPS, vision, and map constraints.

Figure 5.2 shows the estimated position when using standalone GPS measurements. The red dots represent the GPS measurements (at 2 Hz). As can be seen, the GPS measurements no longer reside within the lane lines due to fact that standalone GPS has a drifting bias. The green dots represent the filtered solution (at 100 Hz) with standalone GPS, vision, and map constraints. The filtered solution resides within the lane lines due to the fact that the vision measurement constrains the position to the map. This comparison shows that GPS alone is not enough to determine lane position; however, fusing the GPS with vision and map constrains results in a solution that is lane level accurate. If the vision measurements are unavailable, the filtered solution will converge to the GPS measurements resulting in a loss of lane level accuracy.

Figures 5.3 and 5.4 provide the estimated attitude and the Septentrio GPS receiver measured attitude. The Septentrio GPS receiver is a three antenna receiver that accurately

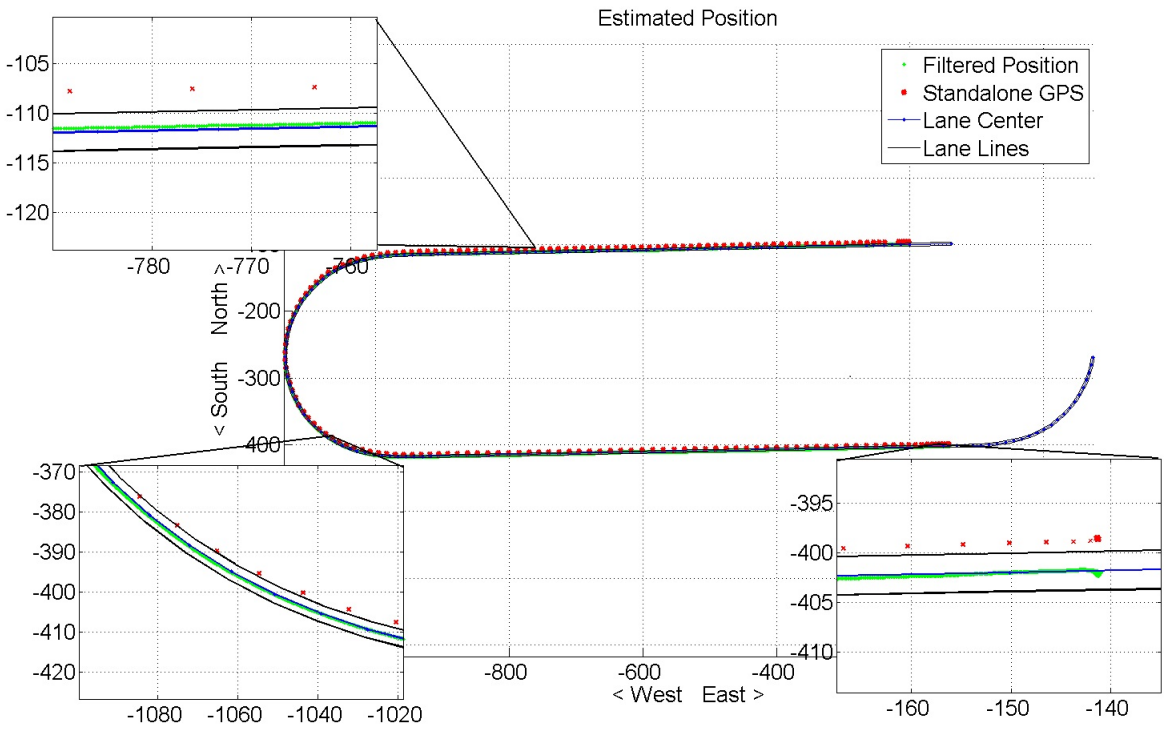


Figure 5.2: Estimated Vehicle Position Using Closely Coupled GPS Updates

measures attitude. The plot shows that the attitude estimated by the filter using a single antenna closely matches the attitude estimated by the triple antenna GPS receiver. The stability of the navigation filter is very dependent on the accuracy of the initial guess at the vehicles attitude. For this data set, the initial pitch and roll was set to zero, and the initial heading was set at -90 degrees. The actual initial heading of the vehicle was around -92 degrees. This initial error results in a two degree heading error until the vehicle starts to turn. Attitude estimates are unobservable without significant excitation (change in attitude) [10]. If the initial guess at the attitude is wrong, the filter can behave in an unstable manner.

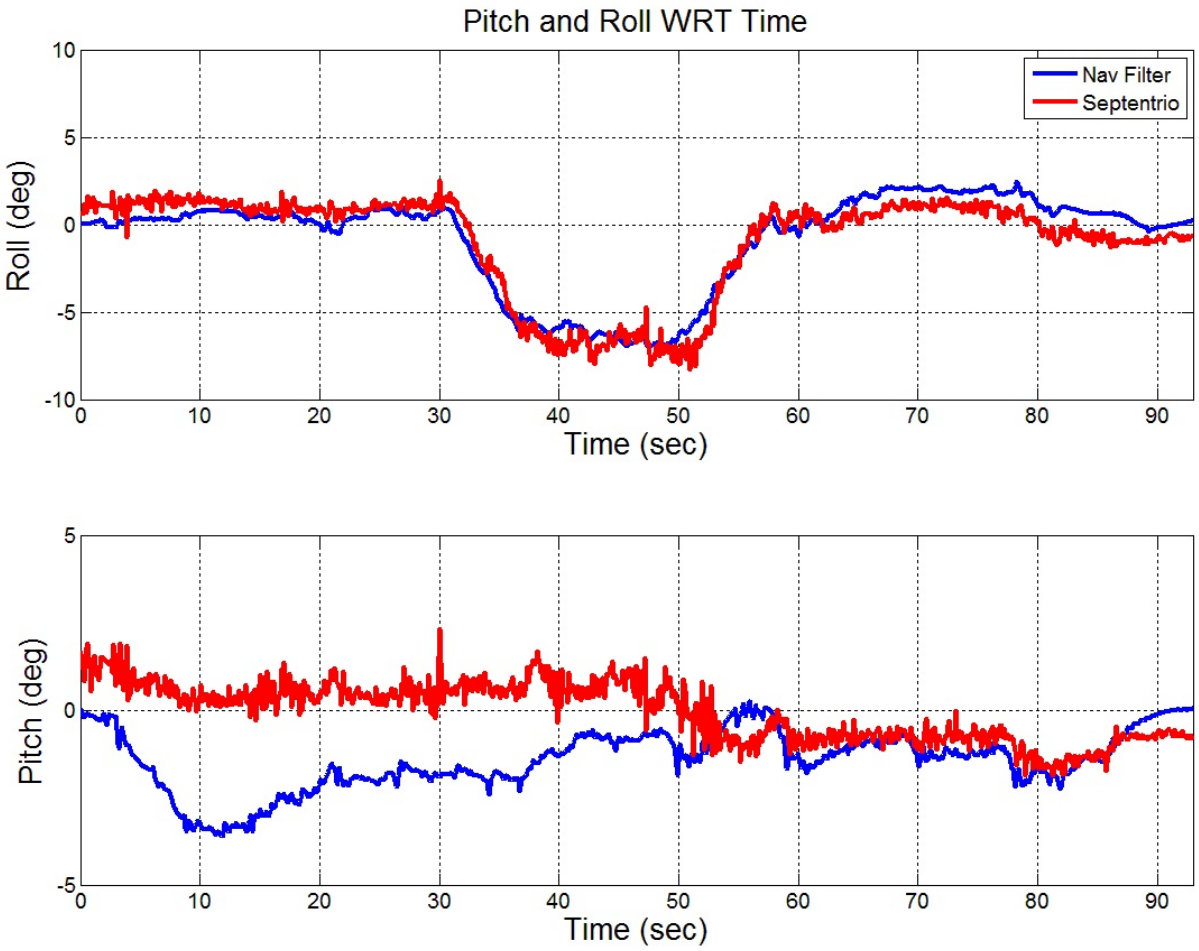


Figure 5.3: Estimated Vehicle Pitch and Roll

## 5.1 Effects of Sensor Failures

The next set of figures show the effects of sensor failures on the system. At thirty seconds into the data run, different sensor outages are simulated to show what happens to the filter when certain sensors become unavailable. The simulated outage last for one minute, after which the measurements are reinstated.

Figure 5.5 is a plot of the estimated total velocity under several different failure conditions. The blue line represents the total velocity reported by the differential GPS alone. The green line represents the system working at full capacity. When vision measurements (yellow line), differential corrections (cyan line), or differential corrections and vision (red line) are removed, the estimated velocity closely resembles the RTK GPS estimated velocity. Only

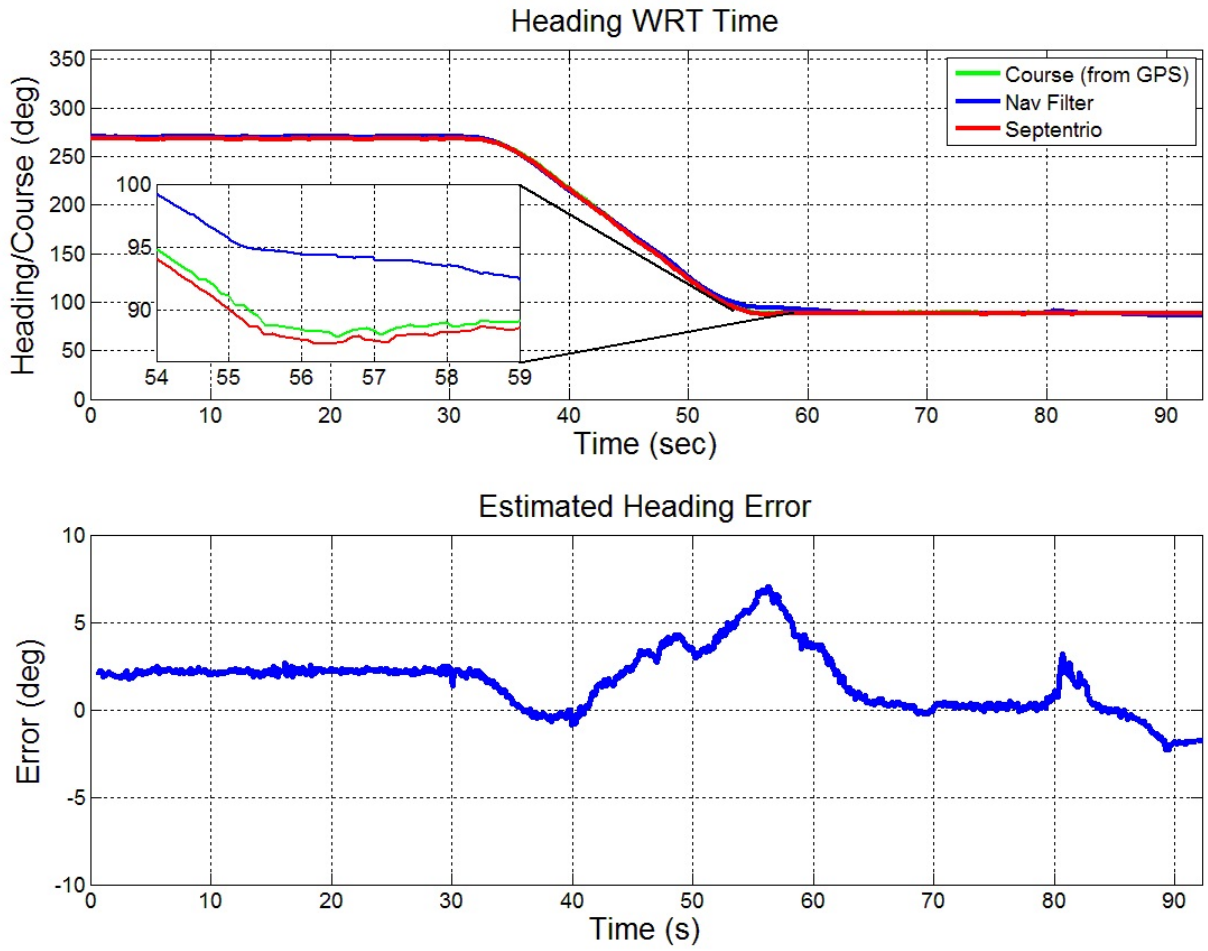


Figure 5.4: Estimated Vehicle Heading

two failure situations result in a loss of velocity estimation. Both failures involve failure of all GPS measurements. Both failure of GPS (magenta line) and failure of GPS and vision (black line) result in loss of velocity estimation; however, there is a noticeable improvement when vision measurements remain operational.

Figure 5.6 shows the performance of the estimated lane position under several different failure conditions. The blue line represents the lane position reported by the differential GPS alone, which was used to represent true position in the lane. The green line represents the system working at full capacity. When only the differential corrections are removed, the filter can still estimate lane position because vision measurements are still available. When GPS is completely turned off, lane position can be estimated correctly because vision

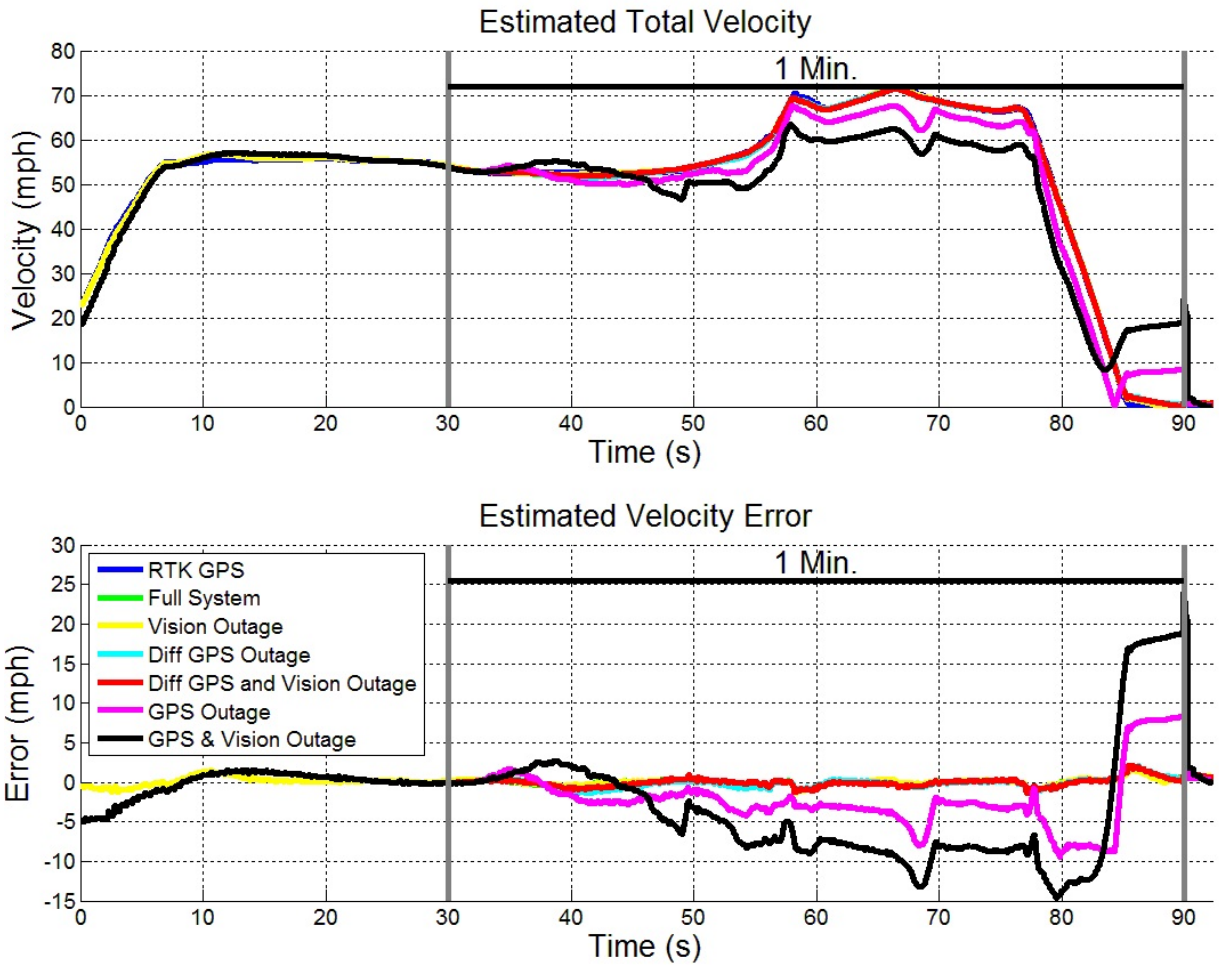


Figure 5.5: Estimated Velocity with Measurement Failures

measurements are still available. Only two failure situations result in a loss of accurate lane position estimation. The first case is when differential corrections and vision measurements are removed. For this situation, only standalone GPS is available which results in a biased lane position estimate. The second case is when GPS and vision are removed. This case represents a loss of all measurement updates. The error in the lane position estimate will continually grow when all measurements are lost. Loss of lane position accuracy for both of these cases occurs with five seconds.

Figure 5.7 is a plot of the error of the estimated lane position. The advantage of using differential GPS can be seen when there are large errors in the vision measurements. Using differential GPS provides better filtering during periods of large vision measurement

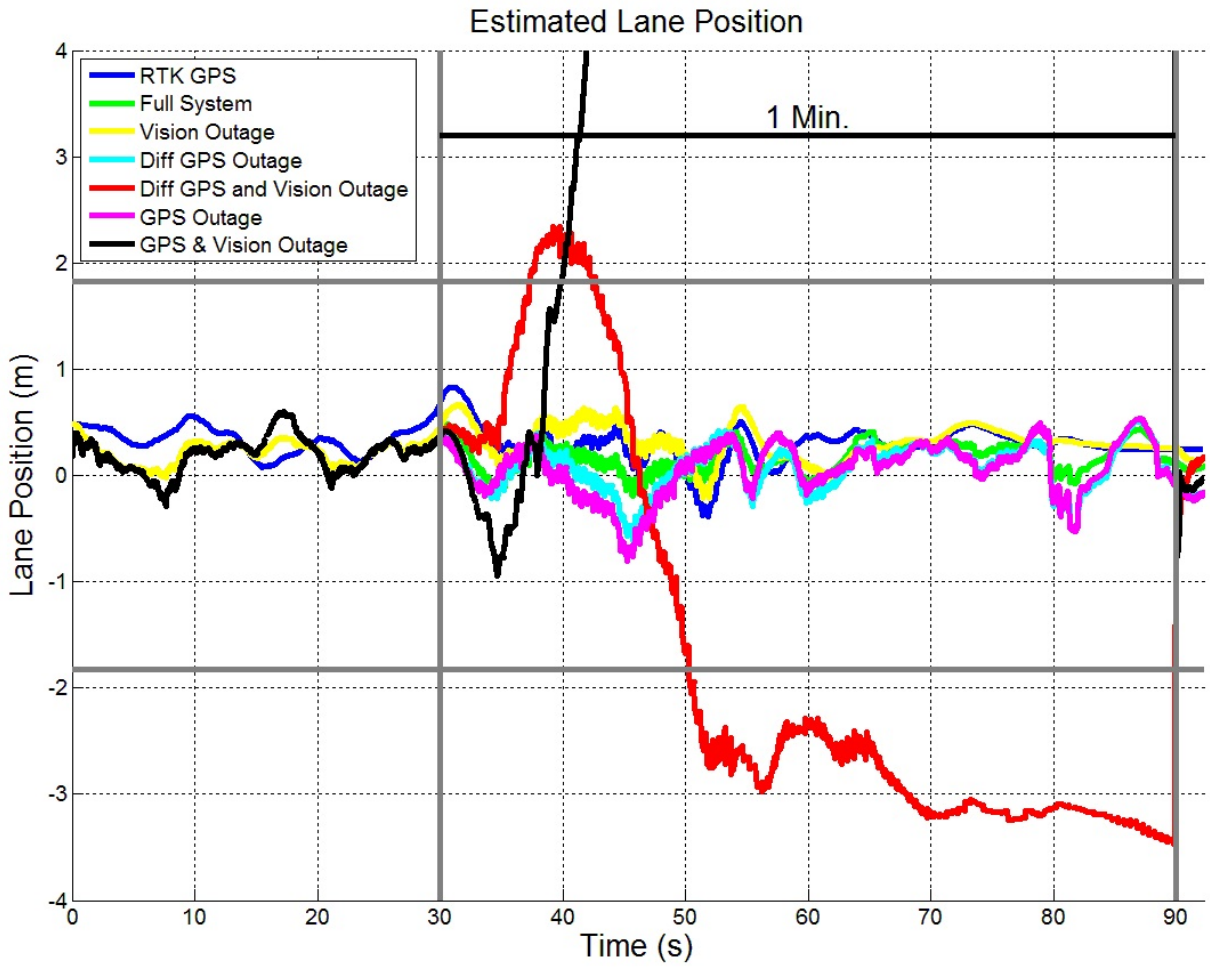


Figure 5.6: Estimated Lane Position with Measurement Failures

errors. For the case when only vision fails (yellow line), the filter solution converges to the GPS measurements, which in this case is differential GPS. This error plot is based off the differential GPS measurement; therefore, when differential GPS is the only measurement used (yellow line), the error is very close to zero. When differential corrections and vision are lost (red line), the filtered solution converges to the GPS measurement; however, since there are no corrections to the GPS, the measurement is biased. Ninety seconds into the data run when all measurements are reinstated, the filter corrects itself for all the failure conditions within a few seconds of reacquisition of measurements.

Figure 5.8 shows the estimated longitudinal position representing the distance from the start of the map along the path of the map. Two failure conditions result in a loss of

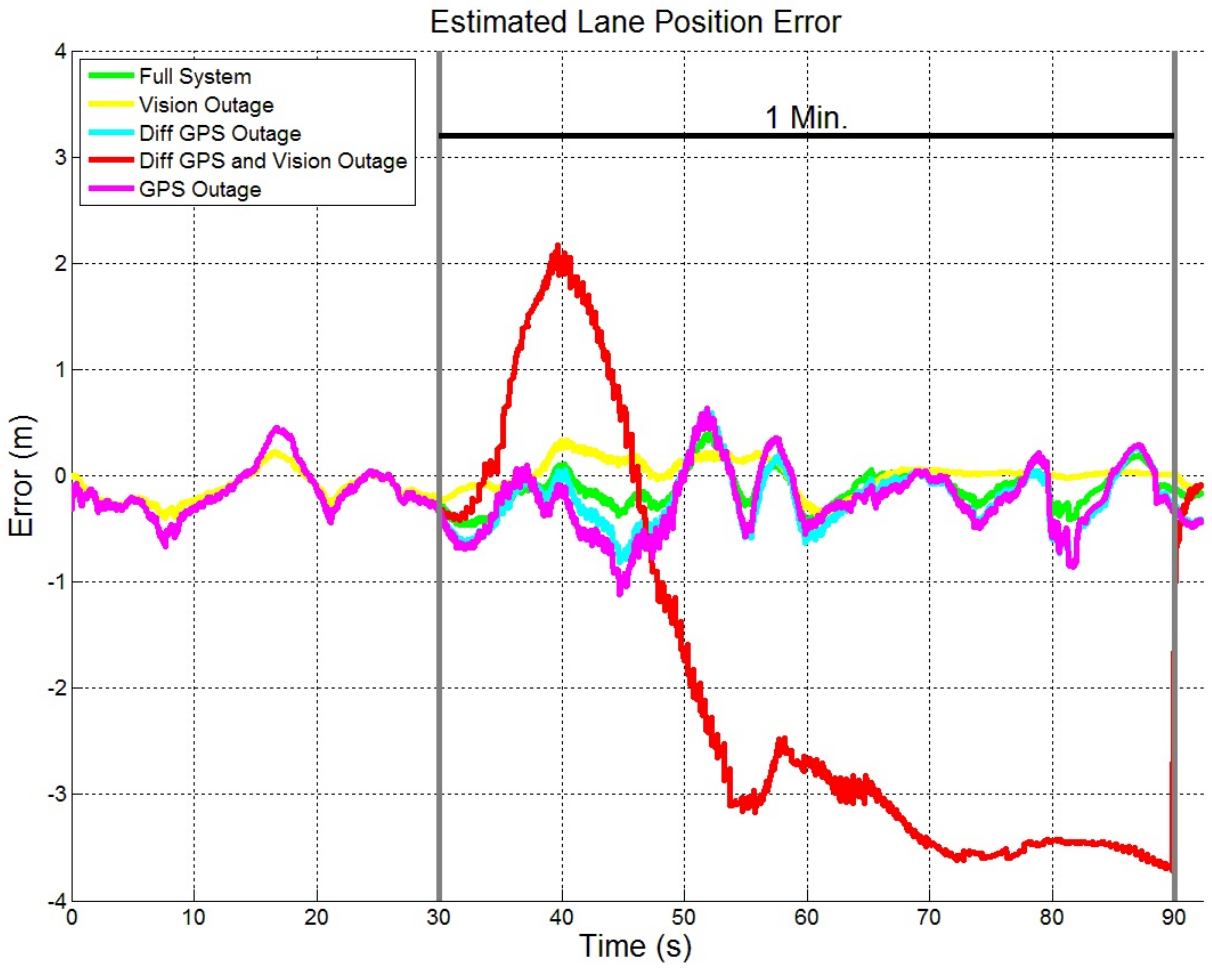


Figure 5.7: Estimated Lane Position Error with Measurement Failures

accuracy in the estimated distance along the map. The first is the GPS outage. For this case only vision measurements are available. As can be seen in Figure 5.6, the lane position estimate still remains accurate for this case. However, since there is no GPS to provide position information in the axis parallel to the road, the estimated distance along the map is dead reckoned causing drift. When only vision measurements are available, the lane position estimate is still available, but the filter loses its location on the map. The second case where this estimate fails is when both GPS and vision are not available.

Figure 5.9 is a plot of the estimated error in longitudinal position. The graph shows that the error in estimated position grows quicker for the case when no vision measurements are available. This figure shows that having vision does help in containing drift in longitudinal

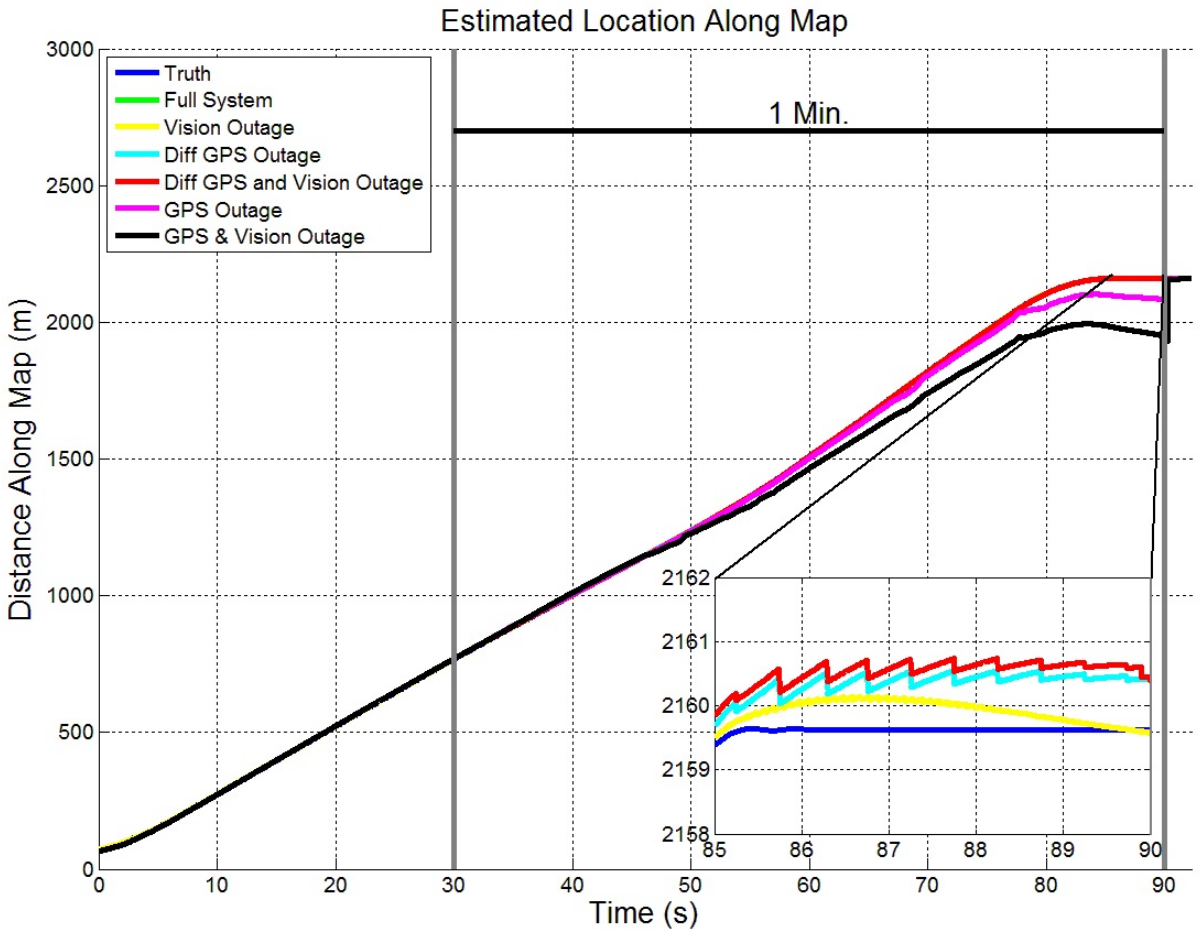


Figure 5.8: Estimated Longitudinal Position with Measurement Failures

position, however, the error for both the loss of GPS (magenta line) and the loss of GPS and vision (black line) cause a continual error growth. Like the estimated lane position, the estimated longitudinal position corrects itself after measurements are reinstated.

Figure 5.10 is an above ground view of the estimated position during the various failures. The star represents the location of the vehicle when the measurements are removed.

Figure 5.11 provides the estimated error in each road axis when no GPS measurements are available. The blue line represents the error when no GPS, map, or vision measurements are available. For this case, there is no measurement updates. Therefore, there is a continual error growth in all axes due to integration of the IMU errors. The black line represents the error when no GPS or vision measurements are available. For this case, the map is available

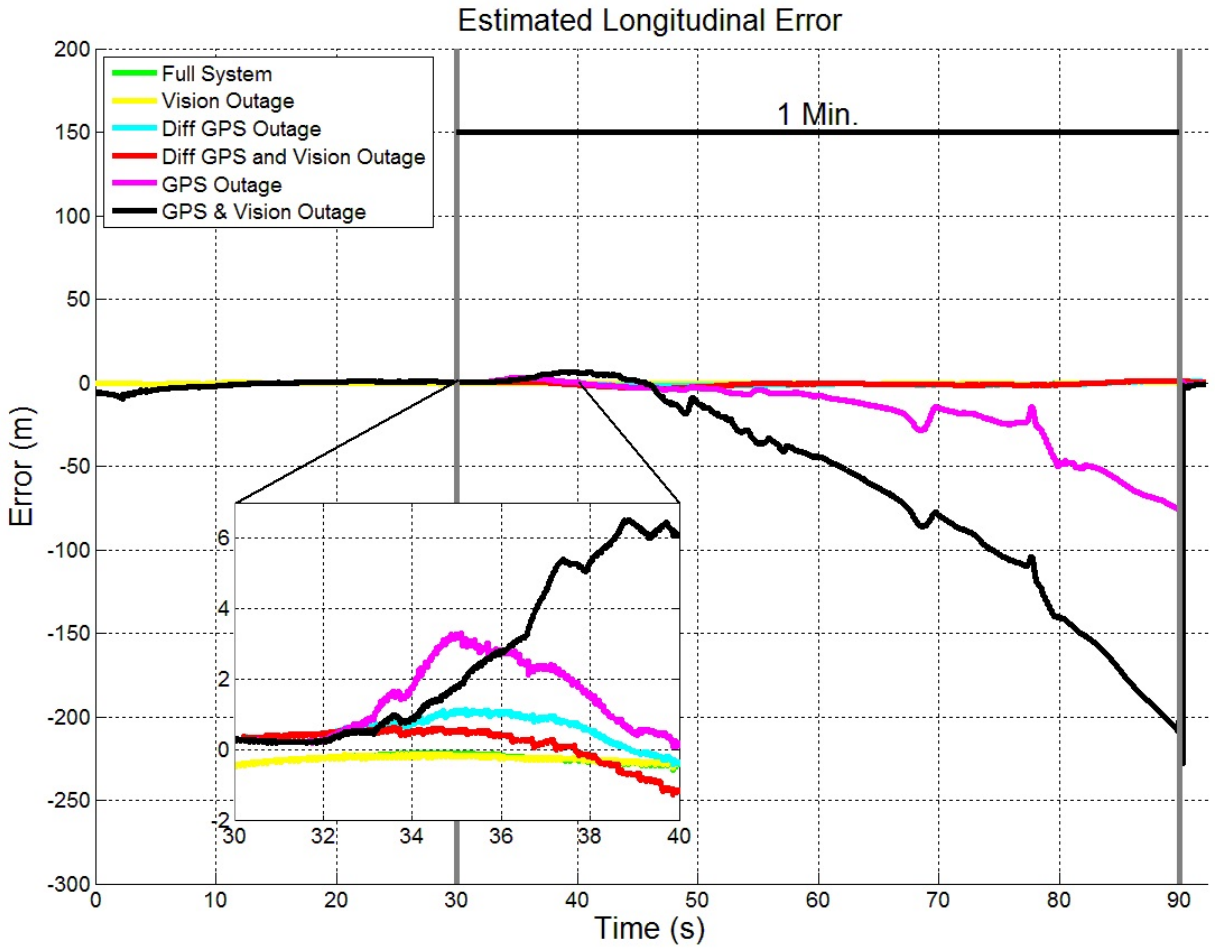


Figure 5.9: Estimated Longitudinal Position Error with Measurement Failures

constraining the error in the vertical road axis. The magenta line shows the error when only GPS is not available. For this case, vision measurements are also available, constraining error in the lateral road axis. The error in the longitudinal axis is not constrained with GPS. Neither the vision measurements nor the height constraint provide full observability in the longitudinal road axis.

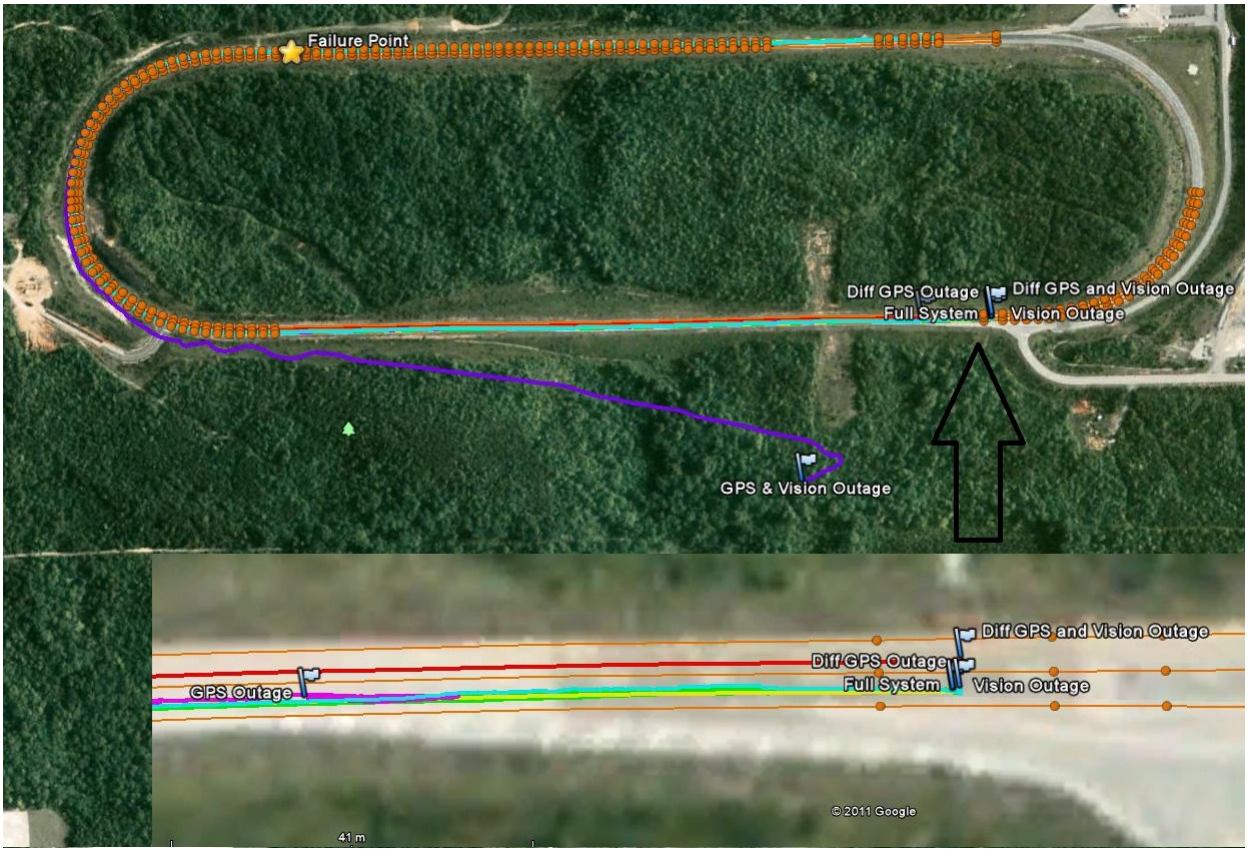


Figure 5.10: Estimated Position with Measurement Failures

## 5.2 Limited Satellite Results

Urban and rural environments both pose different problems for each of the various algorithms. Navigation within a city has proved to be an interesting problem for GPS aided navigation systems due to the blockage of satellites by buildings. Similarly, trees on rural roads can block GPS satellites. However, the use of multiple sensors can provide a solution even with poor GPS satellite visibility. A typical navigation filter based off GPS measurement updates requires at least four GPS observations to remain operational. Each of the four observations is needed to solve an unknown. Three-dimensional position makes up three of the unknowns. The fourth unknown is the clock bias (or the difference in the GPS receiver clock and the GPS system time).

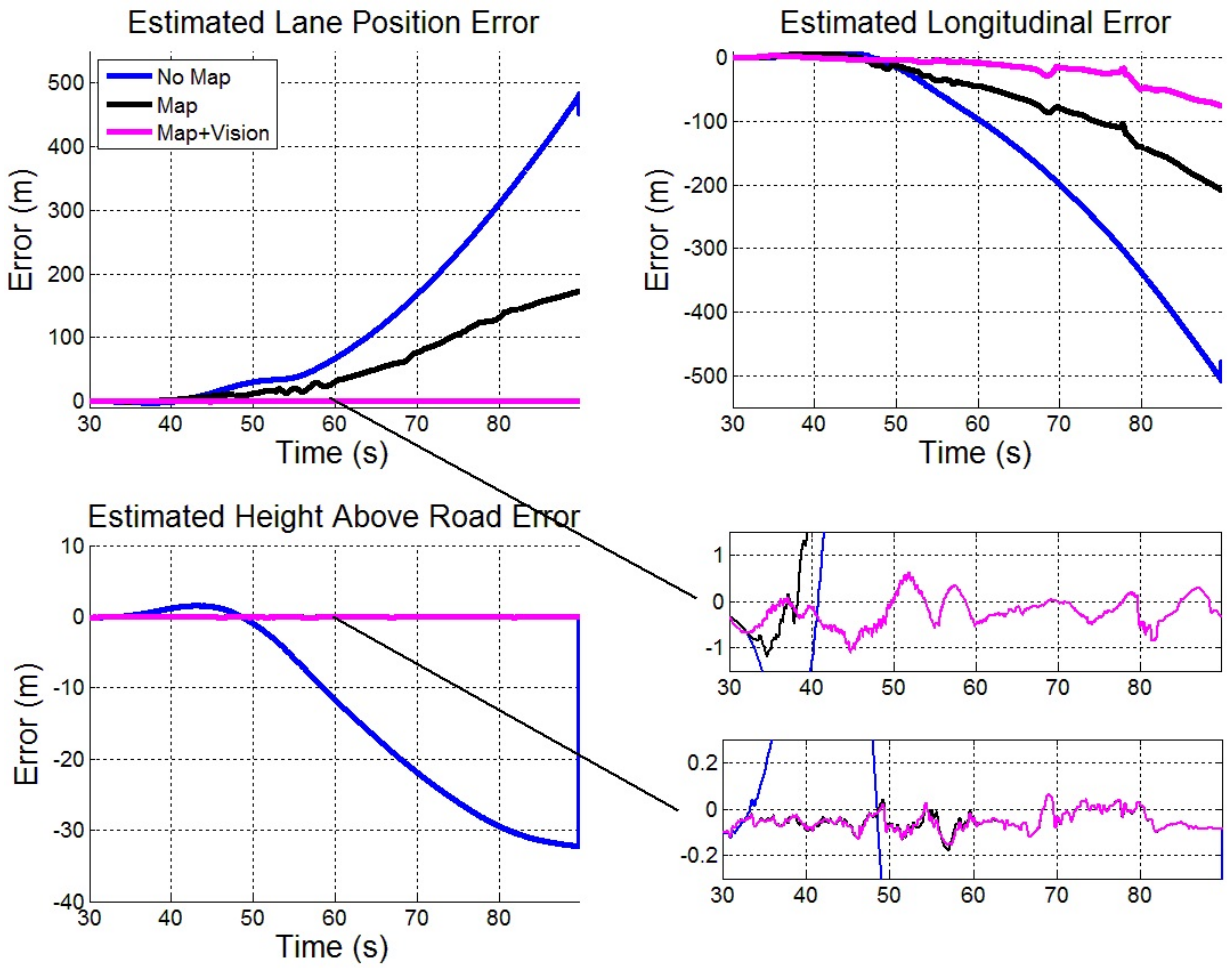


Figure 5.11: Estimated Errors for Various Map and Vision Availability Using No GPS

The vision measurements can measure position in one axis; the axis perpendicular to the road. Since the road map contains vertical information, position in the axis vertical to the road can be constrained. The height of the vehicle above the road is assumed to be constant. Therefore, the only non constrained axis is the axis parallel to the road. Since position is only unconstrained in one axis, only using two GPS observations will result in a fully operational system. One GPS observation is needed for the unknown axis, and the other is needed for receiver clock errors.

Table 5.1: Satellite Azimuth and Elevation Angles

| Satellite | Azimuth Angle (deg) | Elevation Angle (deg) | Carrier-to-Noise-Ratio (dB) |
|---|---|---|---|
| SV 5 | 63.15 | 19.49 | 48 |
| SV 9 | 150.98 | 15.74 | 48 |
| SV 15 | 100.48 | 79.8 | 54 |
| SV 18 | -79.82 | 37.84 | 53 |
| SV 21 | -38.55 | 51.92 | 52 |
| SV 26 | 46.6 | 43.53 | 48 |
| SV 27 | 128.50 | 24.82 | 42 |
| SV 29 | -148.28 | 48.83 | 51 |

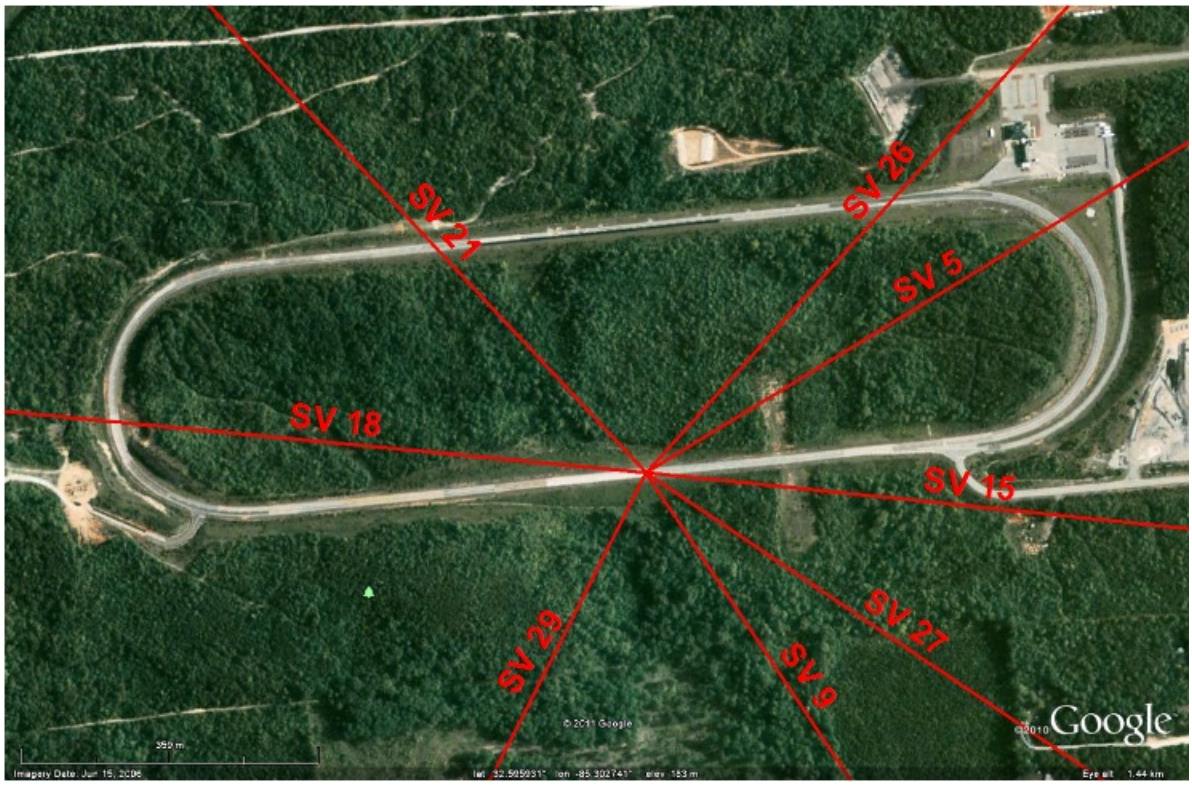


Figure 5.12: Satellite Line of Sight Vectors

Figure 5.12 shows the direction from which all the GPS observations are originating for the data run discussed in the previous section. This figure can be used as a reference for the plots below. The plots below show the data run from the last section; however, at thirty seconds, all but a few selected GPS observations are turned off. After one minute, all the GPS observations are turned back on. The simulated satellite outages will show how

the filter reacts when less than four GPS observations are available and the effects satellite geometry and measurement quality on the filter.

Like the measurement failure results, these results were created by looking at the effects of measurement failures on the same dataset. Thirty seconds into the run, all satellite observations except the satellite observations listed in the legend are turned off. Figure 5.13 shows the estimated velocity and velocity error for various limited satellite constellations.

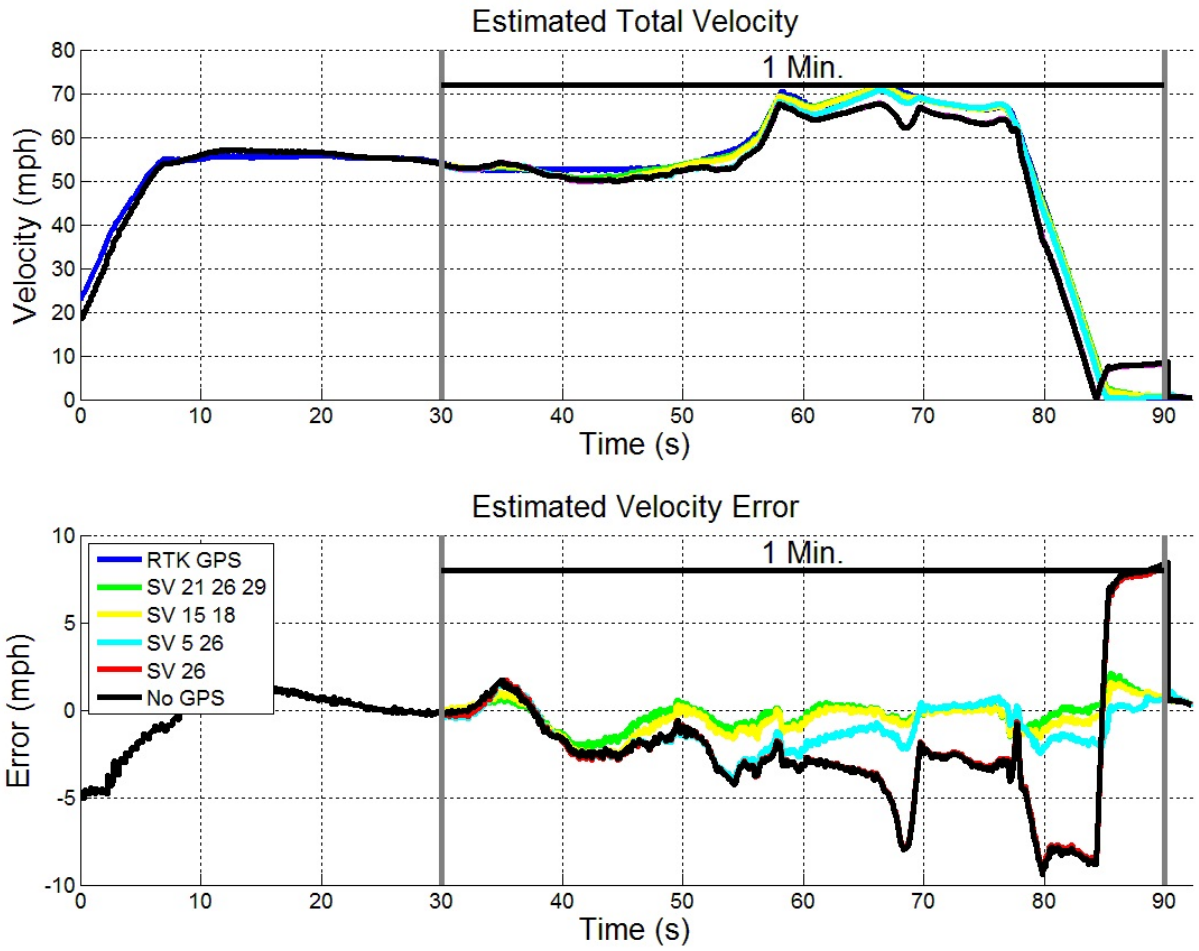


Figure 5.13: Estimated Velocity with Vision and Limited Satellite Visibility

Figure 5.13 shows that estimated velocity degrades as the number of GPS observations decreases. The three observation case (green line) has the least error, followed closely by the SV 15 and 18 combination (yellow line). The SV 5 and 26 combination (cyan) performs worse than the three and other two observations cases; however, this combination performs considerably better than the one and no observation case. There is no noticeable difference

in estimated velocity when using one GPS observation (red line) and when using no GPS observations (black line).

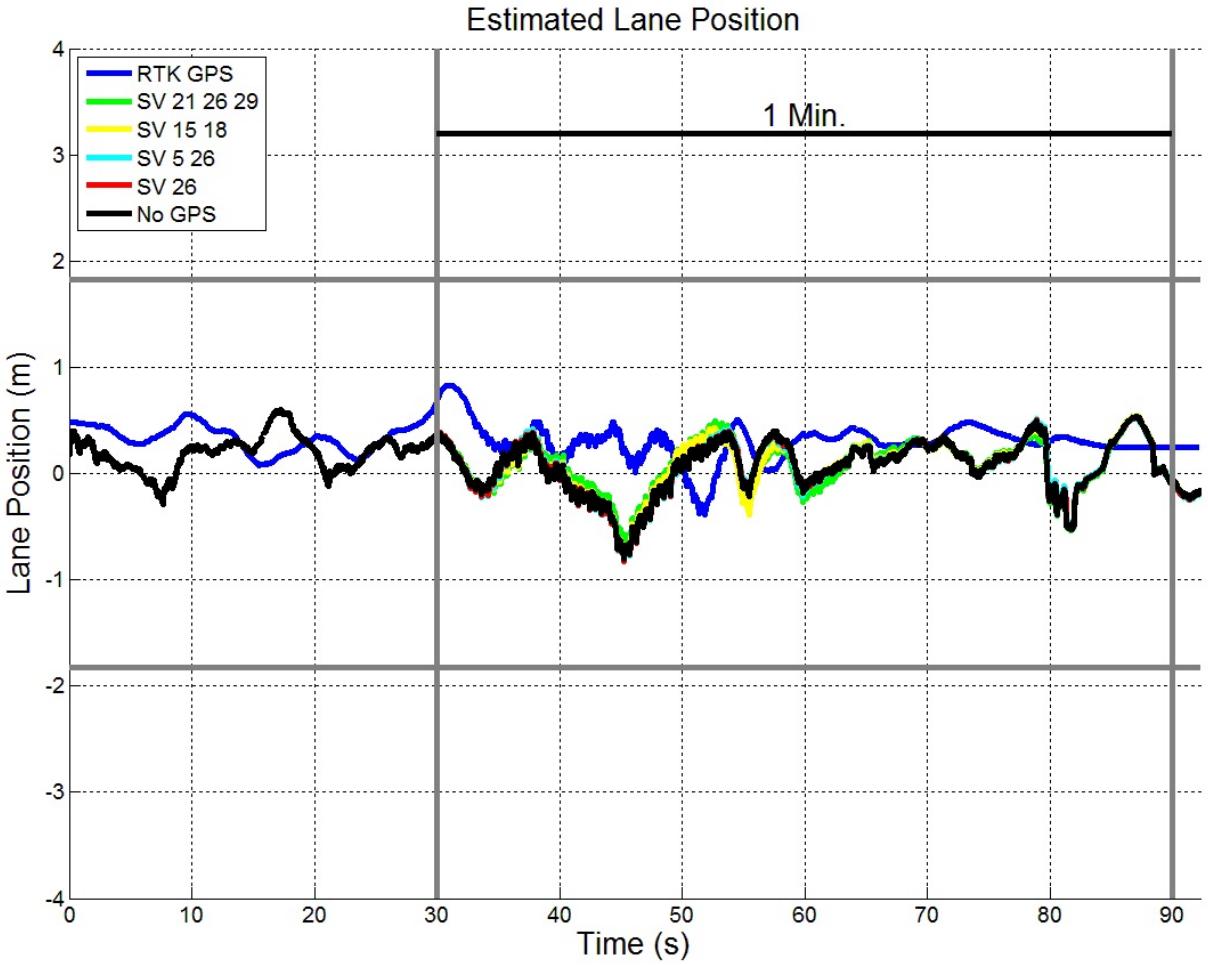


Figure 5.14: Estimated Lane Position with Vision and Limited Satellite Visibility

Figure 5.14 is a plot of the estimated lane position for the various satellite constellations. The blue line is the estimated truth using the RTK GPS measurements. The horizontal gray lines represent the lane lines assuming a twelve foot lane. When vision measurements are used, the lane position estimate remains accurate for all limited satellite constellations. Even when no GPS observations are available, the vision measurements ensure that lateral lane position accuracy is maintained. The component of any GPS observations that lie in the lateral road axis will be ignored because the visions measurements have a much smaller

associated variance. If vision measurements are not available, the navigation filter will not have the observability necessary to estimate lane position.

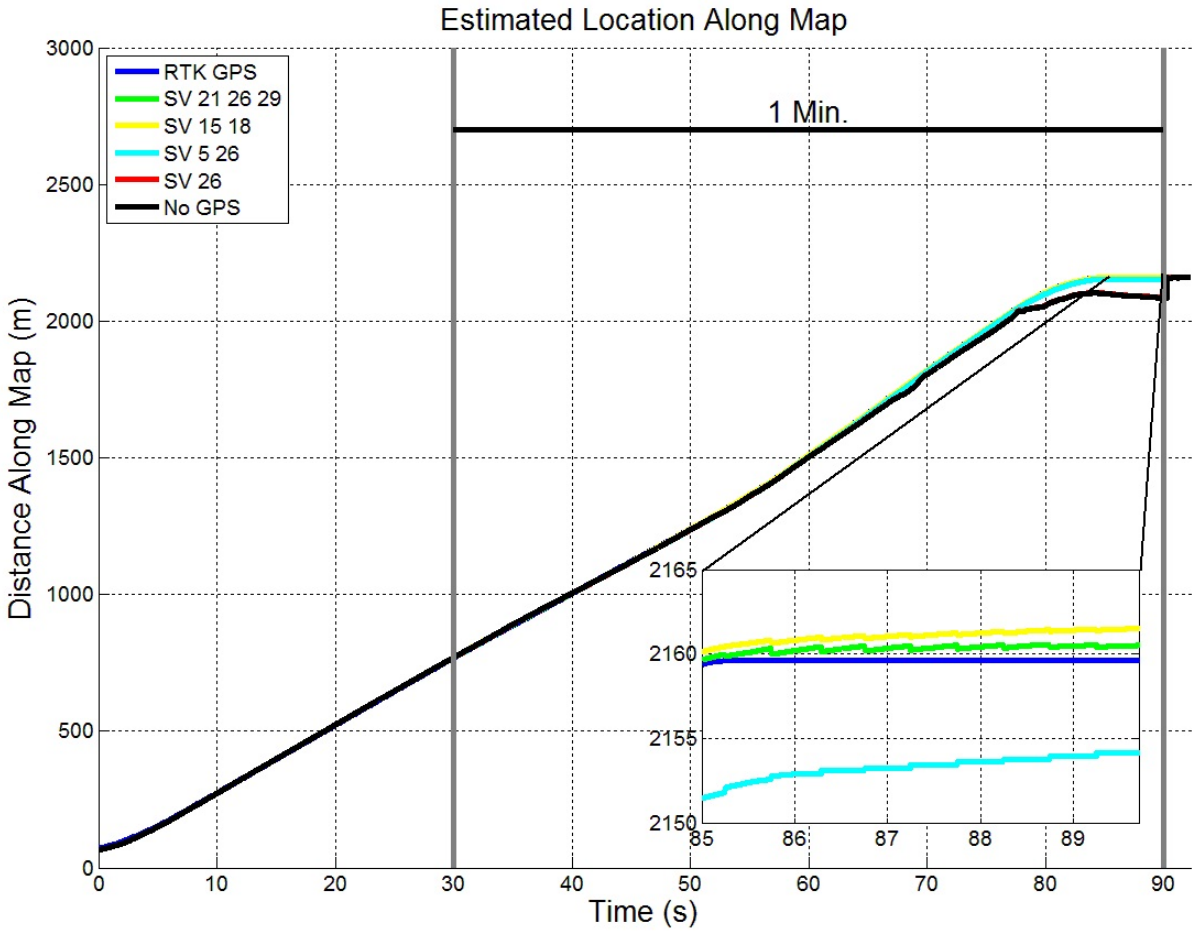


Figure 5.15: Estimated Longitudinal Position with Vision and Limited Satellite Visibility

Figure 5.15 shows the estimated longitudinal position with vision measurements representing the distance from the start of the map along the path of the map. This position axis is where the use of some GPS observations shows the most benefit. The order of performance is the same as Figure 5.13. When there are two or more GPS observations are available, the filter is able to estimate longitudinal position; however, this value may be biased. The zoomed in section of the plot shows the biases at the end of the satellite outage. If less than two GPS observations are available, the filter no longer has the observability necessary

to estimate longitudinal lane position. Also, there is no noticeable difference in drift when using one GPS observation (red line) and using no GPS observations (black line).

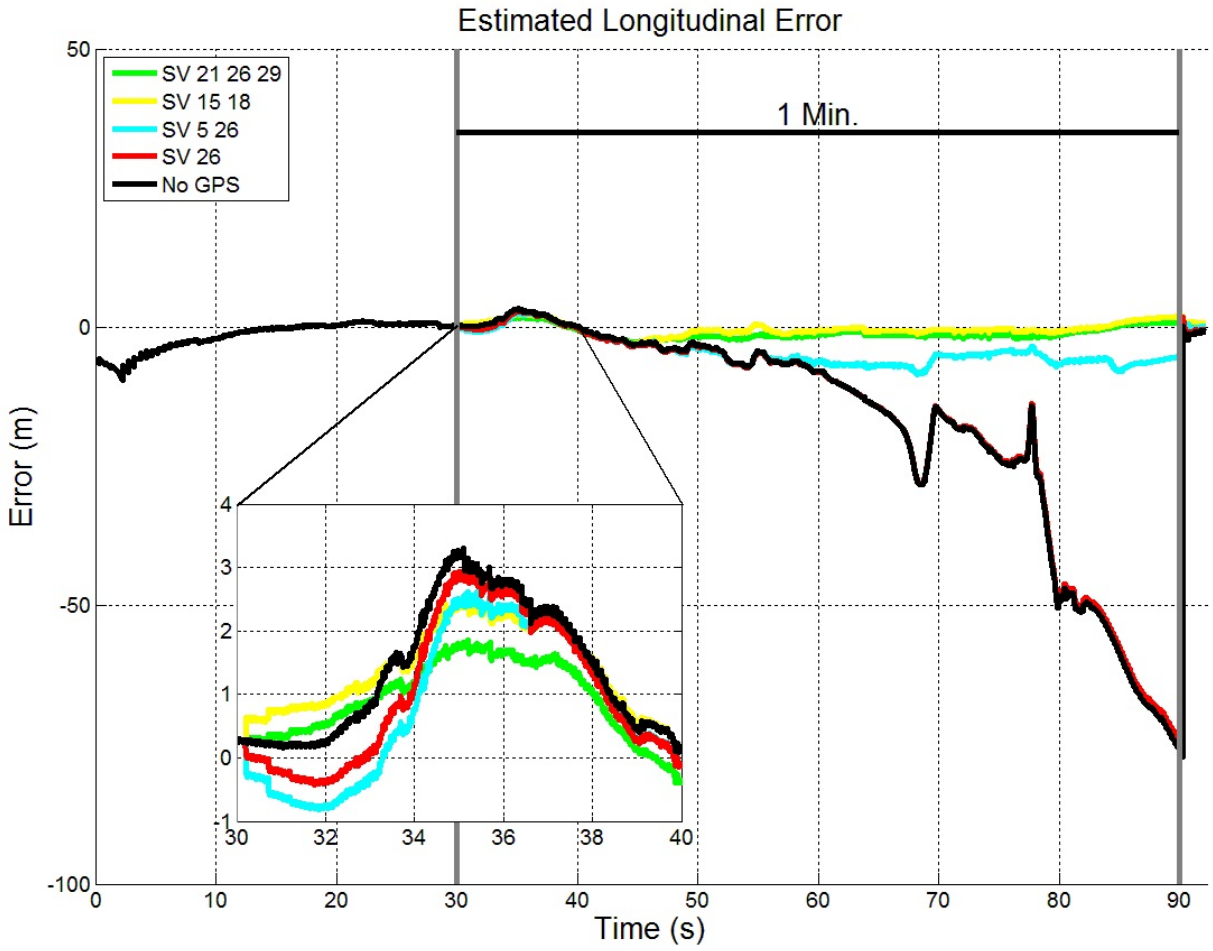


Figure 5.16: Estimated Longitudinal Position Error with Vision and Limited Satellite Visibility

Figure 5.16 is a plot of the estimated error in longitudinal position. The plot does show the estimated longitudinal position contains a large biased for the case when only SV 5 and 26 are used. This bias is most likely due to the lack in observability due to the fact that the azimuth angles to both of these satellites are close together. For the case when only SV 15 and 18 are used, the bias present is along the level seen when using stand-alone GPS with more than four observations. This small error is most likely due to the better observability due to the fact that the azimuth angles to the satellites are far apart. If only two observations are available, then the filter still remains observable; however, there can

be bias in estimated longitudinal position. This bias is a function on the quality of the observations available, and the constellation. The best results appear to come when the two observations are 180 degrees apart in azimuth angle and both of the azimuth angles line in the axis parallel with the direction of the road (one satellite in front of the vehicle and the other behind). Typically, in an urban environment, observable satellites will reside in the axis parallel with the direction of the road. The estimated longitudinal position becomes unobservable if only one or no GPS observations are available.

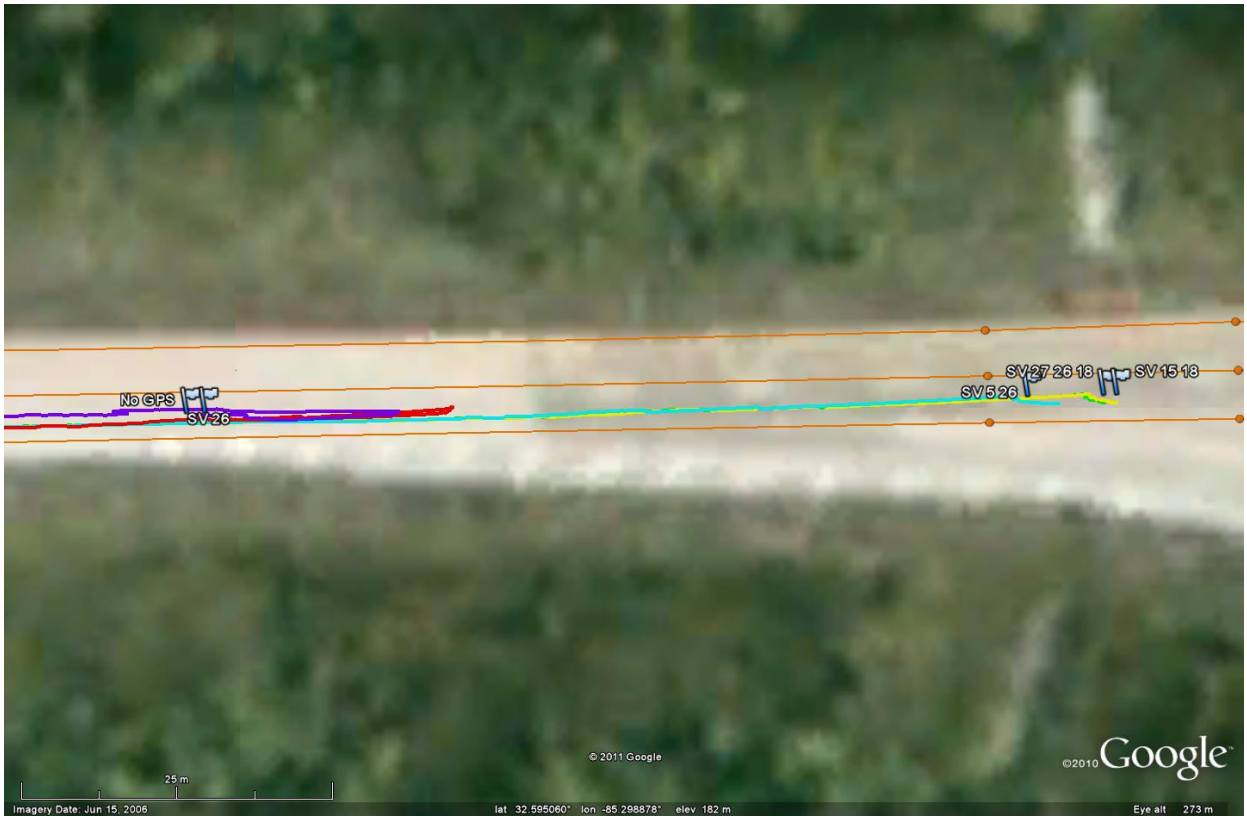


Figure 5.17: Estimated North-East Position with Vision Measurements, Map, and Limited Satellite Visibility

Figure 5.17 provides a top down view at the end of the satellite outage. At the end of the one minute outage, the car has come to a complete stop form 70 mph. For this case, both the map and vision measurements where used. The vision measurements insures that for every possible GPS satellite outage, lateral lane position is always be maintained. The

error in the longitudinal road axis is dependent on GPS observations available. As long as two observations are available, the navigation filter will remain fully observable.

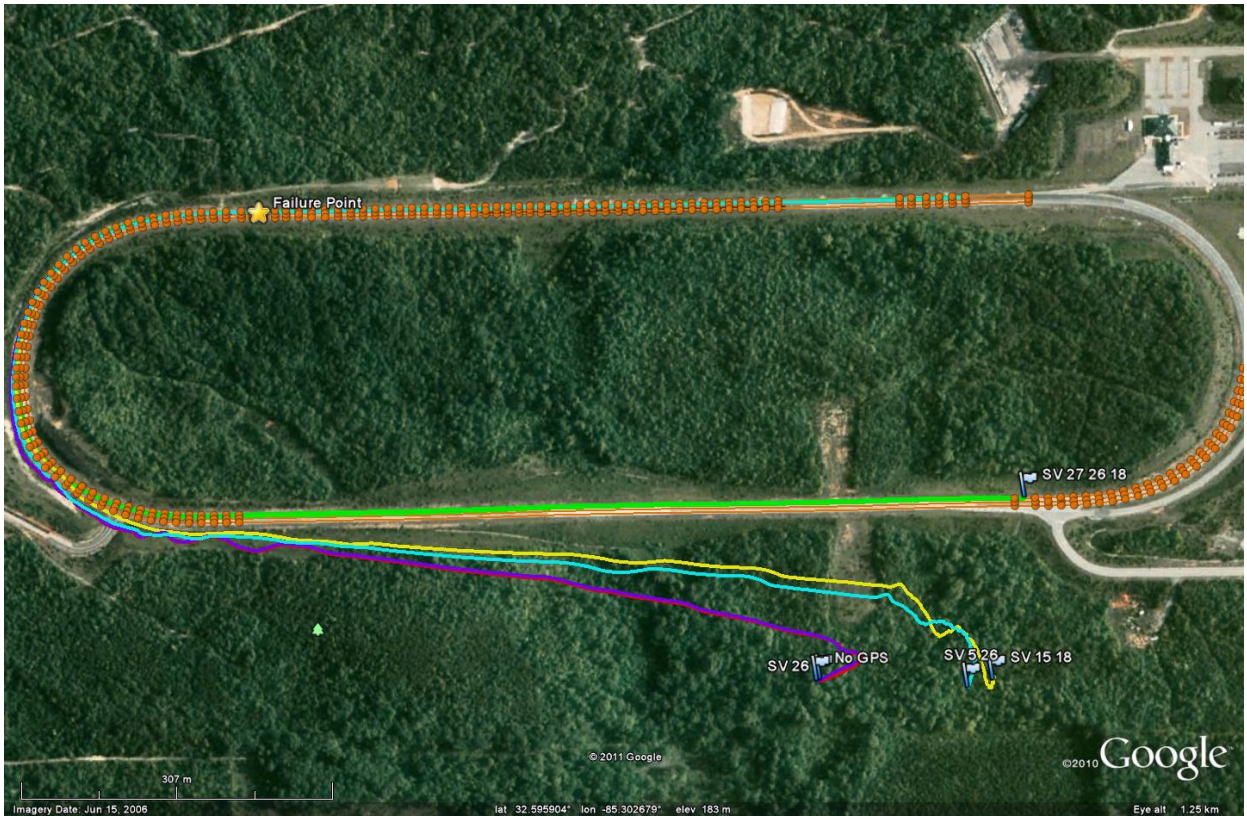


Figure 5.18: Estimated North-East Position with Map and Limited Satellite Visibility

Figure 5.18 shows the estimated position when using only the map with limited satellite visibility. When the map is available, the filter can still use height measurements to constrain the vertical position. With a constrained height, the three GPS observation case is fully observable; however, without the vision measurements, the lane position estimate will be biased. Comparing Figure 5.18 to Figure 5.19 demonstrates a clear improvement in drift when using the height measurement.

Figure 5.19 shows the estimated position when using no map or vision measurements. Like all the other limited satellite results, performance increases with the number of GPS observations available. The three observation case (green line) performs much better than the other cases. The system is not observable with only three GPS observations; therefore,

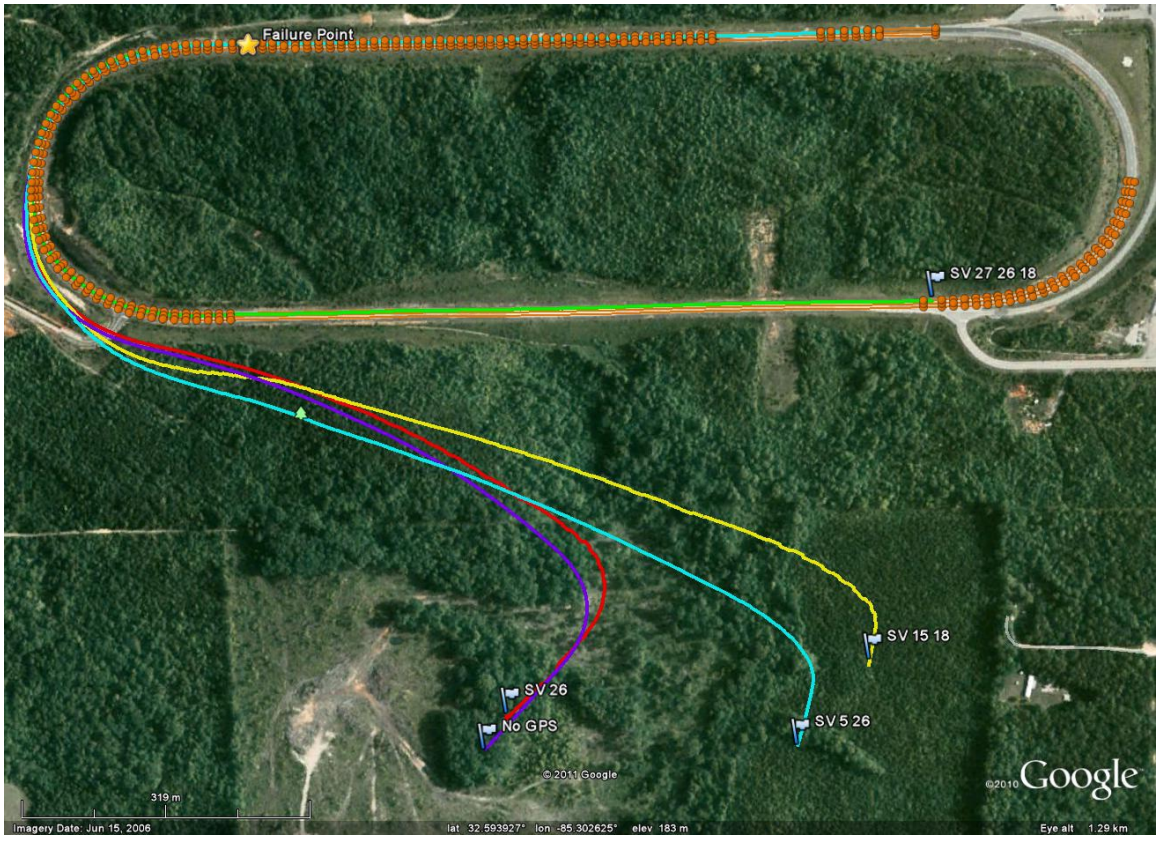


Figure 5.19: Estimated North-East Position with Limited Satellite Visibility

the position will continue to degrade. With three GPS observations, the clock bias and drift is the only unobservable mode; therefore, the drift when using only three GPS observations is dependent on the stability of the clock used by the receiver. There is an improvement in drift rate when using one or two GPS observations; however, the drift for any case where less than three GPS observations are available is very large.

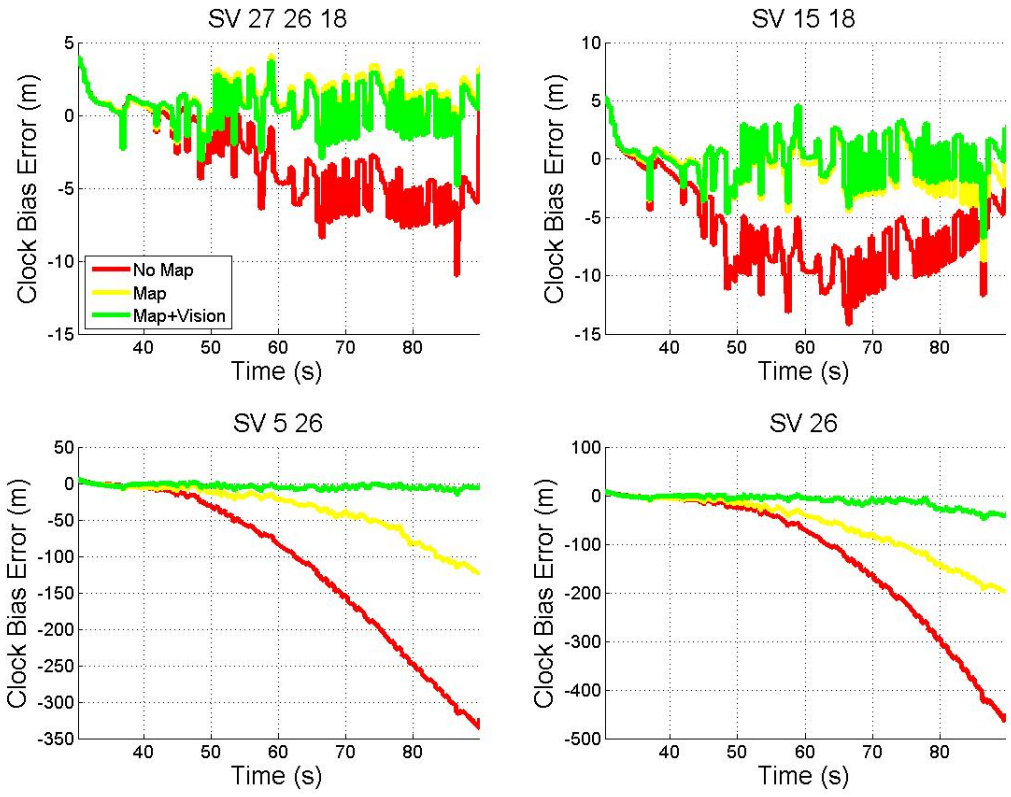


Figure 5.20: Receiver Clock Bias Error for Various Satellite Combinations

Figure 5.20 provides the receiver clock bias error for the various satellite constellations and various availability of the map and vision measurements. The receiver clock bias is the bias (in meters) observed on all GPS pseudorange measurements due to the difference in the GPS receiver clock time and GPS system time. The error was calculated by differencing the estimated clock bias and the receiver clock bias estimated with a full satellite constellation. The plot shows the error in estimated receiver clock bias decreases as additional measurements are added. The estimated receiver clock bias remains observable when at least two GPS observations are available along with the map and vision measurements. The estimated receiver clock bias drifts away from the true value when only one GPS observation, along with vision measurements and the map, are available. This drift is due to a lack of observability when fewer than two GPS observations are available. The SV 15 and 18 combination performs much better than the SV 5 and 26 combination. The carrier-to-noise ratio for SV

15 and 18 are both in the low fifties. The carrier-to-noise ratio for SV 5 and 26 are both in the upper forties. This difference in measurement quality suggest the estimated clock bias performance is dependent on the noise present in the available pseudoranges. Using the map and vision measurements has a much larger impact on estimated receiver clock bias when the carrier-to-noise ratio of the available GPS observations is low.

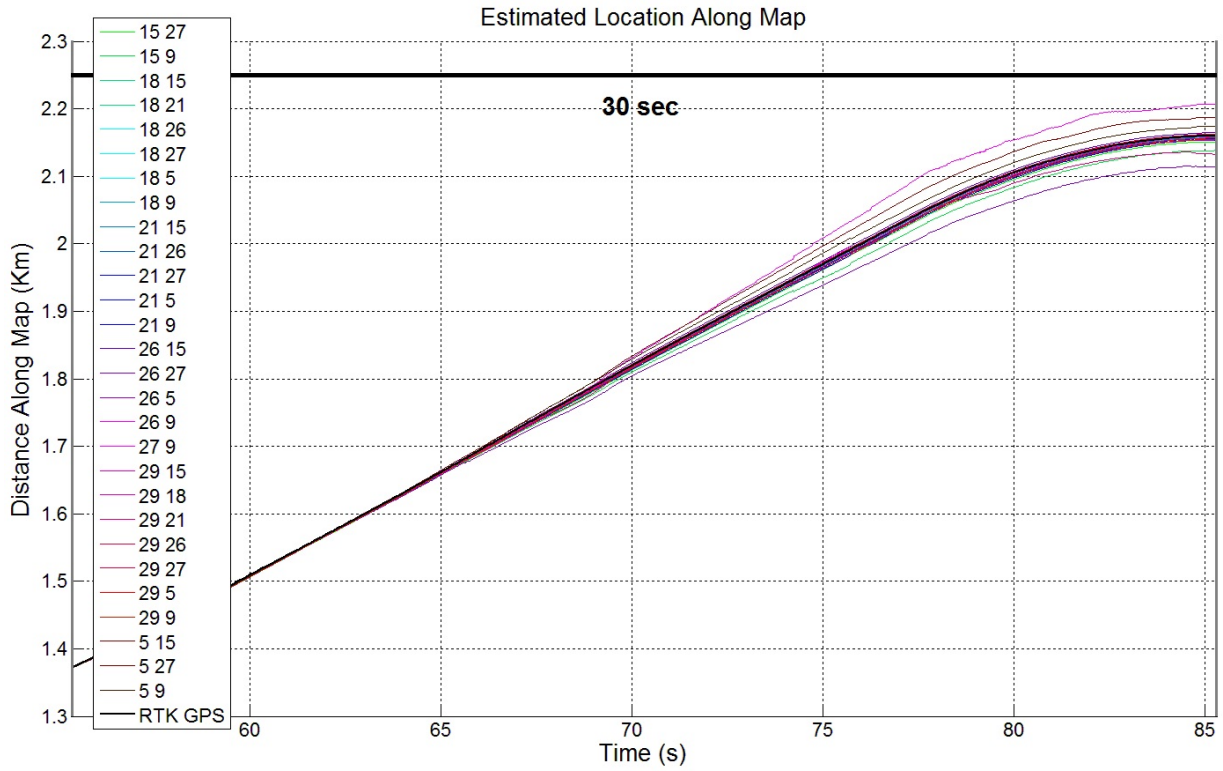


Figure 5.21: Estimated Longitudinal Position for All Possible SV Pairs

In order to better understand the effect of satellite constellation on the case where two GPS observations and vision measurements are used, Figure 5.21 shows estimated longitudinal position for every possible pair of GPS observations. For all cases, the longitudinal position is biased but observable. There are two combinations that result in what appears to be a continual error growth; however, it is not know if the estimated longitudinal position would converge to some steady state bias given enough time.

Table 5.2 shows the longitudinal position bias after one minute of navigating with only two GPS satellites for every possible pair of satellites. The satellite pairs are listed in the

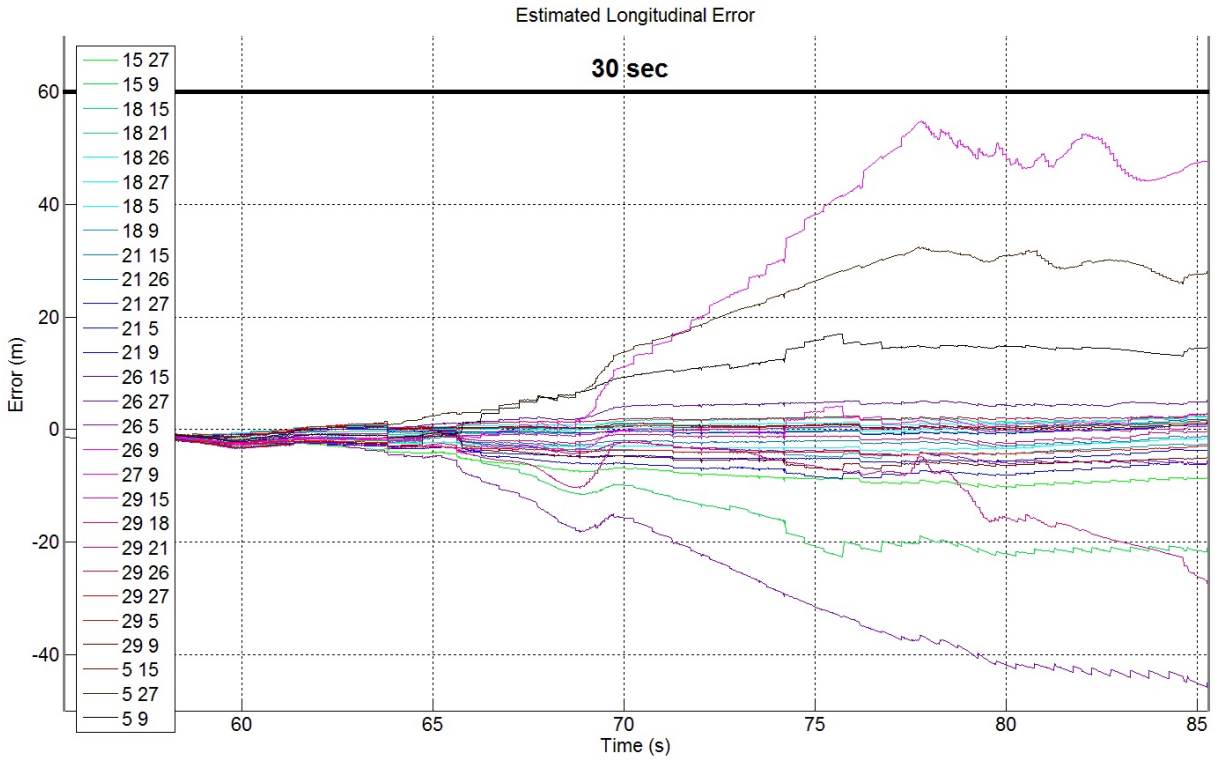


Figure 5.22: Estimated Longitudinal Error for All Possible SV Pairs

table from highest bias (worst performance) to lowest bias (best performance). Four of the satellite combinations resulted in less than a meter of bias. Nine of the satellite combinations resulted in less than a two meter bias. And eighteen of the twenty-eight pairs resulted in less than a 5 meter bias.

Table 5.2 also provides the average carrier-to-noise ratio of the two observations, and the lowest carrier-to-noise ratio of the pair. The carrier-to-noise ratio is a good indication of the noise present in an observation. A larger carrier-to-noise ratio corresponds to low measurement noise on that observation. The carrier-to-noise ratio is measured is decibels (a logarithmic scale). The data shows a correlation between carrier-to-noise ratio and longitudinal position bias. The bias tends to increase as average carrier-to-noise ratio falls. There are some outliers (SV 15 9, SV 21 9, SV 26 15); however, these outliers consists of a large carrier to noise ratio paired with a low carrier-to-noise ratio suggesting that both observations should have good carrier-to-noise ratio to ensure a small longitudinal position bias.

Table 5.2: Longitudinal Position Error after 30 Seconds for Every SV Pair

| SV Pair | Longitudinal Position Error (m) | Average C2N (dB) | Lowest C2N (dB) |
|---|---|---|---|
| SV 26 9 | 47.64 | 48 | 48 |
| SV 26 27 | -45.51* | 45 | 42 |
| SV 5 27 | 27.77 | 45 | 42 |
| SV 29 21 | -26.72* | 51.5 | 51 |
| SV 15 9 | -21.72 | 51 | 48 |
| SV 5 9 | 14.52 | 48 | 48 |
| SV 15 27 | -8.666 | 48 | 42 |
| SV 21 9 | -6.125 | 50 | 48 |
| SV 26 5 | -6.025 | 48 | 48 |
| SV 26 15 | -5.236 | 51 | 48 |
| SV 29 9 | 4.947 | 49.5 | 48 |
| SV 21 27 | -3.619 | 47 | 42 |
| SV 29 26 | 2.981 | 49.5 | 48 |
| SV 29 27 | -2.846 | 46.5 | 42 |
| SV 27 9 | 2.67 | 45 | 42 |
| SV 18 9 | -2.567 | 50.5 | 48 |
| SV 18 26 | 2.445 | 50.5 | 48 |
| SV 18 21 | 2.283 | 52.5 | 52 |
| SV 21 26 | 1.953 | 50 | 48 |
| SV 29 5 | 1.742 | 49.5 | 48 |
| SV 18 5 | 1.682 | 50.5 | 48 |
| SV 18 27 | -1.546 | 47.5 | 42 |
| SV 21 15 | -1.19 | 53 | 52 |
| SV 5 15 | 1.123 | 51 | 48 |
| SV 21 5 | .9541 | 50 | 48 |
| SV 18 15 | .9308 | 53.5 | 53 |
| SV 29 15 | .5867 | 52.5 | 51 |
| SV 29 18 | -.3918 | 52 | 51 |

Ideally both observations will have a carrier-to-noise ratio larger than 50 dB. The effects of using GPS observations with less than a 40 db carrier-to-noise ratio have not been studied.

This data does show that some satellite pairs can result in close to a fifty meter bias. The results shows that with good satellite geometry and good satellite measurements, the navigation filter will remain operational. However, if satellite geometry is bad (line of sight vectors to the satellites are close to perpendicular to the road) and measurement quality is poor (low carrier-to-noise ratio), the filter can experience large errors in longitudinal position.

# Chapter 6

# Conclusions

This thesis has presented a method of using lane position measurements from a camera or LiDAR to update a global navigation filter. A waypoint map is used in order to relate the vision measurement (given in the road coordinate frame) to the global (ECEF coordinate frame). The map also provides an additional height measurement because the height of the vehicle above the road is known and constant. Provided the map is globally accurate, the vision and height measurements provide a much more unbiased measurement of global position than stand-alone GPS. If the map is not globally accurate, the global position estimates will be incorrect and biased. This bias will be a direct representation of the global error in the map. For example, if the map is two meters off in the east direction, the global solution when using the map and vision measurements will be biased by two meters in the east direction. The global accuracy of the map will determine the global accuracy of the estimated global position; however, the global accuracy of the map has no effect on the estimated lane position. If RTK differential GPS or unbiased vision measurements are available, the filter will estimate an unbiased lane position.

Vision and height measurements, along with a map, were shown to greatly reduce the drift experienced when GPS is lost. The vision and height constrain drift in two axis; thus, the solution only drifts in the longitudinal axis of the road coordinate frame. One GPS range could be used to observe position in the longitudinal axis of the road coordinate frame. Using GPS observations adds another unobservable mode (receiver clock bias and drift); therefore, two GPS observations are needed (along with vision measurements and a map) in order to maintain full position observability. At least one of the GPS observations must have a component in the longitudinal axis of the road coordinate frame. As long as both GPS

observations do not lie in the axis perpendicular to the road, full observability is maintained. Two GPS observations are unlikely to have the same azimuth angle or an exactly 180 degrees azimuth angle difference. While the navigation filter remains fully observable with two GPS observations, map, and vision measurements, the performance of positioning in the longitudinal axis of the road is dependent on the constellation of the two GPS observations and the error in the observations. Results from a variety of combinations of satellite pairs were shown. Some combinations of satellites resulted in a meter level bias in longitudinal lane position, while other satellite combinations resulted in a a longitudinal bias on the order of tens of meters. As long as unbiased vision measurements are available, the estimated lateral lane position will be unbiased.

## 6.1 Future Work

A large potential exists for future work in developing lane maps and map keeping algorithms. The information in lane maps has not been standardized. There may be extra information that should be contained in the lane map that was not covered in this work. Examples of information that can be included with each segment are the attitude of the road, distance to left and right lane marking (or lane width), and information on what map (if any) is to the left and right of the current section. The attitude of the road is needed to use the vision measurements of lane position to update the filter. The distance to the left and right lane marking can be used by the vision systems to determine position in the lane without making a constant lane width assumption. Also, setting the distance to the lane lines to zero could signify no lane marking in the current section ,and allow the filter to ignore vision measurements in sections that do not have painted lane lines (such as in an intersection). Adding information on what map lies to the left and the right of the current section would allow the filter to know what map and index to use when changing lanes.

The use of wheel odometry should be explored as an effective measurment for periods when GPS is not available or when the number of GPS observations is limited. Wheel

odometry would provide a measured position in the longitudinal road axis; however, wheel odometry consists of integrating the wheel speed sensor. This integration will cause a continual error growth in the odometry estimate. The drift associated with wheel odometry is small compared to the drift cause by IMU integration. Using wheel odometry could improve degradation of the longitudinal position in the absence of GPS, but the filter would not be a fully observable without GPS. The system would however be able to maintain an accurate position for much longer when the filter is unobservable (GPS is not available).

Bibliography


[1] J. Britt and D. M. Bevly, "Lane tracking using multilayer laser scanner to enhance vehicle navigation and safety systems," in *Internation Technical Meeting. Anaheim, California*, 2009.

[2] C. Rose and D. M. Bevly, "Vehicle lane position estimatation with camera vision using bounded polynomial interpolated lines," in *Internation Technical Meeting. Anaheim California*, 2009.

[3] T. D. Gillespie, *Fundamentals of Vehicle Dynamics*. Society of Automotive Engineers, 1992.

[4] J. A. Farrell, *Aided Navigation: GPS with High Rate Sensors*. McGraw Hill, 2008.

[5] P. D. Groves, *Principles of GNSS, Inertial, and Multisensor Integrated Navigation Systems*. Artech House, 2008.

[6] R. E. Kalman, "A new approach to linear filtering and prediction problems," *Rans. Of the ASME-Journal of Basic Engineering*, vol. 82 (series D), pp. 35–45, 1960.

[7] ARINC Research Corporation, 2250 E. Imperial Highway, Suite 450 El Segundo, CA 90245-3509, *Navstar GPS Space Segment / Navigation User Interfaces*, Oct 1993.

[8] Septentrio, Ubicenter, Philipssite 5 B-3001 Leuven, Belgium, *PolaRx2/2e Use Manual*, 3.2.0 ed., January 2007.

[9] H. Leppakoski, H. Kuusniemi, and J. Takala, "Raim and complementary kalman filtering for gnss reliability enhancement," in *Proc. IEEE/ION Position, Location, And Navigation Symp*, pp. 948–956, 2006.

[10] I. Rhee, M. F. Abdel-Hafez, and J. L. Speyer, "Observability of an integrated gps/ins during maneuvers," vol. 40, no. 2, pp. 526–535, 2004.

[11] J. W. Allen and D. M. Bevly, "Relating local vision measurements to global navigation satellite systems using waypoint based maps," in *Proc. IEEE/ION Position Location and Navigation Symp. (PLANS)*, pp. 1204–1211, 2010.

[12] J. W. Allen and D. M. Bevly, "Performance evaluation of range information provided by dedicated short range communication (dsrc) radios," in *2010 ION GNSS Savannah, Georgia*, 2010.

[13] J. W. Allen and D. M. Bevly, "Use of vision sensors and lane maps to aid gps/ins under a limited gps satellite constellation," in *2009 ION GNSS Savannah, Georgia*, 2009.

[14] J. W. Allen, C. Rose, J. Britt, and D. M. Bevly, "Intelligent multi-sensor measurements to enhance vehicle navigation and safety systems," in *2009 International Technical Meeting. Anaheim, California*, 2009.

[15] J. Clanton, "Gps and inertial sensors enhancement for vision-based highway lane tracking," Master's thesis, Auburn University, 2006.

[16] G. Welch and G. Bishop, "An introduction to the kalman filter." TR 95-041 Department of Computer Science University of North Carolina at Chapel Hill Chapel Hill, NC 27599-3175 July 24, 2006, 2006.

[17] R. Toledo-Moreo, D. Betaille, and F. Peyret, "Lane-level integrity provision for navigation and map matching with gnss, dead reckoning, and enhanced maps," vol. 11, no. 1, pp. 100–112, 2010.

[18] B. D. Tapley, B. E. Schutz, and G. H. Born, *Statistical Orbit Determination*. Elsevier Academic Press, 2004.

[19] S. Nassar, Z. Syed, X. Niu, and N. El-Sheimy, "Improving mems imu/gps systems for accurate land-based navigation applications," in *ION NTM*, 2006.

[20] S. Mammar, S. Glaser, and M. Netto, "Time to line crossing for lane departure avoidance: a theoretical study and an experimental setting," vol. 7, no. 2, pp. 226–241, 2006.

[21] J. Kibbel, W. Justus, and K. Furstenberg, "Lane estimation and departure warning using multilayer laserscanner," in *Proc. IEEE Intelligent Transportation Systems*, pp. 607–611, 2005.

[22] P. C. Hughes, *Spacecraft Attitude Dynamics*. Dover Publications, 2004.

[23] W. L. Brogan, *Modern Control Theory*. Prentice-Hall, 1991.

[24] G. F. Franklin, J. D. Powell, and A. Emami-Naeini, *Feedback Control of Dynamic Systems*. Pearson Education, 5th ed., 2006.

# Appendices

# Appendix A

## Coordinate Frame Rotation and Translation

Lane position measurements are given in the road based coordinate frame. The road based coordinate frame can be approximated with a waypoint based map. A rotation matrix is need to rotate coordinates in the navigation coordinate frame to the road coordinate frame because the navigation filter coordinate frame is not oriented the same way as the road coordinate frame. Since the navigation coordinate frame and the road coordinate frame do not have the same origin, coordinate frame translation must also be covered.

A rotation matrix is a matrix that if multiplied by a vector of values expressed in an initial coordinate frame will result in a vector of values expressed in a new coordinate frame. The new coordinate frame has some different attitude from the initial coordinate frame. The difference in attitude will govern the values in the rotation matrix. A rotation matrix can be constructed using Euler angles. The rotational direction of Euler angles are based off the right handed coordinate system. In short, rotation about an axis that points towards the observer results in a counter-clockwise positive rotation. Rotation about an axis that points away from the observer results in a clockwise positive rotation. Rotation matrices are orthogonal; therefore, the inverse of a rotation matrix is equal to its transpose. Equation (A.1) describes this principle.

$$(C_{\alpha}^{\beta})^{-1} = (C_{\alpha}^{\beta})^{T} = C_{\beta}^{\alpha} \tag{A.1}$$

Rotation matrices are denoted by $C_{\alpha}^{\beta}$. This rotation matrix maps coordinates in the $\alpha$ coordinate frame to the $\beta$ coordinate frame.

### A.1 Two-Dimensional Rotations

Two-dimensional coordinate frame rotation matrices are $2 \times 2$ matrices based off one attitude angle. Figure A.1 shows the principle of a two-dimensional rotation. The $(i,j)$ coordinate frame is the starting coordinate frame, and the $(i',j')$ coordinate frame is the final coordinate frame. For the coordinate frame in Figure A.1, the right handed coordinate frame rule defines the axis of rotation as pointing down (or away from the observer); therefore, clockwise rotation results in a positive Euler angle. Equation (A.2) shows the rotation matrix that will map coordinates in the $(i,j)$ coordinate frame to the $(i',j')$ coordinate frame.

$$C_{(i,j)}^{(i',j')} = \begin{bmatrix} \cos(\theta) & \sin(\theta) \\ -\sin(\theta) & \cos(\theta) \end{bmatrix} \tag{A.2}$$

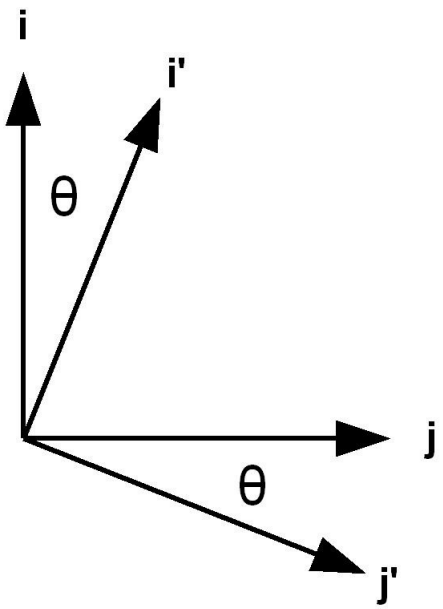


Figure A.1: Two-Dimensional Rotation

## A.2 Three-Dimensional Rotations

Three-Dimensional coordinate frame rotation matrices are $3 \times 3$ matrices based off three Euler angles. A three-dimensional coordinate frame rotation can be thought of as a series of three two-dimensional rotations [22]. Figure A.2 shows the rotation series used for all three-dimensional rotations used in this work.

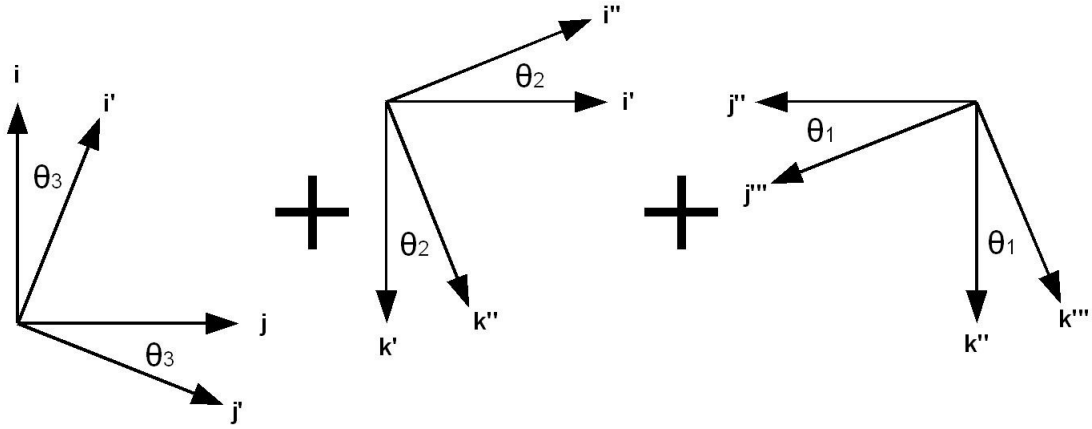


Figure A.2: Three-Dimensional Rotation Sequence

The first rotation is about the z ($k$) axis. The second rotation is about the new y ($j'$) axis. The third rotation is about the new x ($i''$) axis. Equation (A.3) shows how the three-dimensional rotation matrix is constructed. $s_1$ is the sine of $\theta_1$ and $c_1$ is the cosine of $\theta_1$. $s_2$ is the sine of $\theta_2$ and $c_2$ is the cosine of $\theta_2$. $s_3$ is the sine of $\theta_3$ and $c_3$ is the cosine of $\theta_3$.

$$C_{(i,j)}^{(i''',j''')} = \begin{bmatrix} 1 & 0 & 0 \\ 0 & c_1 & s_1 \\ 0 & -s_1 & c_1 \end{bmatrix} \begin{bmatrix} c_2 & 0 & -s_2 \\ 0 & 1 & 0 \\ s_2 & 0 & c_2 \end{bmatrix} \begin{bmatrix} c_3 & s_3 & 0 \\ -s_3 & c_3 & 0 \\ 0 & 0 & 1 \end{bmatrix} = \begin{bmatrix} c_2c_3 & c_2s_3 & -s_2 \\ s_1s_2c_3 - c_1s_3 & s_1s_2s_3 + c_1c_3 & s_1c_2 \\ c_1s_2c_3 + s_1s_3 & c_1s_2s_3 - s_1c_3 & c_1c_2 \end{bmatrix} \tag{A.3}$$

### A.3 Coordinate Frame Translation

The origin of the road based coordinate frame is not located at the same point in space as the origin of the navigation coordinate frame origin. When mapping coordinates in the navigation coordinate frame to the road coordinate frame, the coordinate frame must be moved and rotated. Figure A.3 shows an example of a rotated and translated coordinate frame.

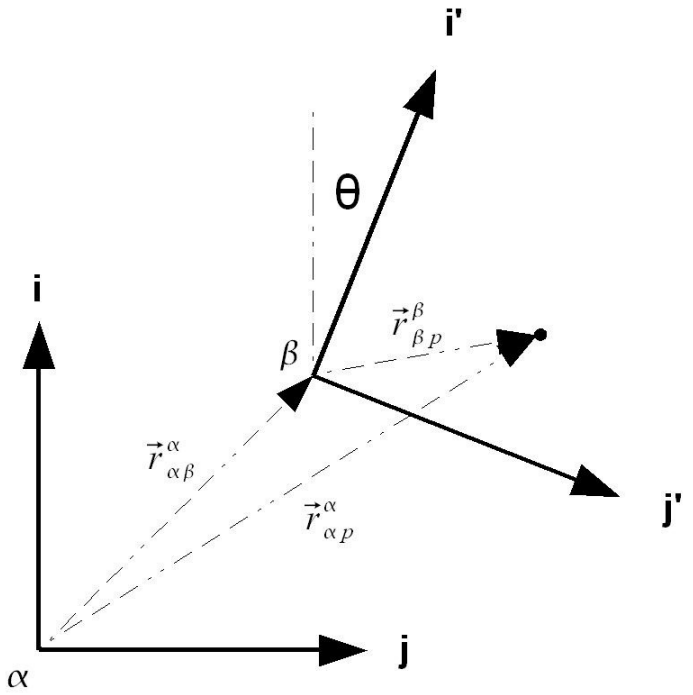


Figure A.3: Two-Dimensional Coordinate Frame Translation and Rotation

Equation (A.4) shows how to map coordinates in coordinate frame that has been moved and rotated. $\vec{r}^{\,\alpha}_{\alpha p}$ is the position vector expressed in the initial coordinate frame ($\alpha$), and $\vec{r}^{\,\beta}_{\beta p}$ is the position vector expressed in the rotated and translated coordinate frame ($\beta$). $\vec{r}^{\,\alpha}_{\alpha\beta}$ is a vector expressed in the initial coordinate that points from the initial coordinate frame to the new coordinate frame. $C_{\alpha}^{\beta}$ is the rotation matrix from coordinate frame alpha to coordinate frame beta.

$$\vec{r}^{\,\beta}_{\beta p} = C_{\alpha}^{\beta}\left[\vec{r}^{\,\alpha}_{\alpha p} - \vec{r}^{\,\alpha}_{\alpha\beta}\right] \tag{A.4}$$

Coordinates in the final coordinate frame can be mapped back to the initial coordinate frame using Equation (A.5).

$$\vec{r}_{\alpha p}^{\,\alpha} = C_{\beta}^{\,\alpha}\vec{r}_{\beta p}^{\,\beta} + \vec{r}_{\alpha\beta}^{\,\alpha} \tag{A.5}$$

## A.4 Global Coordinate Frame Rotations

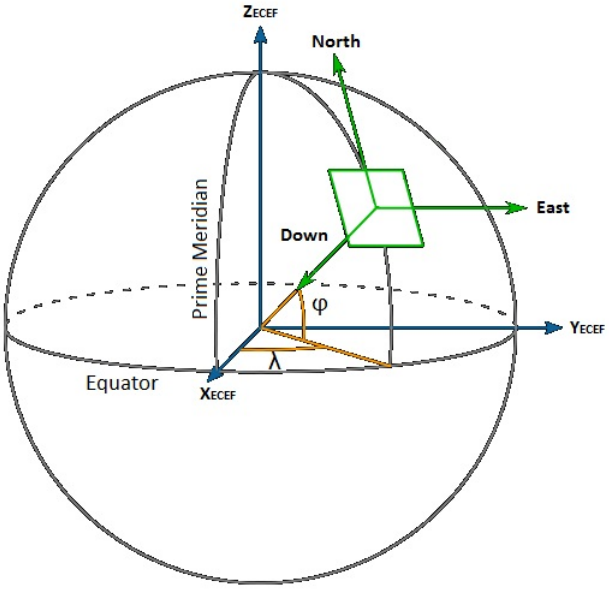


Figure A.4: North-East-Down Coordinate Frame

Sometimes it may be necessary to map coordinates in the Earth Centered Earth Fixed (ECEF) coordinate frame to the North East Down (NED) coordinate frame. The North East plane of the NED coordinate frame is tangential to a reference ellipsoid. The reference ellipsoid is an ellipsoid that mimics the surface of the earth. Using the latitude ($\phi$) and longitude ($\lambda$) of the origin of the NED coordinate frame, a rotation matrix that maps ECEF coordinates to NED coordinates can be constructed. Equation (A.6) shows the rotation matrix that maps coordinates in the ECEF coordinate frame to the NED coordinate frame. The transpose of this matrix will map coordinates from the NED coordinate frame to the ECEF coordinate frame.

$$C_{e}^{\,n} = \begin{bmatrix} -\sin(\phi)\cos(\lambda) & -\sin(\phi)\sin(\lambda) & \cos(\phi) \\ -\sin(\lambda) & \cos(\lambda) & 0 \\ -\cos(\phi)\cos(\lambda) & -\cos(\phi)\sin(\lambda) & -\sin(\phi) \end{bmatrix} \tag{A.6}$$

Equation (A.7) coverts ECEF position coordinates ($\vec{r}_{ep}^{\,e}$) to NED position coordinates ($\vec{r}_{np}^{\,n}$). Notice that, along with the latitude and longitude of the origin of the NED coordinate frame, the position of the origin expressed in the ECEF coordinate frame ($\vec{r}_{en}^{\,e}$) must be known.

$$\vec{r}_{np}^{\,n} = C_{e}^{\,n}\left[\vec{r}_{ep}^{\,e} - \vec{r}_{en}^{\,e}\right] \tag{A.7}$$

Equation (A.8) coverts NED position coordinates to ECEF position coordinates.

$$\vec{r}^{\,e}_{ep} = C_e^{\,nT}\vec{r}^{\,n}_{np} + \vec{r}^{\,e}_{en} \tag{A.8}$$

Equation (A.9) coverts ECEF velocity coordinates to NED velocity coordinates. Notice that velocity mapping is independent of the position of the NED coordinate frame. The latitude and longitude of the NED coordinate frame is still needed to construct the rotation matrix.

$$\vec{v}_n = C_e^{\,n}\vec{v}_e \tag{A.9}$$

Equation (A.10) coverts NED velocity coordinates to ECEF velocity coordinates.

$$\vec{v}_e = C_e^{\,nT}\vec{v}_n \tag{A.10}$$

# Appendix B

## Observability Analysis

The type of navigation filter used in this thesis is the discrete extended Kalman filter (DEKF). The DEKF is an state estimator that is optimally tuned given noise characteristics of inputs and measurements. A state estimator is a mathematical algorithm that estimates states of system given the inputs to the system, measurements of some of the states, a mathematical description of the system, and how the measurements relate to the system. Observability refers to the ability of the estimator to estimate all of the states based off a set of measurements of some of the states. In order to estimate all the states, it is not necessary to measure all the states. For example, IMU biases can be estimated without an actual measurement of the values. Observability analysis takes the state to measurement relationship to determine if the estimator will be able to properly estimate all the states. If the estimator is observable, then it is able to estimate all the states given the measurements available. It is important to note that the observability necessary; however it does not guaranty the estimator will be be able to estimate all the states. The stability of the estimates is also a function of measurement quality, accuracy of the measurement and state equations, and nonlinearities in both the measurement and state equations.

The observability matrix is a matrix that represents the relationship of the measurement equations to the state equations. If this matrix is non-singular (or the rank of the matrix is equal to the number of state (n)) then the system is observable. Equation (B.1) is used determine the observability matrix ($O$) [23].

$$O = \begin{bmatrix} A \\ HA \\ HA^2 \\ \vdots \\ HA^{n-1} \end{bmatrix} \tag{B.1}$$

The observability matrix is a function of the system matrix ($A$) and the observation matrix ($H$). This type of analysis is only valid for systems that are time invariant (The system matrix ($A$) does not change over time. The system equations (navigation kinematic equations) used in this thesis are time variant. Equation (B.2) is used to determine the observability matrix for a time varying system [24].

$$O(t_0, t_1) = \int_{t_0}^{t_1} \phi(t, t_0)^T H(t)^T H(t) \phi(t, t_0) dt \tag{B.2}$$

The value of the observability matrix is estimated by discretely integrating (Euler integration) the equation above and checking the rank of the observability matrix at each measurement epoch. $\phi(t, t_0)$ is the state transition matrix and $H(t)$ is the current observation

matrix. Once the time variant observation matrix has reached full rank, it will remain at full rank. Therefore, in order to continually check observability, the observability matrix and the state transition matrix should be reset once the observability matrix becomes full rank. Once the observability matrix is reset, the rank of the matrix will fall back to zero. Reseting the observability matrix will result in a jagged line when plotting the observability with respect to time. As long as the plot is jagged, the system is observable. If the line settles to some value less than the number of states, the system will be unobservable.

The navigation filter does not pass the observability test using the time invariant analysis unless the attitude of the vehicle (IMU) is measured along with the global position of the vehicle. The velocity of the vehicle is not needed for full observability; however, it is beneficial to also use velocity measurements. If the attitude of the IMU is fixed to some constant known value, then the filter will pass the time invariant observability test.

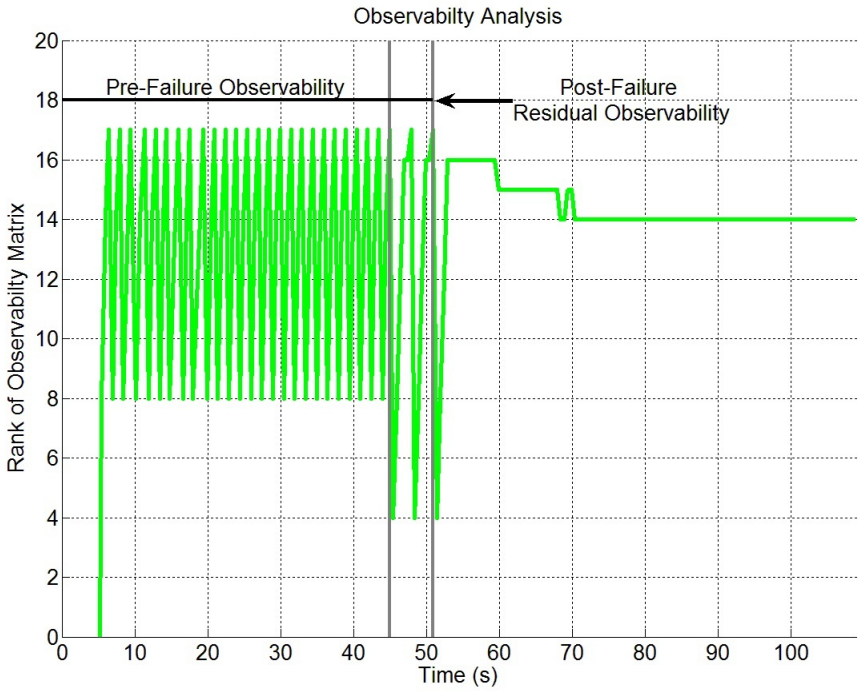


Figure B.1: Filter Observability with Respect to Time

Figure B.1 shows the rank of the observability matrix for the data used in the results chapter of the thesis. For this run, only the GPS pseudorange and pseudorange rate measurements are used initially, then after the failure point, only two GPS observations are used. The GPS measurements were received at two 2 Hz. The observability matrix reaches full rank once every second (every two GPS measurements). The system requires two measurements to be observable due to the coupling of the attitude states and the IMU acceleration bias states. After the failure point, the observability matrix becomes full rank twice more. This post failure observability is unusual because the estimator should not be observable with only two GPS pseudorange measurements. This effect only happens when two or more GPS observations are available. The length and frequency of the post failure observability

varies with the GPS observations used. Just because the observability matrix is full rank after the failure does not guarantee that the state estimates will remain stable.

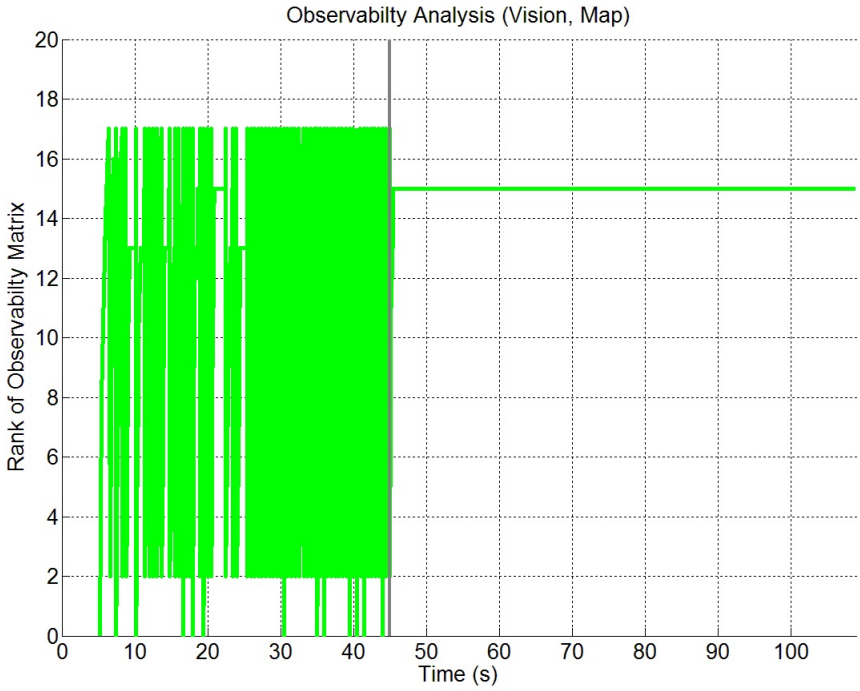


Figure B.2: Filter Observability (Full System) (GPS Outage)

Figure B.2 provides the rank of the observability matrix for the same data. For this run the GPS pseudorange and pseudorange rate measurements along with vision lane position measurements and a map are used pre-failure. The frequency at which the matrix become full rank is increased when using the vision measurements because the vision measurements are received at 10 $Hz$. Upon closer investigation, the rank of the observation matrix will never reach full rank on a vision measurement. The observation only becomes full rank when a GPS measurement is used. Post-failure, only the vision measurements are used to update the filter. The observability matrix rank does what is expected and remains at 15, two less than full rank. The two unobservable modes are GPS receiver clock errors and the longitudinal road axis.

Figure B.3 shows the run in Figure B.2 except after the failure, two GPS observations are used instead of none. The observability matrix continues to reach full rank as long as any two GPS observations are available.

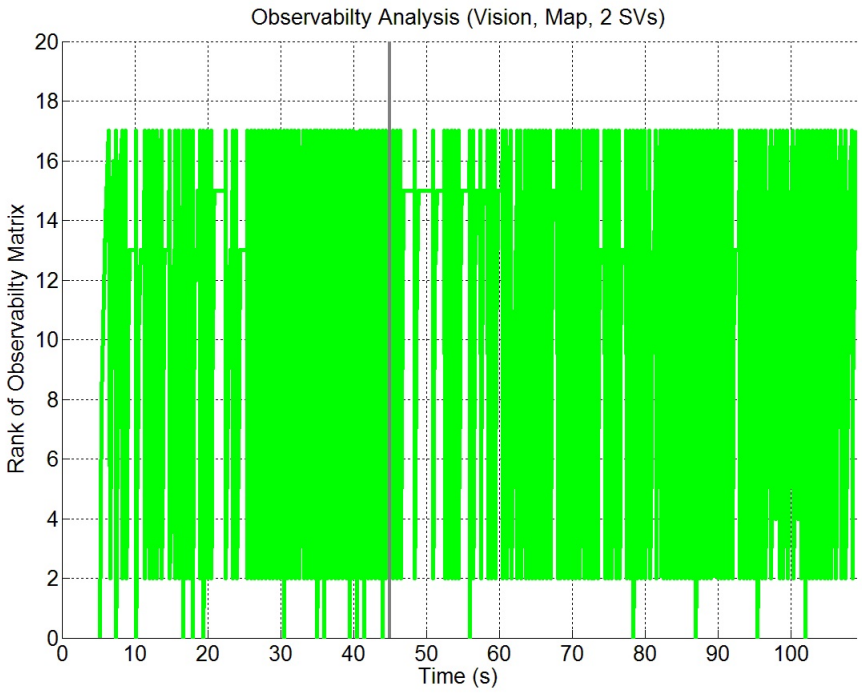


Figure B.3: Filter Observability (Full System) (2 GPS Observations during Outage)

Appendix C

Table of Variables

Table C.1: Variables

| | |
|---|---|
| $C_b^e$ | Rotation Matrix from Body to ECEF axis |
| $C_n^r$ | Rotation Matrix from NED to Road axis |
| $C_e^r$ | Rotation Matrix from ECEF to Road axis |
| $C_e^n$ | Rotation Matrix from ECEF to NED axis |
| $C_{MECH}$ | IMU Mechanization Matrix |
| $\rho_m$ | Measured Pseudorange |
| $c$ | Speed of Light |
| $dt_{sv}$ | Satellite Clock Correction |
| $f_m$ | Measured Signal Frequency |
| $L_1$ | Frequency of the L1 GSP Signal |
| $\hat{r}$ | Estimated Range to GPS Satellite |
| $\hat{\dot{r}}$ | Estimated Range Rate to GPS Satellite |
| $dt_u$ | User Clock Bias |
| $\dot{dt_u}$ | User Clock Drift |
| $\vec{r}_{eb}^{\,e}$ | Position Vector of Body in the ECEF Coordinate Frame |
| $\vec{e}_{er}^{\,e}$ | Position Vector of Road Waypoint in the ECEF Coordinate Frame |
| $\vec{r}_{rb}^{\,r}$ | Position Vector of Body in the Road Coordinate Frame |
| $\vec{v}^{\,e}$ | Velocity Vector in the ECEF Coordinate Frame |
| $\vec{\psi}^{\,e}$ | Attitude Vector of Body |
| $\vec{\gamma}$ | Attitude Vector of Road |
| $d_r$ | Length of Road Segment |
| $\phi$ | Latitude |
| $\lambda$ | Longitude |
| $\theta$ | Pitch |
| $\psi$ | Heading |

Table C.2: Variables

| | |
|---|---|
| $e$ | Position East |
| $n$ | Position North |
| $d$ | Position Down |
| $e_n$ | Unit Vector n |
| $P$ | State Covariance Matrix |
| $A$ | System Matrix |
| $A_d$ | Discrete System Matrix |
| $B$ | Noise Input Matrix |
| $Q$ | System Covariance Matrix |
| $dt$ | Time Between IMU Measurements |
| $\vec{z}$ | Measurement Residual Vector |
| $\vec{y}$ | Measurement Vector |
| $\hat{\vec{y}}$ | Estimated Measurement Vector |
| $h$ | Measurement Equation |
| $H$ | Measurement Model Matrix |
| $R$ | Measurement Covariance Matrix |
| $\sigma_\rho$ | Standard Deviation of Pseudorange Measurement |
| $\sigma_{\dot{\rho}}$ | Standard Deviation of Pseudorange Rate Measurement |
| $x_{sv}$ | Position of GPS Satellite in the x axis of the ECEF Coordinate Frame |
| $y_{sv}$ | Position of GPS Satellite in the y axis of the ECEF Coordinate Frame |
| $z_{sv}$ | Position of GPS Satellite in the z axis of the ECEF Coordinate Frame |
| $\dot{x}_{sv}$ | Velocity of GPS Satellite in the x axis of the ECEF Coordinate Frame |
| $\dot{y}_{sv}$ | Velocity of GPS Satellite in the y axis of the ECEF Coordinate Frame |
| $\dot{z}_{sv}$ | Velocity of GPS Satellite in the z axis of the ECEF Coordinate Frame |